



2012

## GLYCEROL-3-PHOSPHATE IS A NOVEL REGULATOR OF BASAL AND INDUCED DEFENSE SIGNALING IN PLANTS

Bidisha Chanda

University of Kentucky, [bidisha.chanda@gmail.com](mailto:bidisha.chanda@gmail.com)

[Right click to open a feedback form in a new tab to let us know how this document benefits you.](#)

---

### Recommended Citation

Chanda, Bidisha, "GLYCEROL-3-PHOSPHATE IS A NOVEL REGULATOR OF BASAL AND INDUCED DEFENSE SIGNALING IN PLANTS" (2012). *Theses and Dissertations--Plant Pathology*. 16.  
[https://uknowledge.uky.edu/plantpath\\_etds/16](https://uknowledge.uky.edu/plantpath_etds/16)

This Doctoral Dissertation is brought to you for free and open access by the Plant Pathology at UKnowledge. It has been accepted for inclusion in Theses and Dissertations--Plant Pathology by an authorized administrator of UKnowledge. For more information, please contact [UKnowledge@lsv.uky.edu](mailto:UKnowledge@lsv.uky.edu).

## **STUDENT AGREEMENT:**

I represent that my thesis or dissertation and abstract are my original work. Proper attribution has been given to all outside sources. I understand that I am solely responsible for obtaining any needed copyright permissions. I have obtained needed written permission statement(s) from the owner(s) of each third-party copyrighted matter to be included in my work, allowing electronic distribution (if such use is not permitted by the fair use doctrine) which will be submitted to UKnowledge as Additional File.

I hereby grant to The University of Kentucky and its agents the irrevocable, non-exclusive, and royalty-free license to archive and make accessible my work in whole or in part in all forms of media, now or hereafter known. I agree that the document mentioned above may be made available immediately for worldwide access unless an embargo applies.

I retain all other ownership rights to the copyright of my work. I also retain the right to use in future works (such as articles or books) all or part of my work. I understand that I am free to register the copyright to my work.

## **REVIEW, APPROVAL AND ACCEPTANCE**

The document mentioned above has been reviewed and accepted by the student's advisor, on behalf of the advisory committee, and by the Director of Graduate Studies (DGS), on behalf of the program; we verify that this is the final, approved version of the student's thesis including all changes required by the advisory committee. The undersigned agree to abide by the statements above.

Bidisha Chanda, Student

Dr. Pradeep Kachroo, Major Professor

Dr. Lisa J. Vaillancourt, Director of Graduate Studies



GLYCEROL-3-PHOSPHATE IS A NOVEL REGULATOR OF BASAL AND  
INDUCED DEFENSE SIGNALING IN PLANTS

---

DISSERTATION

---

A dissertation submitted in partial fulfillment of the requirements  
for the degree of Doctor of Philosophy in the  
College of Agriculture at the  
University of Kentucky

By  
BIDISHA CHANDA  
Lexington, Kentucky

Director: Dr. Pradeep Kachroo, Associate Professor of Plant Pathology  
Lexington, Kentucky

2012

Copyright © BIDISHA CHANDA

## ABSTRACT OF DISSERTATION

### GLYCEROL-3-PHOSPHATE IS A NOVEL REGULATOR OF BASAL AND INDUCED DEFENSE SIGNALING IN PLANTS

Plants use several strategies to defend themselves against microbial pathogens. These include basal resistance, which is induced in response to pathogen encoded effector proteins, and resistance (R) protein-mediated resistance that is activated upon direct or indirect recognition of pathogen encoded avirulence protein(s). The activation of R-mediated signaling is often associated with generation of a signal, which, upon its translocation to the distal uninfected parts, confers broad-spectrum immunity against related or unrelated pathogens. This phenomenon known as systemic acquired resistance (SAR) is one of the well-established forms of induced defense response. However, the molecular mechanism underlying SAR remains largely unknown. Induction of plant defense is often associated with a fitness cost, likely because it involves reprogramming of the energy-providing metabolic pathways. Glycerol metabolism is one such pathway that feeds into primary metabolism, including lipid biosynthesis. In this study, I evaluated the role of glycerol-3-phosphate (G3P) in host-pathogen interaction. Inoculation with the hemibiotrophic fungal pathogen *Colletotrichum higginsianum* led to increased accumulation of G3P in wild-type plants. Mutants impaired in biosynthesis of G3P showed enhanced susceptibility, suggesting a correlation between G3P levels and basal defense. Conversely, increased biosynthesis of G3P correlated with enhanced resistance. The Arabidopsis genome encodes one copy of glycerol kinase (GK), which catalyzes phosphorylation of glycerol to G3P, and five copies of G3P dehydrogenase (G3Pdh), which catalyze reduction of dihydroxyacetone phosphate to G3P. Analysis of plants mutated in various G3Pdh's showed that plastidal lipid biosynthesis was only dependent on the GLY1 isoform but the pathogen induced G3P pool required the function of GLY1 and two other G3Pdh isoforms. Interestingly, compromised G3P biosynthesis in GK and G3Pdh mutants also compromised SAR, which was restored when G3P was provided exogenously. Detailed biochemical analysis showed that G3P was transported to distal tissues and that this process was dependent on a lipid transfer protein, DIR1. Together, these results show that G3P plays an important role in both basal- and induced-defense responses.

Key words: Glycerol-3-phosphate (G3P), Systemic acquired resistance, Glycerol, Plant immunity, Basal resistance

BIDISHA CHANDA  
June 12, 2012

GLYCEROL-3-PHOSPHATE IS A NOVEL REGULATOR OF BASAL AND  
INDUCED DEFENSE SIGNALING IN PLANTS

By  
BIDISHA CHANDA

Pradeep Kachroo  
*Director of Dissertation*

Lisa J. Vaillancourt  
*Director of Graduate Studies*

June 12, 2012

*Date*

## ACKNOWLEDGEMENTS

I would like to take this opportunity to thank my major advisor Dr. Pradeep Kachroo for his support during the course of my PhD program. His constant encouragement, constructive criticisms and suggestions always helped me keep focused on my objectives, which led to the successful completion of my PhD. His unsurpassed knowledge and sense of perseverance always inspired and motivated me. I always respected his overzealous passion and dedication for his work. I will always remain ever grateful to him for all of my achievements during this period.

I would also like to express my gratitude to Dr. Aardra Kachroo for her valuable suggestions, comments and ideas during my PhD program. Her ideas were always helpful to streamline my experiments.

My heartfelt thanks are also due to Dr. Ludmila Lapchyk for her untiring help both in crucial and casual times. I would like to thank Amy Crume for maintaining the green house and plant growth facility. I would like to thank John Johnson for analysis of our fatty acid samples.

Special thanks are to the lab members for making a jovial working atmosphere. I would like to thank Dr. Srivathsa Venugopal, for helping me in the project related to role of glycerol metabolism in *Arabidopsis* against *Colletotrichum higginsianum*; Ye Xia, for helping me in SAR experiments, Keshun Yu for helping me with the TLC and JA, AA estimations, Ken-Taro Sekine for localization of GLY1, Mihir Kumar Mandal for providing with the DIR1 protein and Qing Ming Gao.

I would like to thank Etta Nuckles for allowing me to borrow from her ever-ready stock of *C. higginsianum* subcultured plates.

My sincerest thanks are also due to my committee members Dr. Lisa Vaillancourt, Dr. Kenneth Seebold, Dr. Aardra Kachroo and Dr. Bruce Downie.

I would especially like to thank Dr. Bruce Downie for teaching me the basics of HPLC.

I would like to thank Dr. Duroy Navarre for analyzing my SA samples and Dr. Michael Goodin for pSITE vectors. My sincere thanks to Dr. Lisa Vaillancourt for timely update of all graduate forms and fellowships.

I would like to thank my external examiner Dr. Edward DeMoll for taking out his time for my defence seminar. I would also like to thank Dr. Peter Eastmond for providing mitochondrial G3Pdh mutant seeds. I would also like to thank ABRC for the seeds, Kansas Lipidomics Centre for lipid analysis, AGTC for sequencing and Dr. David Hildebrand for the TLC plates. Lastly, I would like to thank the department of Plant Pathology for making my stay here enjoyable and memorable.

The journey towards the completion of PhD would not be possible without the emotional and moral support from my family members especially my parents and in-laws. Completion of PhD also would have been impossible without the support and help from my husband. I would also take the opportunity to thank my friends Mohammed, Merrari, Maria, Ester and Sladana for their unconditional love and support.

## TABLE OF CONTENTS

Acknowledgements.....	iii
List of tables.....	vii
List of figures.....	viii
CHAPTER 1: INTRODUCTION.....	1
Objectives.....	3
CHAPTER 2: MATERIALS AND METHODS	
Plant growth conditions and genetic analyses.....	4
Bacterial transformation.....	4
Arabidopsis transformation.....	5
Plant treatments.....	6
Pathogen infection ( <i>Pseudomonas syringe</i> Pv. <i>tomato</i> ).....	6
( <i>Colletotrichum higginsianum</i> ).....	7
Trypan-blue staining.....	7
DNA extraction.....	8
RNA extraction and northern analysis.....	8
Synthesis of probe and hybridization.....	9
Sequencing.....	9
Synthesis of cDNA.....	10
<i>In planta</i> G3P mobility assays.....	10
Phosphatase assay.....	10
Collection of phloem exudate, preparation of total protein extracts and proteinase K treatment.....	11
Confocal microscopy.....	11
Fatty acid profiling.....	12
Lipid profiling.....	12
Extraction and quantification of azelaic acid.....	13
Extraction and quantification of Salicylic acid and SAG.....	13
Extraction and quantification of Jasmonic acid.....	13

Glycerol, G3P and neutral sugar quantifications.....	14
Camalexin Quantifications.....	15
H <sub>2</sub> O <sub>2</sub> Quantification.....	15
CHAPTER 3: Glycerol-3-phosphate is a critical mobile inducer of systemic immunity in plants.....	
Introduction.....	20
Results .....	21
G3P synthesis is essential for SAR .....	21
Many G3Pdh isoforms contribute to SAR .....	22
GLY1 and GLI1 contribute to total G3P pool.....	23
Exogenous G3P restores defective SAR.....	24
G3P-conferred SAR is dependent on DIR1.....	26
DIR1 is required for the translocation of G3P.....	26
G3P conferred SAR is dependent on AZI1.....	27
CHAPTER 4: Determine role of glycerol metabolism in basal defense against hemibiotrophic fungal pathogen <i>Colletotrichum higginsianum</i>	
Introduction.....	61
Results .....	62
G3P levels correlate with infection response to <i>C. higginsianum</i> .....	62
A mutation in <i>G3Pdh<sub>chl</sub></i> and <i>G3Pdh<sub>cyt2</sub></i> confer enhanced susceptibility to <i>C. higginsianum</i> ..	64
The enhanced susceptibility of <i>g3pdh</i> mutants is not due to a defect in SA, camalexin or ROS pathways.....	65
CHAPTER 5: DISCUSSION.....	79
References.....	83
Appendix-A List of abbreviations.....	96
Vita.....	100

## LIST OF TABLES

Table 2.1. Plant materials used in the study.....	16
Table 2.2. List of primers used in the study.....	18



## LIST OF FIGURES

Figure 3.1. GLY1 and GLI1 are plastidal and cytosolic enzymes, respectively.....	29
Figure 3.2. Impaired SAR in <i>gly1</i> and <i>gli1</i> plants correlates with a defect in G3P metabolism but not fatty acid (FA) or lipid flux .....	32
Figure 3.3. Mutations in <i>G3Pdh</i> isoforms do not impair fatty acid or lipid profile .....	35
Figure 3.4. G3P levels increase in response to pathogen inoculation .....	37
Figure 3.5. Pathogen-induced increase in G3P precedes that of SA, AA and JA.....	39
Figure 3.6. G3P levels increase in response to pathogen inoculation .....	40
Figure 3.7. The <i>gly1</i> and <i>gli1</i> plants are not impaired in SA or MeSA pathways.....	42
Figure 3.8. The <i>gly1</i> and <i>gli1</i> plants are not impaired in JA pathways.....	43
Figure 3.9. The <i>gly1</i> and <i>gli1</i> plants are not impaired in AA pathways.....	44
Figure 3.10. Exogenous application of G3P improves SAR in Col-0 plants, and G3P- conferred SAR is dependent on SID2.....	46
Figure 3.11. Dose-response relationship for G3P .....	47
Figure 3.12. G3P does not alter SA levels.....	48
Figure 3.13. G3P does not alter JA levels .....	49
Figure 3.14. G3P does not alter AA or oleic acid (18:1) levels or show antimicrobial activity .....	51
Figure 3.15. Whole plant pretreatment with SA, but not local application, restores SAR in <i>gly1</i> and <i>gli1</i> plants .....	52
Figure 3.16. G3P-conferred SAR is dependent on DIR1.....	54
Figure 3.17. G3P and DIR1 are dependent on each other for translocation into distal tissues .....	56
Figure 3.18. Autoradiograph of extracts from infiltrated (I) and distal (D) leaves of plants infiltrated with <sup>14</sup> C-G3P + DIR1.....	58
Figure 3.19. Arabidopsis plants express phosphatase that converts G3P to glycerol .....	59
Figure 3.20. Arabidopsis mutants impaired in G3P biosynthesis are insensitive to AA...60	

Figure 4.1. Pathogen response, G3P and glycerol levels in <i>C. higginsianum</i> inoculated plants.....	67
Figure 4.2. <i>In planta</i> growth and pathogen response in <i>Colletotrichum higginsianum</i> -inoculated plants and G3P and neutral sugar levels.....	70
Figure 4.3. A mutation in <i>G3Pdh<sub>chl</sub></i> and <i>G3Pdh<sub>cyt2</sub></i> confer enhanced susceptibility to <i>C. higginsianum</i> . ....	73
Figure 4.4 Pathogen response in plants pretreated with G3P.....	75
Figure 4.5. The enhanced susceptibility of <i>g3pdh</i> mutants is not due to a defect in SA, camalexin or ROS pathways.....	78

# CHAPTER 1

## INTRODUCTION

Plants are constantly challenged by a wide range of microbial pathogens and pests. The microbial pathogens are broadly categorized as biotrophs or necrotrophs, depending on their growth pattern on the host. Biotrophic pathogens require living plant cells to grow and are thought to redirect the host metabolism for their survival (Pieterse et al., 2009). On the other hand, necrotrophs cause necrosis and death of the host tissues and feed on the dead cells. Hemibiotrophs, a third group of pathogens exhibit an early biotrophic phase which then transitions into necrotrophic mode of growth (Panstruga et al., 2003). During a compatible or susceptible interaction, biotrophic and hemibiotrophic pathogens are thought to facilitate their colonization by suppressing the host immune system (Pieterse et al., 2009). Plants in turn have evolved various mechanisms to restrict the pre or post-invasion growth of pathogens. The first line of defense involves recognition of pathogen-derived molecules also known as pathogen associated molecular patterns (PAMPs) by the host encoded pathogen recognition receptors (PRRs) (reviewer in Dangl and Jones 2001). The immunity resulting from such an interaction is known as the PAMP triggered immunity (PTI) or basal resistance. One of the well characterized examples of PTI include FLAGELLIN SENSITIVE 2 (FLS2)-mediated resistance against bacterial flagellin protein flg22 that is required for bacterial virulence and motility (Parker et al., 2009). FLS2 is a transmembrane receptor kinase containing an extracellular leucine rich repeat (LRR) domain, a transmembrane domain, and a cytoplasmic serine/threonine kinase domain. The plants lacking functional FLS2 show enhanced susceptibility to *Pseudomonas syringae* (Zipfel et al., 2004; Boller et al., 2009). Similarly, ELONGATION FACTOR Tu RECEPTOR (EFR) recognizes bacteria encoded elf18 peptide. Activation of the PRRs leads to series of signaling events resulting in the accumulation of reactive oxygen species (ROS), callose deposition, activation of MAP kinase signaling cascade and increased transcription of several defense related genes (Zipfel et al., 2004; Thilmony et al., 2006).

Some pathogens have evolved effectors that can suppress PTI. In turn plants have evolved to recognize such pathogens via their resistance (R) proteins, which directly or indirectly recognize pathogen encoded effector(s) (also termed avirulence factors, avr). This form of defense is known as effector triggered or R-mediated immunity (ETI), and is often associated with the development of a hypersensitive response (HR) at the site of pathogen entry. HR is associated with rapid cell death in the zone of pathogen invasion that leads to programmed cell death (PCD) (Greenberg, 1997). Cells undergoing PCD sends off signals to the other cells to activate defense responses. ETI also results in the activation of defense response including accumulation of reactive oxygen species (ROS), salicylic acid (SA), and pathogenesis-related (PR) proteins. The avirulence factors often promote pathogen virulence on hosts lacking the R protein. The Arabidopsis genome encodes ~150 R proteins and a majority of these contain a LRR domain at the C-terminal and a nucleotide-binding (NB) domain towards the N-terminal. The NB-LRR proteins are subcategorized based on the presence of a Toll/interleukin-1 receptor-like (TIR) or a coiled coil (CC) domain at their N-terminal end (Martin et. al., 2003). The indirect interaction between R-Avr is explained based on the “guard model”, according to which R is activated in response to the avr-mediated alteration of a host guardee protein. For example, R proteins RPM1 and RPS2 are activated in response to avr factor-mediated phosphorylation or cleavage of the host protein RIN4, respectively.

The local defenses triggered by ETI and often by PTI (Mishina and Zeier, 2007) elicit defense in the distal uninfected tissues leading to a long lasting broad-spectrum resistance against secondary infections. This phenomenon, known as systemic acquired resistance (SAR), involves translocation of a mobile signal(s) from the local to distal tissues. Several factors contributing to SAR have been uncovered and these include components of the SA pathway, methyl SA, and jasmonic acid (JA) and a lipid transfer protein (LTP) encoded by *DIR1* (*DEFECTIVE IN INDUCED RESISTANCE 1*). More recently, a nine-carbon dicarboxylic acid, azelaic acid (AA) was shown to induce SAR by priming SA biosynthesis. AA conferred SAR was dependent on *DIR1* as well as *AZELAIC ACID INSENSITIVE1* (*AZI1*) encoded LTP-like protein. Normal induction of SAR also requires the function of the *GLYCEROL DEPENDENT1* (*GLY1*) encoded GLYCEROL-3-

PHOSPHATE (G3P) DEHYDROGENASE, which catalyzes the conversion of dihydroxyacetone phosphate (DHAP) to G3P (Kachroo et. al., 2004). GLY1 or its allele SFD1 is also required for the normal biosynthesis of plastidal glycerolipids, which is initiated upon ACT1 catalyzed acylation of G3P with oleic acid (18:1) (Kachroo et. al., 2004). Besides GLY1, the Arabidopsis genome encodes four isoforms of G3Pdh and a glycerol kinase, which are likely to contribute to the total G3P pool.

## **Objectives**

Plant defense is associated with the interplay of different phytohormones such as salicylic acid (SA), ethylene and jasmonic acid (JA), this is associated with activation of defense genes such as the pathogenesis-related genes (PR) genes (Pieterse et. al., 2009). Apart from phytohormones many components of the primary metabolism are reported to take part in defense signaling either directly as a defense signal component or indirectly by recruiting energy for reprogramming of the metabolic pathways to boost up the immune system (Bolton, 2009; Rolland, 2002). Emerging evidence in our laboratory suggest that components of the primary metabolic pathways serve as key regulators of the host defense signaling. In this study. I investigated the role of G3P metabolism in disease physiology of plants. The objectives of my work were to:

- I) Determine the role of G3P in SAR
- II) Determine the role of G3P in basal defense against the hemibiotrophic fungal pathogen *Colletotrichum higginsianum*

## CHAPTER 2

### MATERIALS AND METHODS

#### Plant growth conditions and genetic analyses

Steam sterilized soil was used to sow the seeds listed in Table 2.1 were vernalized overnight at 4°C to synchronize their germination. The transplanted seedlings were covered with transparent plastic domes for 2-3 days. Plants were grown in MTPS 144 (Conviron, Winnipeg, MN, Canada) walk-in chambers at 22°C, 65% relative humidity and 14 h photoperiod. These chambers were equipped with cool white fluorescent bulbs (Sylvania, F096/841/XP /ECO). The photon flux density (PFD) of the day period was 106.9  $\mu\text{moles m}^{-2} \text{s}^{-1}$  (measured using a digital light meter, Phytotronic Inc, MO). Genotypes used in this study are listed in Table 2.1. Crosses were performed by pollinating emasculated flowers of recipient plants with pollen from donor plants. The *g3pdh* mutants were isolated by screening SALK lines obtained from Arabidopsis Biological Resource Center (Table 2.1). The mutant alleles were screened by PCR, cleaved amplified polymorphic sequence (CAPS) (Konieczny and Ausubel, 1993) or derived (d)-CAPS (Neff et al. 1998). The primers used for genotyping are listed in Table 2.2.

#### Bacterial transformation

Both electroporation and heat shock methods were used for *Escherichia coli* transformation. The *E. coli* competent cells were kindly provided by Ludmila Lapchyk. For heat shock method, ~50-100  $\mu\text{L}$  of the cells were mixed with ~50-100 ng of DNA and after a 30 min incubation on ice these cells were subjected to a heat shock at 42°C for 1.30 min followed by a 5 min incubation on ice. Approximately 1 mL of LB broth was mixed with the transformed cells followed by 30 min incubation at 37°C. Cells (100-200

μl aliquots) were plated on LB agar medium containing appropriate antibiotic.

For electroporation, *E. coli* (DH5α) or *Agrobacterium* (strains MP90 and LBA4404) cells were briefly incubated with ~50-100 ng of DNA, placed in a pre-chilled cuvette and electroporated using an electroporator (Genco BRL electroporator, Life technologies, NY, USA) set at 25 μF capacitance, 200 Ω resistance and 2 volts pulse. The electroporated cells were mixed with 1 mL of LB broth, incubated at 37°C (*E. coli*) or 29°C (*Agrobacterium*) for 30 min and plated on LB-agar medium containing appropriate antibiotic(s). The plates were incubated overnight at 37°C (*Escherichia coli*) or 29°C (*Agrobacterium*).

### **Arabidopsis transformation**

A single colony of *Agrobacterium tumefaciens* was cultured overnight in 5 mL of LB at 29°C and a 500 μL of the inoculum from this starter culture was reinoculated into 500 mL of LB and grown overnight at 29°C. Next day the bacterial suspension was centrifuged at 5,000 rpm for 10 min and the pellet was resuspended in the transformation solution containing 2.15 g Murashige and Skoog [MS] basal salt mixture, 30 g sucrose, 0.5 mL of Silwett L-77 in 1 L of distilled water, and the solution was adjusted to pH 5.7 with 1 M KOH. The plants were immersed in rectangular tissue culture boxes (1pot/box) containing the transformation solution, placed in the vacuum dessicator and vacuum infiltrated for ~ 4 min using bench vacuum ports. The transformed plants were gently rinsed under tap water, placed horizontally under a dome for 12-14 h, and subsequently transferred to plant growth chambers. The seeds from the transformed plants were collected after 4-6 weeks, surface-sterilized with 70% ethanol for 1 min, treated with 5% bleach for ~20-30 min in a rotary shaker and washed at least 3 times with sterile water before plating these on 0.5 x Murashige and Skoog media (MS) agar (0.8%) medium containing the appropriate antibiotic. For selection of transgenic plants expressing the *BAR* transgene, seeds were sown on soil that was sprayed with the glufosinate based herbicide, Finale, 5.6 mL/500 mL of water (Farnam Companies, AZ, USA).

## Plant treatments

Glycerol (50 mM; VWR or Invitrogen, CA, USA), G3P (100  $\mu$ M; Sigma-Aldrich, MO, USA), benzothiadiazole (BTH) (100  $\mu$ M; CIBA-GEIGY Ltd, NY, USA) was prepared in water and plants were either sprayed (glycerol, BTH) or injected (G3P) with these chemicals. JA (50  $\mu$ M; Sigma-Aldrich, MO, USA) and MeJA (10%; Sigma-Aldrich, MO, USA) were dissolved in ethanol and methanol, respectively. JA was diluted in water sprayed on the leaves until it run off. MeJA was used directly as a 10% solution. The JA and MeJA-treated plants were covered with a transparent plastic dome. Azelaic acid (1 mM; Sigma-Aldrich, MO, USA) was dissolved in 5 mM 2-[N-morpholino] ethane-sulfonic acid (MES; adjusted to pH 5.6) (Sigma-Aldrich, MO, USA). AA was either sprayed or injected into leaves. Paraquat (Sigma-Aldrich, MO, USA) was prepared in sterile water and 5  $\mu$ L droplets from 15 and 25  $\mu$ M solutions were spot inoculated on the leaves of 3-4 week old plants.

## Pathogen infections

*Pseudomonas syringae* Pv. *tomato*:

The liquid cultures of *Pseudomonas syringae* DC 3000 or *P. syringae* expressing *avrRpt2* were prepared by inoculating a single colony in 10 mL of King's B medium (20 g peptone, 10 mL glycerol, 1.5 g  $K_2HPO_4$ , 1.5 g  $MgSO_4$ , 15 g agar in 1 L of water, pH adjusted to 7.5 with 1N HCl medium containing kanamycin 50  $\mu$ g/ mL and rifampicin (25  $\mu$ g/ ml). After overnight incubation on a shaker the cells were centrifuged at 3,000 rpm for 5 minutes and the pellet was washed and suspended in 10 mM  $MgCl_2$ . The cell density was measured at  $A_{600}$  using a spectrophotometer (Biomate5, Thermo Electron Corporation Biomate, USA). For SAR, the primary leaves were inoculated with  $MgCl_2$  or the avr bacteria  $10^7$  colony-forming unit (CFU)/ml and 24 h later, the distal leaves were inoculated with virulent bacteria ( $10^5$  CFU/ml). Leaf disc (4 mm) samples from the distal leaves were harvested at 0 and 3 dpi using a cork borer. The leaf discs were homogenized in 10 mM  $MgCl_2$  and undiluted (0 dpi) or  $10^3$  fold diluted (3 dpi) homogenates were



plated on King's B agar medium. The plates were incubated at 29 °C for 2-3 days and the bacteria were counted using a colony counter (Scienceware, Bel-Art Product, USA).

### ***Colletotrichum higginsianum***

*Colletotrichum higginsianum* Sacc. (IMI 349063) was obtained from CABI Bioscience. The fungus was maintained on oatmeal agar (Difco, NJ, USA). Four-week-old Arabidopsis plants were used for both spray and spot inoculations. Spore suspensions at concentrations of 10<sup>6</sup> spores/mL were used for various experiments. For spot inoculations, 10 µL of spore suspension was used to inoculate Arabidopsis leaves. After inoculations, the plants were transferred to a PGV36 Conviron walk-in chamber and covered with a plastic dome to maintain high humidity. Disease symptoms were scored between 3 to 11 dpi. A digital Vernier caliper (Fischer scientific, PA, USA) was used to measure lesion size in spot-inoculated leaves. Each experiment included 30 to 50 plants and was repeated at least twice. Statistical significance was determined using a Student's *t*-test.

### **Trypan-blue staining**

Trypan blue stain was prepared to study the growth of the fungus in the leaves. It was prepared by mixing 10 mL acidic phenol, 10 mL glycerol, and 20 mL sterile water with 10 mg of trypan-blue (Sigma-Aldrich, MO, USA). The leaves were placed in the stain in a six-well microtiter plate and vacuum infiltrated using a dessicator until the leaves were thoroughly immersed in the stain. The plate was placed in a water bath set at 90°C for 2 min followed by 2-12 h incubation at room temperature. The stain was removed using a Pasteur pipette and the leaves were destained with chloral hydrate (Spectrum Chemicals, NJ, USA) prepared by dissolving 25 g of salt in 10 mL of sterile water. The leaves were mounted in 80% glycerol and observed under a compound microscope fitted with AxioCam camera (Zeiss, Germany). Images were analyzed using Openlab 3.5.2, Improvision software (Perkin Elmer, MA, USA).

## **DNA extraction**

3-4-week old Arabidopsis plants were used. The leaf samples were frozen in liquid nitrogen and homogenized using a disposable pestle (Fisher Scientific, PA, USA). The homogenized tissue was suspended in 120  $\mu$ L of DNA extraction buffer containing 200 mM Tris-HCl pH 8.0, 25 mM EDTA, 1% SDS and 250 mM NaCl. To this 80  $\mu$ L of phenol: chloroform: isoamyl alcohol (25:24:1) was added and the homogenate was centrifuged at room temperature for 10 min at 12,000 rpm. The supernatant was precipitated with 100  $\mu$ L of isopropanol and the samples were centrifuged for 10 min at 12,000 rpm. The DNA pellet was air dried and suspended in 50-75  $\mu$ L Tris:EDTA (10:1, pH 8.0) or sterile water.

## **RNA extraction and northern analysis**

For RNA extraction two-three leaves of Arabidopsis were frozen in liquid nitrogen and extracted with 1000  $\mu$ L Trizol reagent (Invitrogen, CA, USA). To this, 200  $\mu$ L of chloroform was added followed by mixing by inverting several times and centrifuged at room temperature for 15 minutes at 12,000 rpm. Isopropanol, 0.5 ml was used to precipitate the supernatant. The precipitate was washed with 75% ethanol, air-dried and suspended in 20  $\mu$ L of DEPC-treated water. Quantification of RNA was done spectrophotometrically ( $A_{260}$ ). ~ 7  $\mu$ g total RNA was mixed with 12-14  $\mu$ L of loading mixture (39  $\mu$ g/mL ethidium bromide, 0.39 X MOPS, 13.7% formaldehyde and 39% formamide and 2  $\mu$ L of loading dye (50% glycerol, 1mM EDTA, 0.4% bromophenol blue and 0.4% xylene cyanol). The RNA was separated by electrophoresis on a 1.5% agarose gel containing 3% formaldehyde and 1X MOPS (4.18 g MOPS, 680 mg NaOAc, 37 mg EDTA in 1 L sterile water, pH 7.0).

For northern analysis the RNA gel was washed with 2xSSC and blotted onto Hybond<sup>TM</sup>-NX (Amersham Biosciences, NJ, USA) nylon membrane. After overnight wet-transfer, RNA was fixed under UV for 0.9 min in a CL-1000 ultraviolet Cross-linker (UVP xx).

The membrane was washed in 2xSSC, dried at 65°C and used for hybridization. The membrane was hybridized in sodium phosphate buffer (200mM, pH 7.0) containing sheared salmon sperm DNA (100 µg/mL), 7% SDS and 1.25 mM EDTA.

### **Synthesis of probe and hybridization**

DNA fragments were labeled using DNA polymerase I Klenow fragment. DNA fragments used for labeling were PCR-or gel-purified (Qiagen, USA), denatured and mixed with 1 µL of Klenow enzyme (NEB, 2,000U/mL), 20 µM of hexanucleotide primers, dATP, dGTP, dTTP, BSA and 25 µCi  $\alpha$ -<sup>32</sup>P-dCTP (Perkin Elmer, USA). The reaction was incubated at 37°C for 1 h and the reaction probe was purified using a MicroSpin G-50 sephadex column (GE Healthcare, NJ, USA). The labeled DNA was denatured using one-tenth volume of 2N NaOH, neutralized with one-tenth volume of 1M Tris pH 7.5 and added to the hybridization buffer. Hybridization was routinely carried out overnight. The hybridized membrane was washed once at room temperature with 2xSSC, 0.5% SDS, twice at 65°C with 2xSSC, 0.5% SDS and once at 65°C with 1xSSC, 0.1%SDS solutions. The membrane was exposed using a Storage Phosphor Screen (Amersham Biosciences, CA, USA) and scanned on a Typhoon 9400 Variable Mode Imager (GE Healthcare, NJ, USA). The signal intensity was quantified using ImageQuant TL V2005 software.

### **Sequencing**

Sequencing reactions were carried out in 10 µL volume that contained ~50-100 ng of PCR- or gel-purified DNA (Qiagen, CA, USA), 1 µL of 5 µM primer and 0.5 µL of BigDye Terminator V3.1 (Applied Biosystems, CA, USA) with cycling conditions 96°C for 2 min, followed by 25 cycles of 96°C for 30 sec, 50°C for 5 sec and 60°C for 1 min and finally 4°C for 5 min and 15°C for 10 min. The reaction was precipitated with 0.6 volumes of isopropanol, washed with 70% alcohol and air-dried. The samples were submitted to the Advanced Genetic Technologies Center (AGTC) sequencing facility, University of Kentucky.

## **Synthesis of cDNA**

For cDNA synthesis, ~5-7 $\mu$ g of RNA was denatured at 65°C and annealed with oligo dT<sub>17</sub>. The reaction mixture was supplemented with 1  $\mu$ L reverse transcriptase (200U/ $\mu$ L), 1  $\mu$ L RNAase inhibitor (40U/ $\mu$ L), 0.5 mM dNTPs and 10 mM DTT and incubated at 42°C for 1 h. The reaction was stopped by incubating the tubes at 65°C for 15 min and subsequently used for RT-PCR.

## ***In planta* G3P mobility assays**

For *in planta* G3P mobility assays, leaves were infiltrated with 40  $\mu$ M of <sup>14</sup>C-G3P (American Radiolabel Co., USA) or co-infiltrated with 40  $\mu$ M <sup>14</sup>C-G3P and 20  $\mu$ g of DIR1-HIS (Kindly provided by Mihir Mandal). Infiltrated and distal leaves were sampled 6 h or 24 h after treatment, weighed and extracted in 300  $\mu$ L of water. The radioactivity was quantified using a liquid scintillation analyzer (1900-TR, Thermo Scientific). For thin-layer chromatography (TLC), samples were run on pre-coated cellulose plates (0.1 mm; EM Laboratories) using n-butanol: acetic acid: water (2:1:1 by vol) and autoradiographed using a Typhoon PhosphorImager.

Regions corresponding to bands I-IV on TLC plates were scraped and eluted using ~5 column (glass column 5 inches long) volumes of n-butanol:acetic acid:water (2:1:1 by vol). These fractions were concentrated under a stream of nitrogen gas, resuspended in minimal volume of deionized water and analyzed by HPLC, gas chromatography-mass spectrometry (GC-MS) (Hewlett Packard).

## **Phosphatase assay**

For phosphatase assays, 30  $\mu$ g of total protein, prepared in deionized water, was incubated with 20  $\mu$ M <sup>14</sup>C-G3P for 1 h at room temperature. The reaction was inhibited by boiling the protein extracts for 10 min before incubation with <sup>14</sup>C-G3P or by adding phosphatase inhibitors (50 mM sodium phosphate, 100  $\mu$ M sodium orthovanadate, 10 mM  $\beta$ -glycerophosphate and 10 mM sodium pyrophosphate). For thin-layer

chromatography (TLC), samples were run on pre-coated cellulose plates (0.1 mm; EM Laboratories) using n-butanol: acetic acid: water (2:1:1 by vol) and autoradiographed using Typhoon PhosphorImager.

### **Collection of phloem exudate, preparation of total protein extracts and proteinase K treatment.**

For collection of petiole exudates plants were induced for SAR by inoculation with *P. syringae* containing *avrRpt2* ( $10^7$  CFU/mL). Twelve hours later, petioles were excised, surface sterilized in 50% ethanol and 0.006% bleach, rinsed in sterile 1 mM EDTA and submerged in ~1.9 mL of 1 mM EDTA and 100 µg/mL ampicillin. Exudates were collected over 48 h and infiltrated into healthy plants. Infiltrated leaves were harvested after two days for *PR-1* gene expression studies. For SAR studies, virulent pathogen was inoculated in the distal leaves 12, 24 or 48 h after infiltration of MgCl<sub>2</sub>, exudates or avirulent pathogen. For protein extract, exudates collected from wild-type plants were precipitated with ammonium sulfate, dialyzed overnight, quantified and used for SAR. Proteinase K (60 µg/mL) treatment was carried out by incubating exudate or exudate protein fractions for 2 h at 37 °C.

### **Confocal microscopy**

For confocal imaging, samples were scanned on an Olympus FV1000 microscope (Olympus America, Melville, NY). GFP or RFP were excited using 488 and 543 nm laser lines, respectively. The various constructs were transformed to *A. tumefaciens* strain LBA4404. Agrobacterium strains carrying various proteins were infiltrated into *Nicotiana benthamiana* plants expressing RFP- or CFP-tagged nuclear protein H2B in wild-type *benthamiana* plants (Martin et al., 2009). After 48 h, water-mounted sections of leaf tissue were examined by confocal microscopy using a water immersion PLAPO60XWLSM 2 (NA 1.0) objective on a FV1000 point-scanning/point-detection laser scanning confocal 3 microscope (Olympus) equipped with lasers spanning the spectral range of 405–633 nm.

### **Fatty acid profiling**

Leaf tissue was placed in glass tubes containing 2 mL of 3% H<sub>2</sub>SO<sub>4</sub> in methanol containing 0.001% butylated hydroxytoluene (BHT). After 30 min incubation at 80°C, 1 mL of hexane with 0.001% BHT was added. The glass tubes were vortexed briefly and allowed to partition, the upper hexane phase was then transferred to vials for gas chromatography (GC). A Varian FAME 0.25 mm x 50 m column was used and peaks were detected using flame ionization detector and based on the retention time of the known FA standards (Standardized by John Johnson).

For quantitative FA estimation, leaves (~50 mg) were extracted together with the 17:0 as the internal standard and the relative levels were calculated based on flame ionization detector peak areas. Based on the retention time of the known FA standards the identity of the unknown peak was determined. Mole values were calculated by dividing peak area by molecular weight of the FA and the loss estimate was calculated based on the internal standard.

### **Lipid profiling**

For lipid extraction, six to eight leaves were incubated at 75°C in isopropanol containing 0.001% BHT for ~15 min. To this, 1.5 mL chloroform and 0.6 mL water was added and the samples were agitated at room temperature for 1h. The lipids were re-extracted in chloroform: methanol (2:1, v/v) until the leaves were bleached. The aqueous content was removed by partitioning with 1M KCl and water. The lipid extract was dried under a gentle stream of nitrogen gas and re-dissolved in 0.5 mL of chloroform. Lipid analysis and acyl group identification was carried out by the Automated Electrospray Ionization-tandem Mass Spectrometry facility at Kansas Lipidomics Research Center.

### **Extraction and quantification of azeliac acid**

For azeliac acid estimations from petiole exudates, samples were extracted using a solution containing glacial acetic acid, methanol, chloroform and potassium chloride (0.9%) (1:4:8:8, by vol) and 17:0 fatty acid as an internal standard. The lower phase was dried under compressed nitrogen, and samples were derivatized with N-methyl-N-(tert-butyl)dimethylsilyl trifluoroacetamide (MTBSTFA) containing 1% tert-butyl)dimethylchlorosilane (TBDMCS), suspended in acetonitrile and analyzed by a gas chromatograph on a Varian FAME 0.25 mm × 50 m column equipped with mass spectrometry. For azeliac acid estimations from leaves, fatty acid extraction described above was followed using 17:0 fatty acid as internal standard (10 µg/100 mg FW). Samples were concentrated to 10 µL using nitrogen gas and 1 µL samples were injected into the GC-MS. The azeliac acid peaks were identified using mass spectrometry.

### **Extraction and quantification of Salicylic acid and Salicylic acid glucoside (SAG)**

For SA and SAG extraction, ~300 mg of mock and pathogen inoculated leaves were collected. Sample analysis was done by using an Agilent 1100 (Agilent Technologies, Palo Alto, CA, USA), with a Novapak C18 column (Waters, Milford, MA, USA). Detection was done with diode-array and fluorescence-array detectors. Sample extraction and analysis was carried out by Dr. Duroy Navarre (USDA-ARS, Prosser, Washington).

### **Extraction and quantification of jasmonic acid**

For jasmonic acid estimations from petiole exudates, samples were extracted using a solution containing glacial acetic acid, methanol, chloroform and potassium chloride (0.9%) (1:4:8:8, by vol) and 17:0 fatty acid as an internal standard. The lower phase was dried under compressed nitrogen, and samples were derivatized using diazomethane and suspended in acetonitrile and analyzed by a gas chromatograph equipped with mass spectrometry. A Varian FAME 0.25 mm × 50 m column was used for this analysis.

## **Glycerol, G3P and neutral sugar quantifications**

Approximately 500 mg-1g of leaf tissue was extracted in 80% ethanol containing 2-deoxy-glucose as an as an internal standard. The leaf extract was then boiled for 5-6 minutes and centrifuged for 10 minutes at 8000 rpm. The supernatant was collected in another tube and freeze-dried and then resuspended in 1mL of water and filtered using a 0.45  $\mu\text{m}$  microcentrifuge filter (Spin-X centrifuge tube filter, Costar, 0.45  $\mu\text{m}$  nylon, 2mL tube, CN: 8170). Samples were diluted 2 times before loading onto an HPLC. High performance anion exchange chromatography (ICS 3000; Dionex Inc.) was used to quantify glycerol, G3P, and neutral sugar levels from plants as described (Downie, 1994). The samples were run on a MA1 (4 x 250 mm) column for glycerol, with pulsed electrochemical detection using 1M of NaOH and 200mM NaOH+500mM NaOAc for glycerol, and for G3P and neutral sugars, a PA1 column was used with pulsed electrochemical detection using 200mM of NaOH and 200 mM NaOH + 500mM NaOAc solvents.

The operating conditions for G3P were as follows: Eluent A: water; Eluent B: 200 mM NaOH; Eluent C: 200 mM NaOH; 500 mM NaOAc  
Flow rate: 1mL/min; Detector: ED40 Pulsed Electrochemical detection; The run is isocratic initial conditions of 0-12 min: %B=80; %C=20, a gradient from initial conditions at 12.1 min to %B=0; %C=100 at 22 min; and back to initial conditions from 22.1-32 min: %B=80; %C=20. For neutral sugars the operating conditions are isocratic elution from 0-40 min: %B=9.5; a gradient from initial conditions at 40.1 to: %B=50 at 50 min: a column wash at %C=100 from 50.1-60 min back to initial conditions from 60.1-70 min: %B=9.5. For glycerol the operating conditions are isocratic elution from 0-60 min: %B=48; column wash from 60.1-65 min: at %C=100: back to initial conditions from 65.1-75 min %B=48 at a flow rate over the MA1 column of 0.4 mL/min.



## **Camalexin Quantifications**

Camalexin was quantified as described previously (Zhou et al., 1998). In brief, 100 mg of leaf tissue was incubated in 4 mL of 80% methanol at 80°C for 20 min. The extract was concentrated to 1 mL followed by addition of 1 mL of chloroform. The samples were vortexed, centrifuged at high speed and the lower layer was collected in a new tube and dried under a gentle stream of nitrogen gas. The dried samples were redissolved in 50  $\mu$ L of chloroform and spotted on a silica gel, thin-layer chromatography (TLC) plate (Whatman; 60 A, 19 channel, 20 cm, 250 mm thickness). The chromatogram was developed using an ethyl acetate: hexane (100:15 by vol) solvent system and the camalexin was visualized as blue spots under UV light. The camalexin spots were removed from the TLC plate, extracted in methanol, and the fluorescence was measured using a fluorimeter (315- and 385-nm wavelengths). The concentration of camalexin was determined as mg/g fresh weight by extrapolating from the standard curve (Kindly provided by Qing-Ming Gao, Dept. Plant Pathology, University of Kentucky, Lexington).

## **H<sub>2</sub>O<sub>2</sub> Quantification**

For H<sub>2</sub>O<sub>2</sub> determination, leaves were homogenized in 40 mM Tris-HCl, pH 7.0, and to this 20 mM 2',7'-dichlorofluorescein was added. The samples were incubated for 1 h in the dark and the H<sub>2</sub>O<sub>2</sub> levels were measured using a spectrofluorimeter at 488 and 583 nm wavelengths. The concentration of H<sub>2</sub>O<sub>2</sub> was determined as mmol/mg protein by extrapolating from the standard H<sub>2</sub>O<sub>2</sub> curve.

**Table 2.1. Plant materials used in the study.**

SI No.	Mutants and transgenic seeds	References
1	Columbia-0 (Col-0)	Redei (1992)
2	Wassilewskija (Ws-0)	Aarts et al. (1998)
3	<i>act1</i> (Col-0)	Kunst et al., 1988; Kachroo et al. (2003)
4	<i>gly1-1</i> (Col-0)	Miquel (1998), Kachroo et al. (2004)
5	<i>gli1 (nho1)</i> (Col-0)	Kang et al. (2003), Kachroo et al. (2005)
6	<i>sid2-1</i> (Col-0)	Wildermuth et al. (2001)
7	<i>dir1-1</i> (Ws)	Maldonado et al. (2002)
8	<i>azi1-2</i> (Col-0)	Jung et al. (2009).
9	G3Pdh <sub>CYT1</sub> ; SALK_020444, At2g41540 (Col-0)	Chanda et al. (2011)
10	G3Pdh <sub>CYT2</sub> ; SALK_033040 At3g07690 (Col-0)	Chanda et al. (2011)
11	G3Pdh <sub>CHL</sub> ; SALK_062006 At5g40610 (Col-0)	Chanda et al. (2011)
12	G3Pdh <sub>MIT</sub> ; <i>sdp1-1</i> , At3g10370 (Col-0)	This dissertation, Eastmond (2006)
13	<i>gly1 gli1</i> (Col-0)	Chanda et al. (2011)
14	<i>act1 gly1</i> (Col-0)	Chanda et al. (2011)
15	<i>act1 gli1</i> (Col-0)	Chanda et al. (2011)
16	<i>g3pdh<sub>cyt1</sub> g3pdh<sub>cyt2</sub></i> (Col-0)	This dissertation
17	<i>g3pdh<sub>cyt</sub> gly1</i> (Col-0)	This dissertation
18	<i>g3pdh<sub>cyt1</sub> g3pdh<sub>chl</sub></i> (Col-0)	This dissertation

**Table 2.1. (Continued)**

SI No.	Mutants and transgenic seeds	References
19	<i>g3pdh<sub>cyt2</sub> g3pdh<sub>chl</sub></i> (Col-0)	This dissertation
20	<i>g3pdh<sub>cyt2</sub> gly1</i> (Col-0)	This dissertation
21	<i>gly1 g3pdh<sub>chl</sub></i> (Col-0)	This dissertation
22	35S- G3Pdh <sub>CYT1</sub> -GFP (Col-0)	This dissertation
23	35S- G3Pdh <sub>CYT2</sub> -GFP (Col-0)	This dissertation
24	35S- G3Pdh <sub>CHL</sub> -GFP (Col-0)	This dissertation
25	35S- G3Pdh <sub>MIT</sub> -GFP (Col-0)	This dissertation

**Table 2.2. List of primers used in this study.** The name, sequence and the purpose for which the primers were used are listed. The enzymes used for d-CAPS or CAPS markers are mentioned in parenthesis.

Name	Primer
<i>NPT</i> (Kan) (Genotyping)	CAA GAT GGA TTG CAC GCA GGT GCT CTT CAG CAA TAT CAC GGG
<i>HPT</i> (Hyg) (Genotyping)	ACC TAT TGC ATC TCC CGC CGT CCG GAT GCC TCC GCT CGA AGT
Lbb1 (Genotyping)	GCGTGGACCGCTTGCTGCAACT
<i>PDF1.2</i> (Probe)	AAT GAG CTC TCA TGG CTA AGT TTG CT AAT CCA TGG AAT ACA CAC GAT TTA GC
<i>gly1-1</i> dCAPS (BstN1) (Genotyping)	AAC CGA TGT TCT TGA GCG TAC TCG CCAG CAA CAA CCT AAA AAC CCC CAG ATT C
<i>sid2-1</i> CAPS (Mfe I) (Genotyping)	CTG TTG CAG TCC GAA AGA CGA CTA GAG CTG ATC TGA TCC CGA
<i>gli1</i> dCAPS (BStN I) (Genotyping)	CAG AGA GAG ACT ACT GTT GTT TGG A CTG CAG ATG GAG CTG GTA CGA GCA TC
<i>act1</i> CAPS (BsmF I) (Genotyping)	GCC ATC AAG TGT TCA TCT ACT GGA AGT CAT ACA AGG TTG CTA
SALK_020444      At2g41540 (Genotyping)	GAT GTG AAA CTA CCC CTT CCC CTG TGG AGC TGC TAA ATG GAG

**Table 2.2. (Continued)**

SALK_062006 At5g40610 (Genotyping)	ATT ACC CAT TTC CAA ACC GTC TTG AAA CTT TGG GCA AAG TTG
SALK_033040 At3g07690 (Genotyping)	TGC AGT GAA CGA GAA CAT GAG ACC TCC TCA ACA ATT CTT CCC
At2g41540 G3Pdh <sub>CYT1</sub> attB1 Fwd-Rev (overexpression)	AAA AAG CAG GCT TAA TGG TGG GAA GCA TTG AGG CA AGA AAG CTG GGT AAG GCT GAC CAA GAA GGG AAG G
At3g07690 G3Pdh <sub>CYT2</sub> attB1 Fwd-Rev (overexpression)	AAA AAG CAG GCT TAA TGA TGG ATC ATT TGG TGG AG AGA AAG CTG GGT AAG GTT TCT GAC CAA GAA GCC A
At5g40610 Chl attB1 Fwd-Rev (overexpression)	AAA AAG CAG GCT TAA TGC GCT TCC GAT CAT TCT TC AGA AAG CTG GGT ATA GTT TGT TCT CGC GGT ATT G
$\beta$ -Tubulin (RT)	CGT GGA TCA CAG CAA TAC AGA GCC CCT CCT GCA CTT CCA CTT CGT CTT
Actin (RT)	ACA CTG TGC CAA TCT ACG AGG GTT ACA ATT TCC CGC TCT GCT GTT GTG

## CHAPTER 3

### **Glycerol-3-phosphate is a critical mobile inducer of systemic immunity in plants**

**This work was published in Nature Genetics, 2011, *Nature Genetics*, 43: 421–427.**

#### **Introduction**

Systemic immunity is a form of defense that provides resistance against a wide range of pathogens in plants and animals alike (Durrant et al., 2004; Vlot et al., 2008; Iriti et al., 2007). In plants, inoculation with an avirulent (avr) pathogen often results in the generation of a mobile signal, which upon translocation to distal tissues activates broad-spectrum resistance not just at the site of infection but throughout the plant. This form of resistance is commonly called systemic acquired resistance (SAR). In cucumber (*Cucumis sativus*), the production of the mobile signal occurs within 3 h of inoculation with the avr pathogen in the local leaves (Smith et al., 1998) and the inoculated leaf must remain attached for at least 4 h after inoculation for SAR to be induced (Rasmussen et al., 1991). Although the identity of the mobile signal remains elusive, many factors contributing to SAR have been discovered. These include, DEFECTIVE IN INDUCED RESISTANCE1 (DIR1) (Maldonado et al., 2002), a protein that shows homology to the lipid transfer protein (LTP) family, salicylic acid (Vlot et al., 2009), methyl salicylic acid (MeSA) (Park et al., 2007), azelaic acid (Jung et al., 2009), auxin (Truman et al., 2010) and, possibly, jasmonic acid (Truman et al., 2007; Attaran et al., 2009). Recent studies have also shown that an intact cuticle is required for the mobile signal to initiate SAR (Xia et al., 2009; Xia et al., 2010). Notably, a defect in cuticle formation affects perception of the mobile signal in the distal tissues but not synthesis and/or translocation of this signal from the site of primary infection (Xia et al., 2009; Xia et al., 2010).

SAR is also dependent on the activity of the *GLYCEROL* DEPENDENT 1-encoded

(*GLY1*) encoding a GLYCEROL-3-PHOSPHATE (G3P) DEHYDROGENASE (G3Pdh) (Nandi et al., 2004). The *GLY1*-encoded G3Pdh reduces dihydroxyacetone phosphate to generate G3P, an obligatory component and precursor for the biosynthesis of all plant glycerolipids. Consequently, a mutation in *GLY1* results in reduced carbon flux through the plastidal pathway of lipid biosynthesis, which leads to a reduction in the hexadecatrienoic (16:3) fatty acids (Miquel et al., 1998; Kachroo et al., 2004; Nandi et al., 2004). G3P is also synthesized through the GLYCEROKINASE-catalyzed phosphorylation of glycerol. A mutation in *GLYCEROL INSENSITIVE1 (GLI1)* or *NHO1*-encoded GLYCEROKINASE compromises non-host resistance to pathogens (Lu et al., 2001; Kang et al., 2003) but does not affect 16:3 levels (Kachroo et al., 2005). This suggests that the G3P synthesized through G3Pdh- and glycerokinase-catalyzed reactions is used in different cellular processes and/or is present in different cellular compartments. Although both *gly1* and *gli1* are well known for their defective defense responses, a role for *gli1* in SAR has not been reported, and the defective SAR in *gly1* plants has been associated with a defect in the fatty acid–lipid biosynthesis pathway (Chaturvedi et al., 2009).

## RESULTS

### G3P synthesis is essential for SAR

A mutation in *GLY1*, but not in *GLI1*, reduces carbon flux through the plastidal fatty acid biosynthesis pathway (**Fig. 3.2A**). This is consistent with the plastidal and cytosolic localization of *GLY1* and *GLI1*, respectively (Chanda et al., 2011, **Fig. 3.1**). To determine if the impaired plastidal fatty acid–lipid pathway of plants with *gly1* mutations (*gly1* plants) was responsible for their defective SAR, it was tested in the *act1* mutant, which is defective in G3P ACYLTRANSFERASE activity (catalyzes the first committed step in plastidal lipid biosynthesis; **Fig. 3.1**) and is consequently severely compromised in the biosynthesis of total and major plastidal lipids as well as the total fatty acid pool (**Fig. 3.2A**). The *act1* plants were completely competent in inducing SAR (**Fig. 3.2 C**). Likewise, the *fad7* and *fad7 fad8* double mutants defective in the biosynthesis of trienoic

fatty acids were also able to induce SAR (Xia et al., 2010). These findings suggested that the defective SAR in *gly1* plants was a result of some factor(s) other than their impaired fatty acid–lipid pool. To determine if GLY1 catalyzed biosynthesis of G3P was essential for SAR, I analyzed SAR in the *gli1* mutant, which like the *gly1* mutant, is likely to accumulate reduced levels of G3P. The *gli1* plants were compromised in SAR (**Fig. 3.2C**). Moreover, *act1 gly1* and *act1 gli1* double mutants were also compromised in SAR, suggesting that the *gly1* and *gli1* mutations are epistatic to *act1* (**Fig. 3.2D**). As expected, *gly1 gli1* double mutant plants were also compromised in SAR. Together, these data suggested that G3P generated through both G3Pdh and GLYCEROKINASE was important for SAR.

### **Many G3Pdh isoforms contribute to SAR**

Besides GLY1, the *Arabidopsis* genome contains four other isoforms of G3Pdh, and three of these have been shown to encode proteins with G3Pdh activity (Wei et al., 2001; Shen et al., 2003; Shen et al., 2006; Quettier et al., 2006) (**Fig. 3.1**), suggesting that these too might contribute to the total G3P pool in the plant and, thereby, SAR. To test their roles in SAR, I isolated homozygous mutant plants containing T-DNA insertions within three of the *G3Pdh* isoforms (At2g41540, At3g07690 and At5g40610). RT-PCR analysis of the knockout plants confirmed absence of the full-length transcripts (**Fig. 3.3A**). All the *G3Pdh* knockout plants showed wild-type like fatty acid profiles (**Fig. 3.3B**). Normal levels of 16:3 in the *G3Pdh* knockout single or double mutant plants suggested that the three pertinent G3Pdh isozymes likely do not contribute to plastidal lipid biosynthesis (**Fig. 3.3C**). Consistent with this conclusion, both total and individual lipid profiles of three *G3Pdh* knockout lines tested were similar to those of wild-type plants (**Fig. 3.3D**, **Fig. 3.3E**). This indicated that these G3Pdh isozymes are likely not major contributors of G3P used in plastidal or extraplastidal lipid biosynthesis. However, two of the *G3Pdh* knockout lines (cytosolic-At3g07690 and chloroplastic-At5g40610) were, indeed, compromised in SAR (**Fig. 3.3F**). Together, these results suggested that the G3P required



for SAR is likely derived from the activities of at least one glycerokinase and three different G3Pdh enzymes; albeit not all of this G3P is used for lipid biosynthesis.

### **GLY1 and GLI1 contribute to total G3P pool**

I next assessed the role of G3P in SAR by analyzing G3P levels in inoculated and distal tissues of wild-type plants at 6 and 24 h post inoculation (hpi) with the avr pathogen. These time points correspond either to the time of transportation of the mobile signal to the distal tissues (~6 h) or initiation of SAR in the distal tissues (12–24 h; Chanda et al. 2011). G3P levels increased in both inoculated and distal tissues by 6 hpi, and distal tissues contained significantly higher levels of G3P compared to the inoculated leaves (**Fig. 3.4A**). G3P also accumulated in petiole exudates within 6 hpi and gradually declined by 48 hpi (**Fig. 3.4B**). The increase in G3P preceded detectable increases of salicylic acid, jasmonic acid or azelaic acid (**Fig. 3.5**). In comparison to wild-type plants, *gly1*, *gli1*, *At3g07690* knockout and *At5g40610* knockout plants showed much reduced accumulation of G3P (**Fig. 3.6**). Together, these data suggested that G3P levels increase during SAR in inoculated and distal tissues as well as in petiole exudates, and that the compromised SAR in *gly1*, *gli1*, *At3g07690* knockout and *At5g40610* knockout plants correlated with their reduced G3P accumulation. These data further suggest that GLI1, GLY1, G3Pdh-*At3g07690* and G3Pdh-*At5g40610* participate in SAR as well as in pathogen-induced G3P accumulation in a functionally non-redundant manner, and that pathogen-induced G3P is derived from the combined activities of at least three G3Pdh isoforms and glycerokinase. Notably, neither mutations in GLI1 nor the G3Pdh isoforms affected basal levels of G3P (**Fig. 3.4B** and **Fig. 3.6A**, **Fig. 3.6B**). This suggested that increased activities of the other isoforms and/or substrate turnover contributed to basal G3P. For instance, glycerol, which is the substrate for GLI1, can be converted to DHAP (Fillinger et al., 2001; Venugopal et al., 2009), which serves as a substrate for the G3Pdh-catalyzed reaction. Unlike G3P, the *gly1* and *gli1* plants accumulated normal levels of salicylic acid (**Fig. 3.7**), jasmonic acid (**Fig. 3.8**) and azelaic acid (**Fig. 3.9**). Moreover, high expression of *PR-1* gene was induced in both *gly1* and *gli1* plants in response to pathogen inoculation, salicylic acid or MeSA application (**Fig. 3.7D–3.7F**) and the

*PDF1.2* gene in response to jasmonic acid treatment (**Fig. 3.8A**), suggesting that they were not defective in salicylic acid or jasmonic acid responsiveness or conversion of inactive MeSA to active salicylic acid. Thus, apparently impaired SAR in the low G3P containing *gly1* or *gli1* mutants was not due to a defect in any of these pathways.

### **Exogenous G3P restores defective SAR**

Next, I directly tested if impaired SAR in *gly1* and *gli1* mutants could be rescued by application of G3P. Indeed, co-infiltration of G3P with the avr pathogen not only improved SAR in wild-type plants but also induced SAR in *gly1* and *gli1* plants, albeit to lower levels than in wild-type plants (**Fig. 3.10A**). Notably, G3P treatment alone also had a nominal effect on SAR (**Fig. 3.10A**), and this SAR-inducing capacity of G3P increased significantly ( $P < 0.001$ ) when G3P was mixed together with petiole exudates collected from plants infiltrated with  $MgCl_2$  (referred to as  $EX_{MgCl_2}$ ) or the avr (*avrRpt2*) pathogen (referred to as  $EX_{AVR}$ ) (**Fig. 3.10B**). It was also found that  $EX_{AVR}$  from *gly1* or *gli1* plants was unable to confer SAR in these plants. However,  $EX_{AVR}$  from wild-type plants was able to confer normal SAR in both *gly1* and *gli1* plants (Chanda et al., 2011). Notably, G3P with  $EX_{MgCl_2}$  or  $EX_{AVR}$  from wild-type, *gly1* and *gli1* plants was fully competent in inducing SAR on *gly1* and *gli1* plants (Chanda et al., 2011). Together, these data confirmed that impaired SAR in *gly1* and *gli1* plants was associated with their inability to accumulate G3P and that this defect could be complemented by providing G3P exogenously. These data further suggested that G3P-induced SAR requires a component present in petiole exudates of healthy plants. The SAR response in wild-type plants infiltrated with  $EX_{MgCl_2} + G3P$  was comparable to the SAR seen in plants inoculated with  $EX_{AVR}$  (**Fig. 3.10B**). To determine the time frame of G3P efficacy, I assessed SAR at different times after treatment with G3P. The wild-type plants were first infiltrated with  $MgCl_2$ ,  $MgCl_2 + G3P$ ,  $EX_{MgCl_2}$  or  $EX_{MgCl_2} + G3P$ . The distal leaves of these plants were inoculated with the vir pathogen at 6, 12, 24 or 48 h after infiltration and bacterial growth was monitored at 0 and 3 dpi. In contrast to  $MgCl_2$ ,  $MgCl_2 + G3P$  or  $EX_{MgCl_2}$ , treatment with  $EX_{MgCl_2} + G3P$  induced strong SAR, which was most effective when the vir pathogen was inoculated 6–12 h post infiltration (**Fig. 3.10C**). These data suggest that the

effectiveness of G3P-conferred SAR correlates with the time frame within which the mobile signal is presumably transported to the distal tissues (Rasmussen et al., 1991; Smith et al., 1998; Chanda et al., 2011). These data further suggested that an exudate-derived host factor is required for G3P-triggered SAR. Analysis of the dose-response relationship showed that physiologically relevant concentrations of G3P (50–100  $\mu\text{M}$ ) were sufficient to induce durable SAR (**Fig. 3.11**).

G3P-conferred SAR was not associated with the induction of salicylic acid, jasmonic acid, or azelaic acid pathways (**Figs. 3.12, 3.13, 3.14**), nor did G3P have any antimicrobial activity at physiologically relevant conditions (**Fig. 3.14D**). Levels of 18:1 (oleic acid) were also not associated with G3P-conferred SAR (**Fig. 3.14C**). A mutation in *gli1* did not affect 18:1 levels (**Fig. 3.2A**), which is consistent with the fact that 18:1 levels are regulated by plastidal G3P (Kachroo et al., 2004). Exogenous G3P also conferred SAR in *act1* plants, which are unable to acylate G3P with 18:1 (**Fig. 3.14E**), thus arguing again a role for 18:1 in G3P-conferred SAR.

Basal levels of *PR-1*, a marker gene induced by increased salicylic acid, in  $\text{EX}_{\text{MgCl}_2} + \text{G3P}$ -treated plants is consistent with the fact that salicylic acid levels did not increase in the exudates, local or distal tissues of G3P-treated plants (**Fig. 3.12A-C**). To test if salicylic acid was required for G3P-conferred SAR, I assayed SAR in *salicylic acid insensitive2* (*sid2*) plants, which are defective in isochorismate-derived salicylic acid biosynthesis (Wildermuth et al., 2001). The  $\text{EX}_{\text{AVR}}$  and  $\text{EX}_{\text{MgCl}_2} + \text{G3P}$  prepared from wild-type leaves were capable of inducing SAR in wild-type but not in *sid2* plants (**Fig. 3.10B**), suggesting that G3P-conferred SAR was dependent on salicylic acid. The fact that G3P application did not increase salicylic acid, and that *sid2* plants contain lower than wild-type levels of salicylic acid (Chanda et al., 2011), suggests that basal salicylic acid levels are both essential and sufficient for G3P-associated SAR. Pretreatment of local leaves with salicylic acid or its active analog benzo (1,2,3) thiadiazole-7-carbothioic acid (BTH) was unable to confer SAR in *gly1* and *gli1* plants (**Fig. 3.15A**), further confirming that both G3P and salicylic acid are required for normal SAR. In comparison

to local treatments, pretreatment of whole plants with salicylic acid significantly ( $P < 0.001$ ) improved SAR in *gly1* and *gli1* plants (**Fig. 3.15B**).

### **G3P-associated SAR is dependent on DIR1**

To determine if the exudate-derived factor required for G3P-mediated SAR was a protein, I tested the SAR-inducing activity of total protein extracts from the petiole exudates of the wild type plants in the presence or absence of G3P. The exudate protein fraction by itself was unable to induce SAR in wild-type plants but induced SAR when applied with G3P (**Fig. 3.16A**). Furthermore, proteinase K treatment of petiole exudates abolished its ability to confer SAR, strongly suggesting that G3P-associated SAR is dependent on one or more proteins present in the petiole exudates.

DIR1 is one of the proteinaceous components known to be required for SAR and is also postulated to function as a lipid transfer protein (Maldonado, 2002). It was found that co-infiltration of G3P with the avr pathogen did not improve SAR in *dir1* plants (Chanda et al., 2011). Thus, G3P-associated SAR was dependent on DIR1. To characterize the role of DIR1, the *Escherichia coli* expressed and purified DIR1-HIS (kindly provided by Dr. Mihir Mandal). Notably, infiltration of DIR1 also conferred SAR in wild-type plants (**Fig. 3.16B**), suggesting that excess DIR1 triggered SAR in the absence of a primary pathogen. Infiltration of DIR1 with G3P conferred significantly ( $P < 0.001$ ) enhanced SAR in comparison to G3P or DIR1 alone (**Fig. 3.16B**). Importantly, when supplied with DIR1, G3P was able to induce SAR in the absence of petiole exudates, supporting the notion that DIR1 was the proteinaceous component in the exudates essential for G3P-induced SAR.

### **DIR1 is required for translocation of G3P**

I next investigated if G3P-induced SAR was associated with the translocation of G3P from inoculated to distal tissues. Infiltration of  $^{14}\text{C}$ -G3P alone into wt leaves did not result in translocation of the radiolabel into distal tissues, but co-infiltration with DIR1-

HIS resulted in increased translocation of the radiolabel to the distal leaves (**Fig. 3.17A**, **Fig. 3.17B**). Together, these results suggest that DIR1 aids the systemic movement of G3P.

Consistent with this conclusion, the avr-inoculated *dir1* plants showed significantly ( $P < 0.001$ ) reduced levels of G3P in their petiole exudates (**Fig. 3.17C**), and infiltration of DIR1 was unable to induce normal SAR in *gly1 gli1* double mutant plants (**Fig. 3.17D**). Chromatographic analysis of the leaf extracts prepared from  $^{14}\text{C}$ -G3P-infiltrated leaves showed little or no G3P, indicating it was metabolized. The  $^{14}\text{C}$  label migrated as four bands (**Fig. 3.17E**, designated I–IV), whether the  $^{14}\text{C}$ -G3P was infiltrated by itself or along with DIR1, in wild-type or *dir1* plants (**Fig. 3.17E**). This suggested that G3P was modified in the infiltrated tissues and that this modification was not dependent on DIR1. As before (**Fig. 3.17A**, **Fig. 3.17B**), radiolabel was detected only in distal leaves of plants infiltrated with G3P + DIR1 (**Fig. 3.17E**). However, unlike in local leaves, the majority of the radiolabel in the distal leaves was in the form of band IV, whereas bands I–III were present only in trace amounts. Bands I–III could be visualized when excess sample was loaded (**Fig. 3.17E** and **Fig. 3.18**). Band IV migrated the same distance as a minor band in the commercial  $^{14}\text{C}$ -G3P control and was likely the result of spontaneous hydrolysis of the phosphate group. Thus, it is possible that G3P was converted to glycerol in both local as well as distal tissues, and that glycerol was likely translocated into distal tissues in a DIR1-dependent manner. A second possibility is that detection of glycerol was the result of phosphatase released upon disruption of the cells during extraction. Indeed, leaf extracts from wild-type or various mutant plants were able to convert  $^{14}\text{C}$ -G3P into glycerol, and this activity could be inhibited by boiling or by the addition of phosphatase inhibitors (**Fig. 3.19A**). Unlike leaf extracts, petiole exudates did not have any detectable phosphatase activity (**Fig. 3.19B**). Addition of phosphate inhibitors before extraction of leaf samples resulted in the detection primarily of band II in the distal tissues of  $^{14}\text{C}$ -G3P + DIR1-treated plants (**Fig. 3.17E**, last lane). These data strongly support the possibility that the glycerol detected in the distal tissues was the result of phosphatase activity released during extraction. To further validate these observations, I assayed SAR in glycerol-treated *gli1* plants, which are unable to metabolize glycerol to G3P. Unlike G3P,

glycerol was unable to induce SAR in *gli1* plants (**Fig. 3.17F**), thus ruling out a role for glycerol in inducing SAR.

### **G3P associated SAR is dependent on AZI1**

Previously it was shown that plants mutated in the *AZI1* encoded lipid transfer protein showed a *dir1*-like phenotype (Jung et al., 2009). To determine if AZI1 was required for G3P- associated SAR I evaluated G3P associated SAR in *azi1* plants. Exogenous G3P was unable to confer normal SAR on *azi1* plants in the presence or absence of primary pathogen even though these treatments induced SAR in wild-type plants (**Fig. 3.20A**). This suggested that G3P associated SAR was also dependent on AZI1. Since localized application of AA is sufficient to confer SAR in distal tissues of wild-type plants (**Fig. 3.20A**), I next evaluated AA-mediated SAR in *gly1* and *gli1* mutant plants. AA was applied to the local leaves and growth of virulent bacteria was monitored in distal tissues at 3 days post inoculation (dpi). AA was unable to induce SAR in G3P biosynthesis mutants (**Fig. 3.20B**), suggesting that AA- associated SAR was dependent on G3P and that AA-and G3P- associated pathways overlapped.

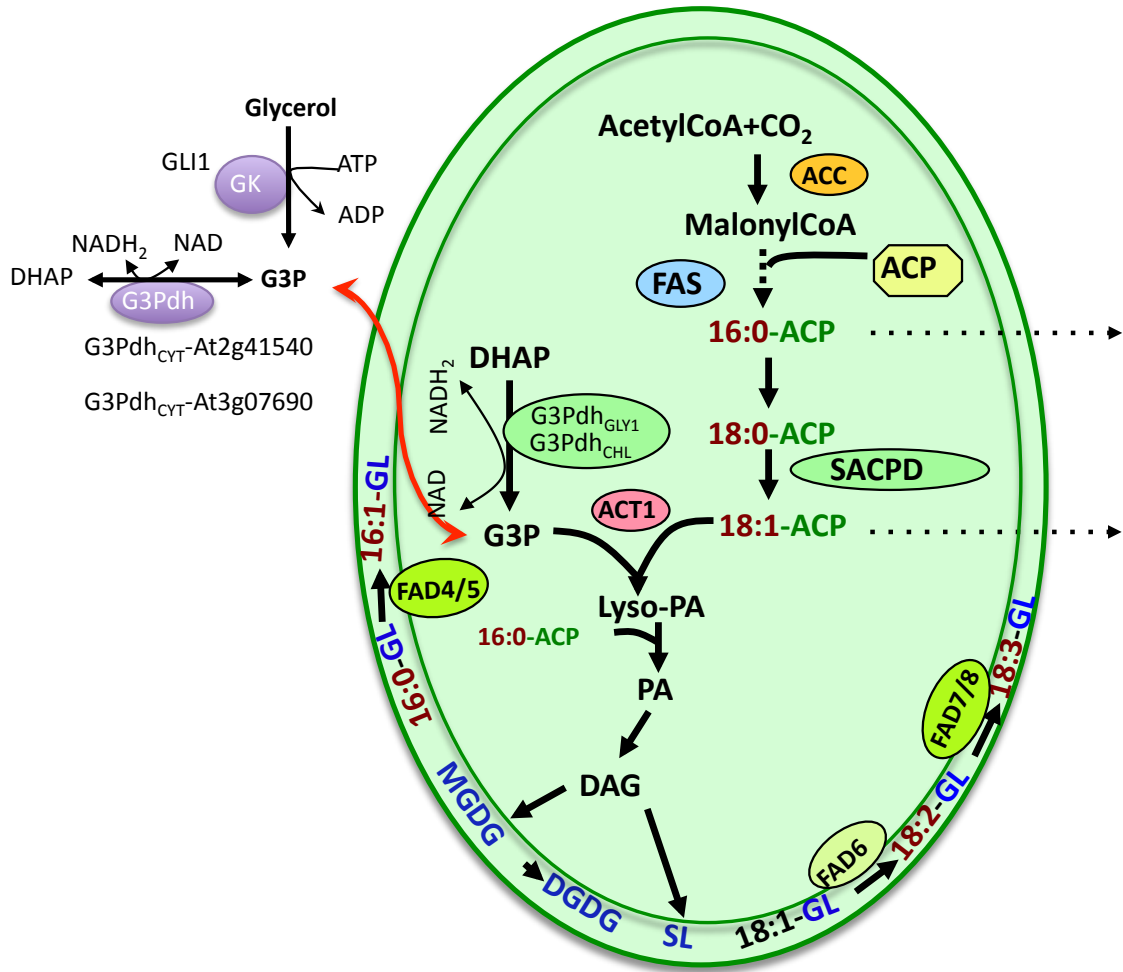
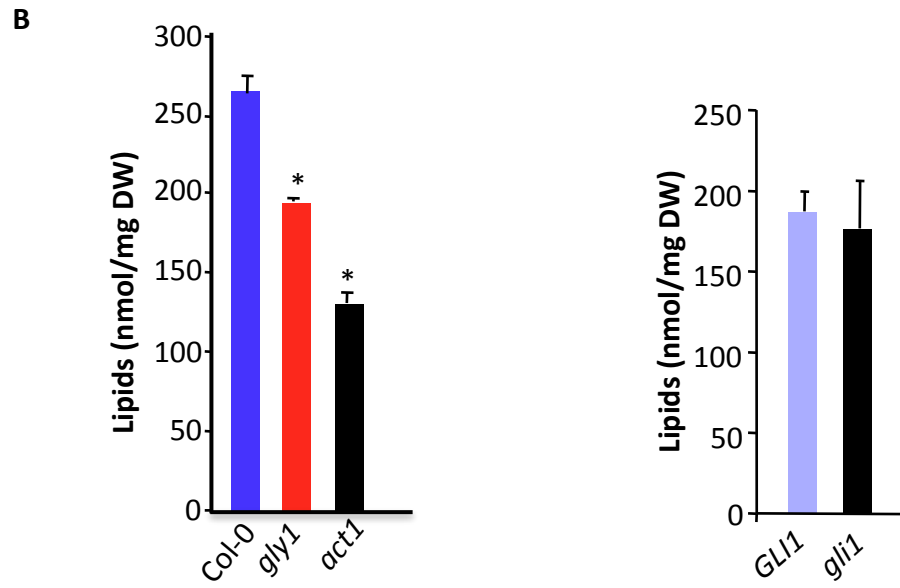
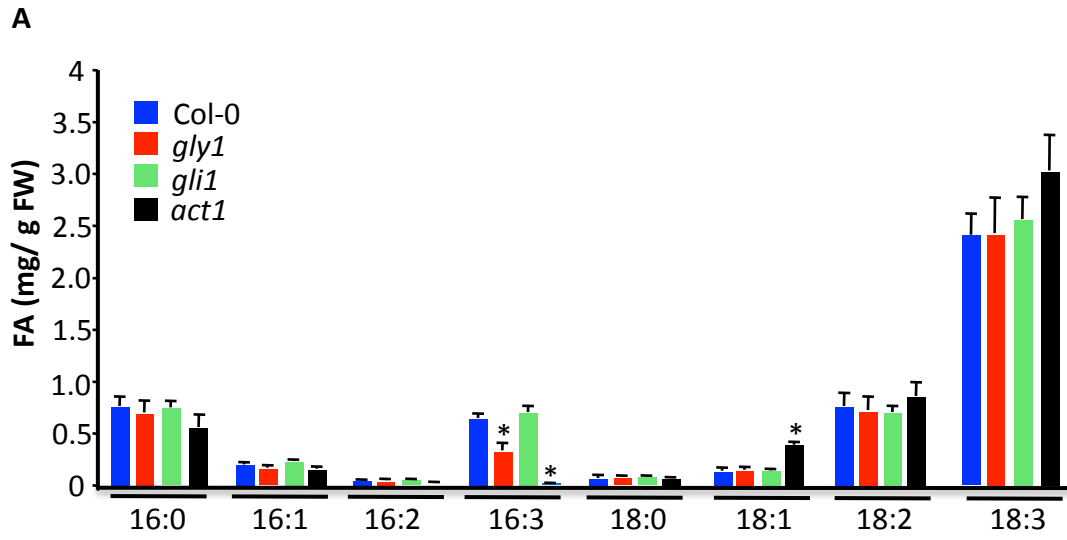
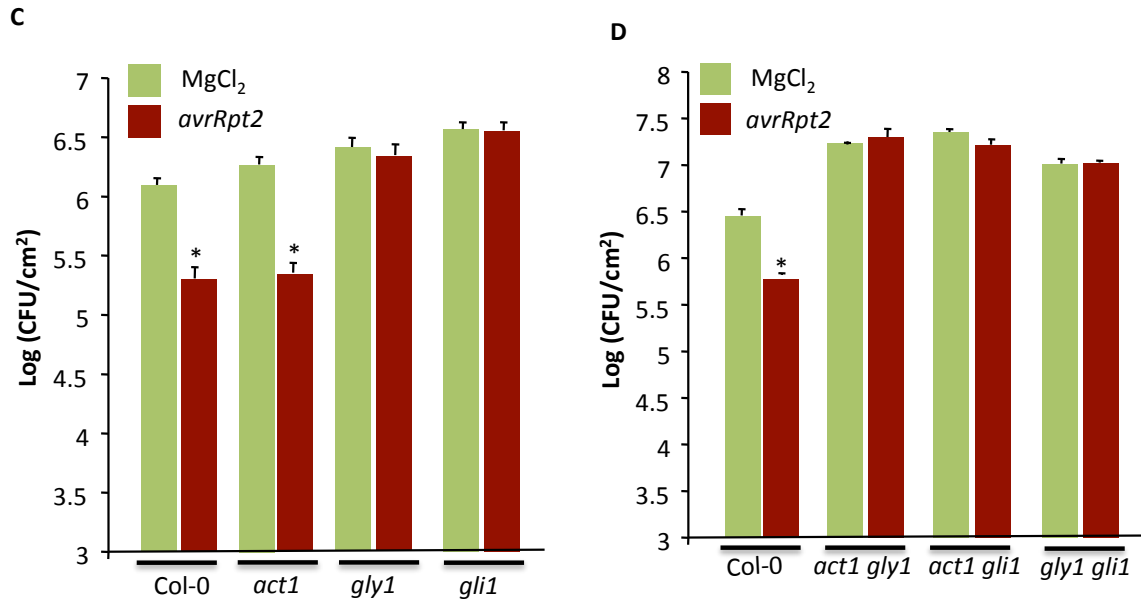


Figure. 3.1. GLY1 and GLI1 are plastidal and cytosolic enzymes, respectively.

**Figure. 3.1. (Continued)** A condensed scheme of glycerol metabolism in plants. Glycerol is phosphorylated to glycerol-3-phosphate (G3P) by GLYCEROL KINASE (GK; GLI1). G3P can also be generated by G3P DEHYDROGENASE (G3Pdh) via the reduction of dihydroxyacetone phosphate (DHAP) in both the cytosol and the plastids (represented by the two largest ovals). G3P generated by this reaction can be transported between the cytosol and plastidal stroma. In the plastids, G3P is acylated with oleic acid (18:1) by the ACT1-encoded G3P ACYLTRANSFERASE. This ACT1-utilizes 18:1 is derived from the STEAROYL-ACYL CARRIER PROTEIN (ACP)-DESATURASE (SACPD)-catalyzed desaturation of stearic acid (18:0). The 18:1-ACP generated by SACPD either enters the prokaryotic lipid biosynthetic pathway through acylation of G3P or is exported out (dotted line) of the plastids as a coenzyme A (CoA)-thioester to enter the eukaryotic lipid biosynthetic pathway. Other abbreviations used are: Lyso-PA, acyl-G3P; PA, phosphatidic acid; PG, phosphatidylglycerol; MGDG, monogalactosyldiacylglycerol; DGDG, digalactosyldiacylglycerol; SL, sulfolipid; DAG, diacylglycerol.

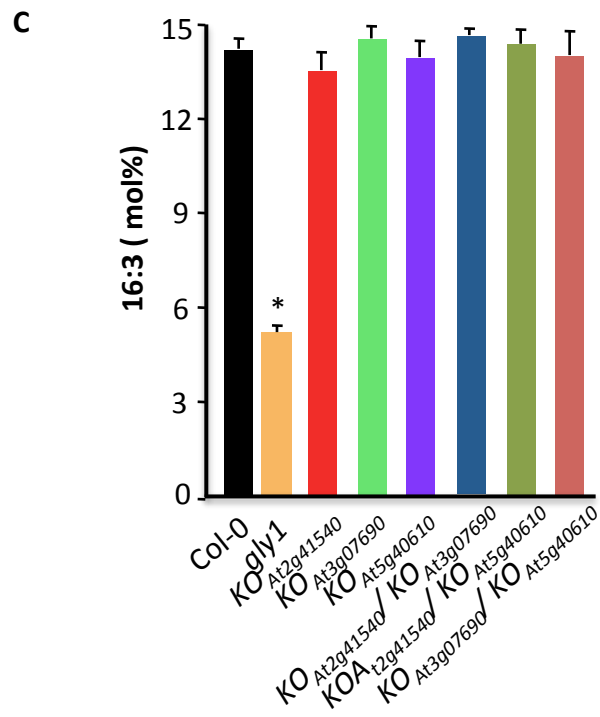
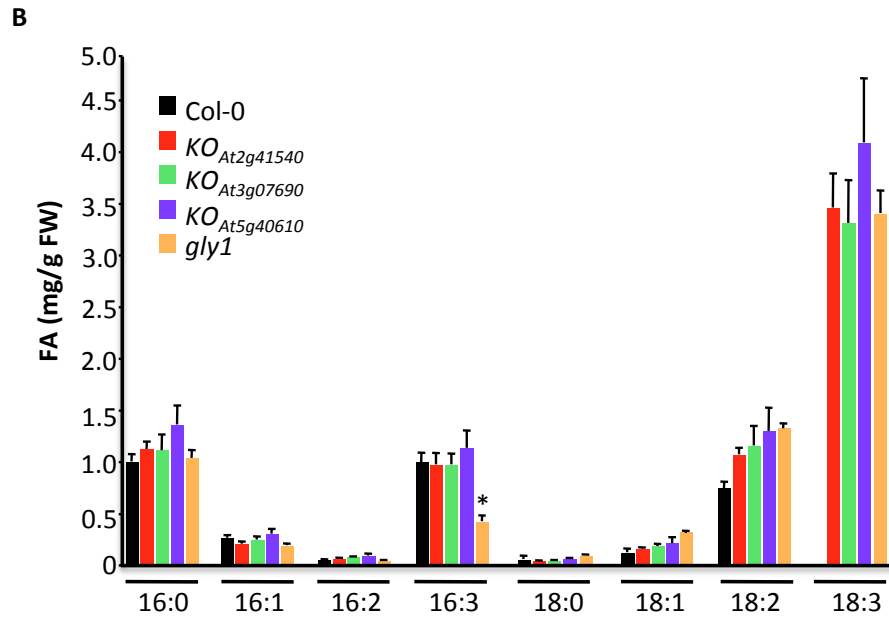
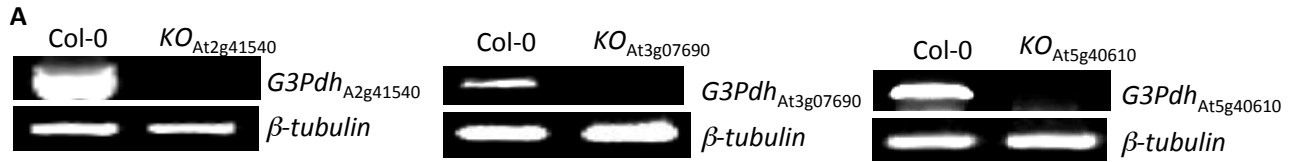


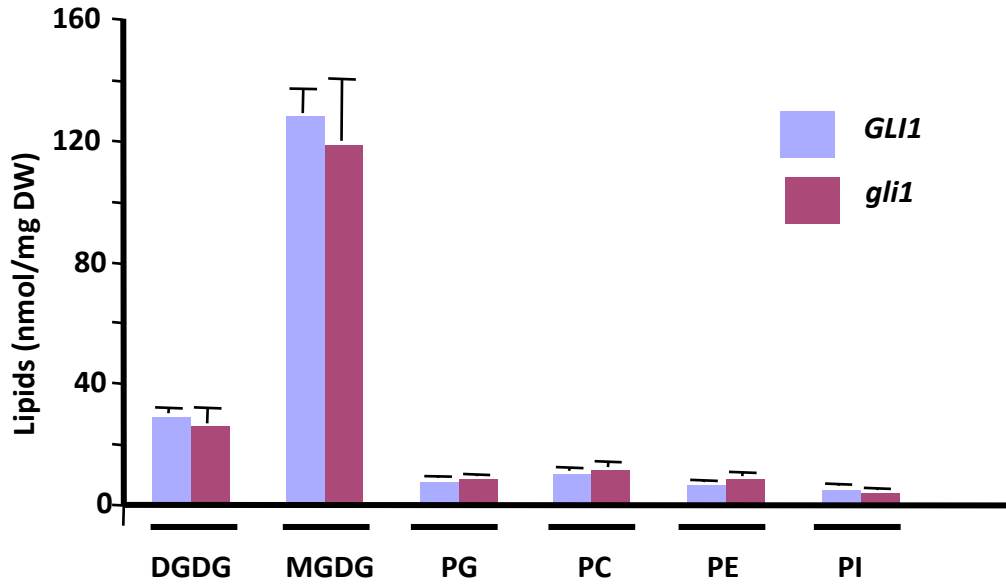
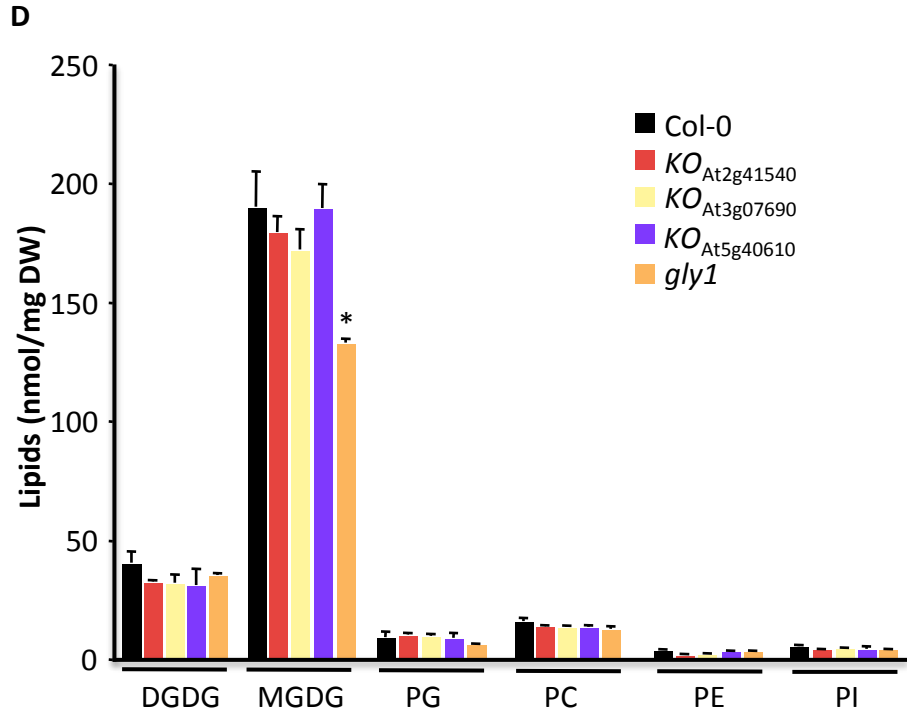




**Figure 3.2. Impaired SAR in *gly1* and *gli1* plants correlates with a defect in G3P metabolism but not fatty acid (FA) or lipid flux.**

(A) Relative levels of fatty acids in 4-week-old Col-0, *gly1*, *gli1* or *act1* leaves. The values are presented as means of six to eight replicates. Asterisks denote a significant difference with wild type (*t*-test,  $P < 0.05$ ). FW indicates fresh weight. (B) Total lipid levels in indicated genotypes. DW indicates dry weight. Asterisks denote a significant difference with wild type (*t*-test,  $P < 0.05$ ). (C) SAR in Col-0, *gly1*, *gli1* or *act1* plants. I inoculated primary leaves with MgCl<sub>2</sub> or *Pseudomonas syringae* expressing *avrRpt2* (black bars) and the distal leaves 48 h later with a virulent strain of *P. syringae*. (D) SAR in Col-0, *act1 gly1*, *act1 gli1* or *gly1 gli1* plants. Asterisks denote a significant difference with respective MgCl<sub>2</sub> treatment. (*t*-test,  $P < 0.0003$ ). The error bars in A-D represent standard deviation (SD).





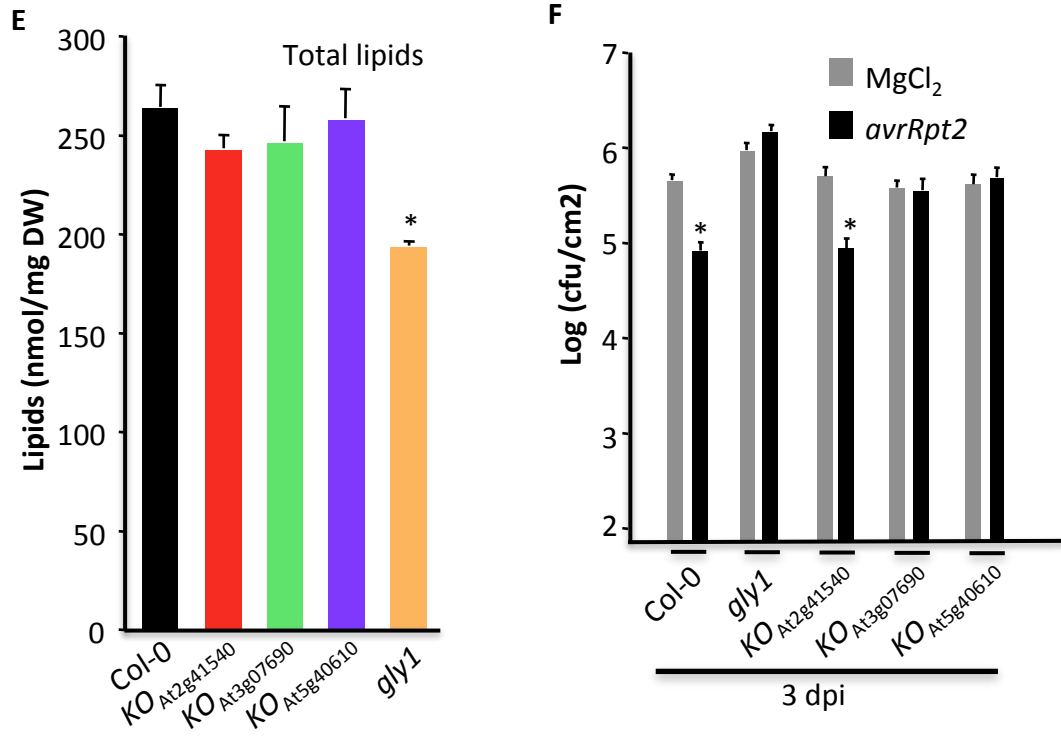
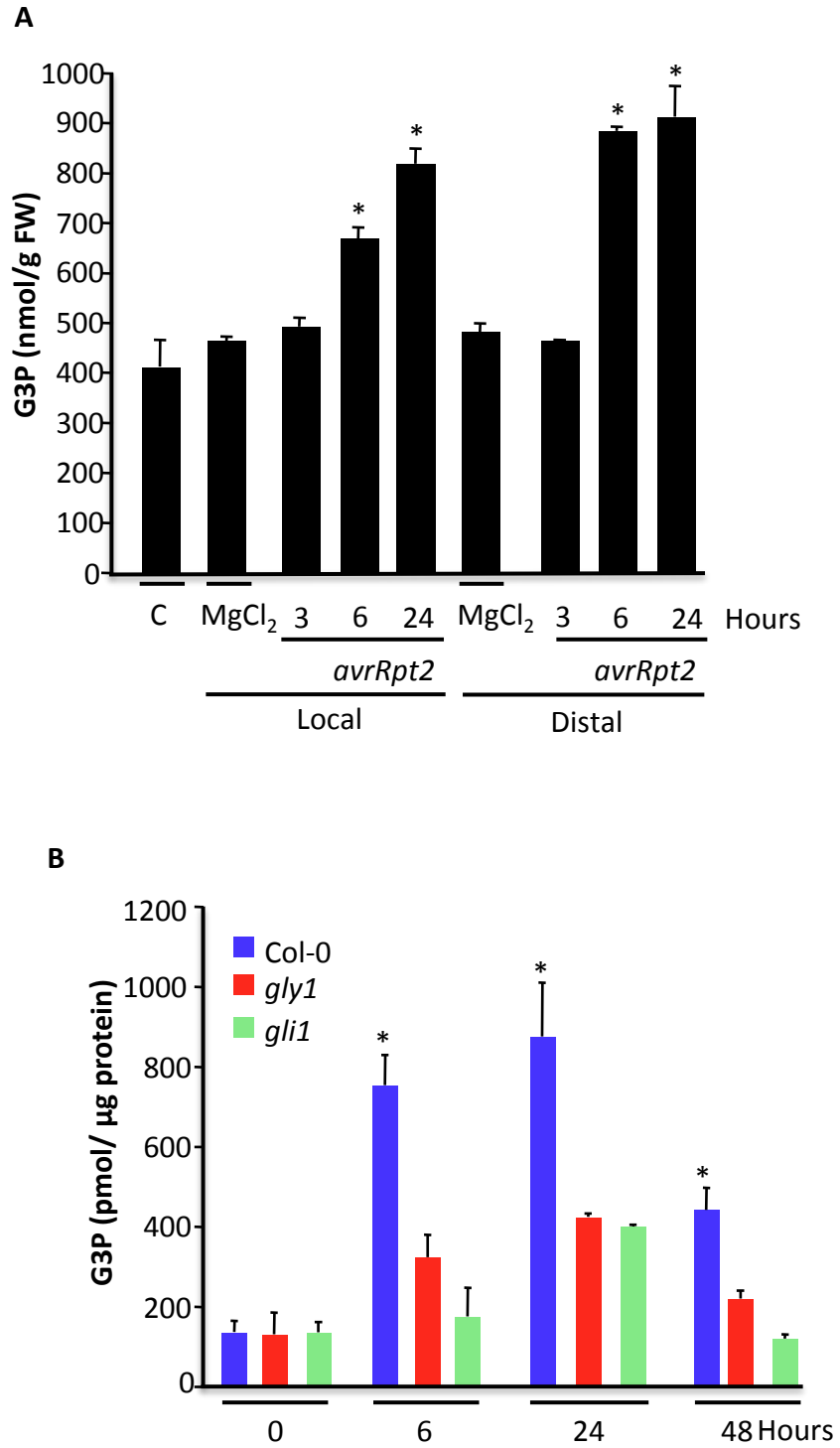


Figure 3.3. Mutations in *G3Pdh* isoforms do not impair fatty acid or lipid profile.

**Figure 3.3. (Continued)**

(A) RT-PCR analysis showing expression levels of indicated *G3Pdh* isoforms in wt and the respective knockout (KO) lines. The level of  $\beta$ -tubulin was used as an internal control to normalize the amount of cDNA template. (B) Levels of FAs in 4-week-old wt (Col-0) and *G3Pdh* KO plants. Asterisk denotes significant difference with wt (*t* test,  $P < 0.05$ ). FW indicates fresh weight. (C) Levels of 16:3 FA in indicated genotypes. Asterisk denotes significant difference with wt (*t* test,  $P < 0.05$ ). (D) Profile of total lipids extracted from wt (Col-0) and *G3Pdh* KO plants. The values are presented as a mean of 5 replicates. Symbols for various components are: DGD, digalactosyldiacylglycerol; MGD, monogalactosyldiacylglycerol; PG, phosphatidylglycerol; PC, phosphatidylcholine; PE, phosphatidylethanolamine; PI, phosphatidylinositol. (E) Total lipid levels in indicated genotypes. DW indicates dry weight. Asterisk denotes significant difference with wt (*t* test,  $P < 0.05$ ). The error bars in d-g represent SD. (F) SAR in Col-0, *g3Pdh* knockout (KO) lines. I inoculated primary leaves with  $MgCl_2$  and Avr pathogen expressing *avrRpt2* and the distal leaves with a virulent strain of *P. syringae*. Asterisks denote a significant difference with respective  $MgCl_2$  treatment. (*t*-test,  $P < 0.001$ )

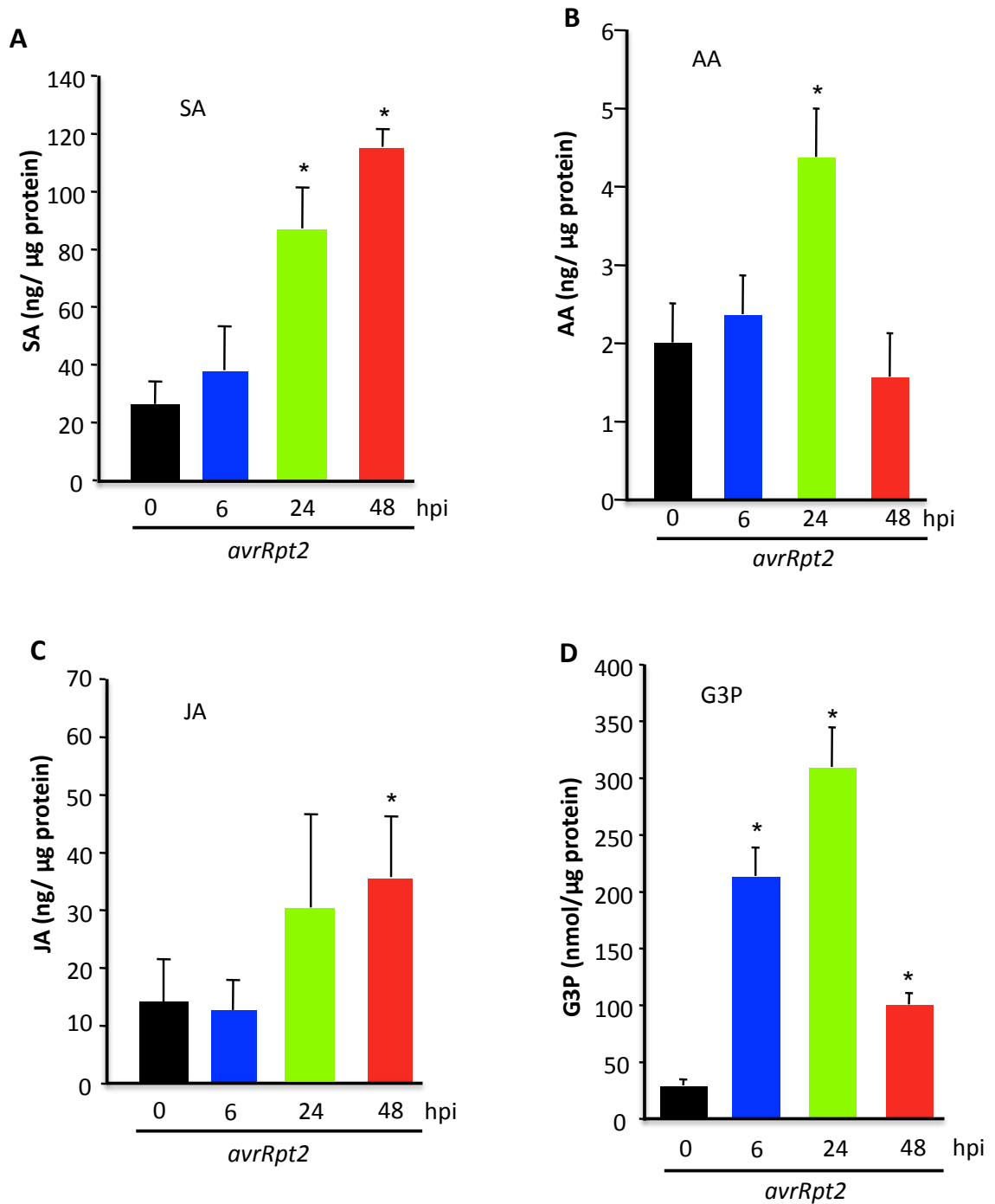


**Figure 3.4 G3P levels increase in response to pathogen inoculation**

**Figure 3.4 (Continued)**

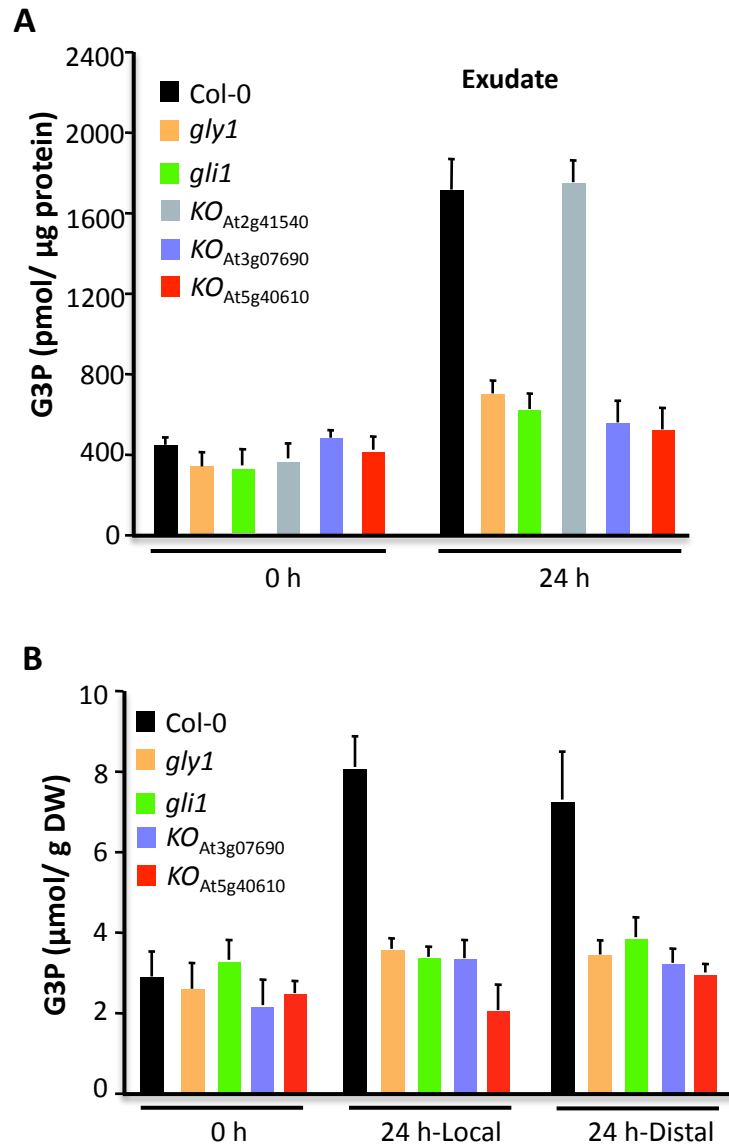
(A) G3P levels in local or distal leaves of Col-0 (wild-type) plants. (B) G3P levels in petiole exudates of Col-0, *gly1* and *gli1* plants at 0, 6, 24 and 48 h post inoculation with the avr pathogen (avrRpt2). Asterisks in b and c denote significant differences (*t*-test,  $P < 0.05$ ). The error bars represent (SD).





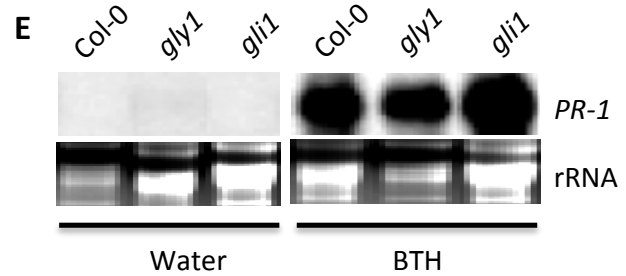
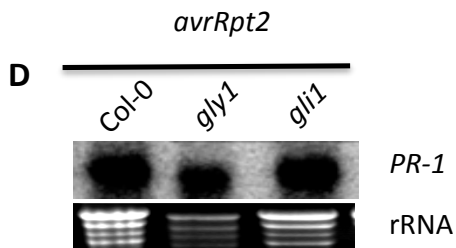
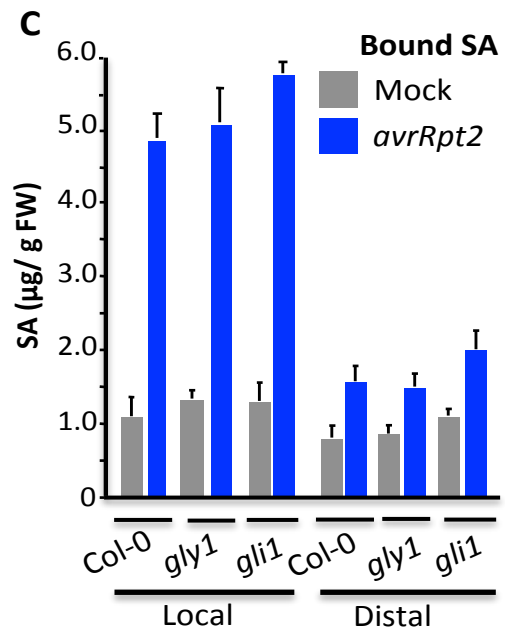
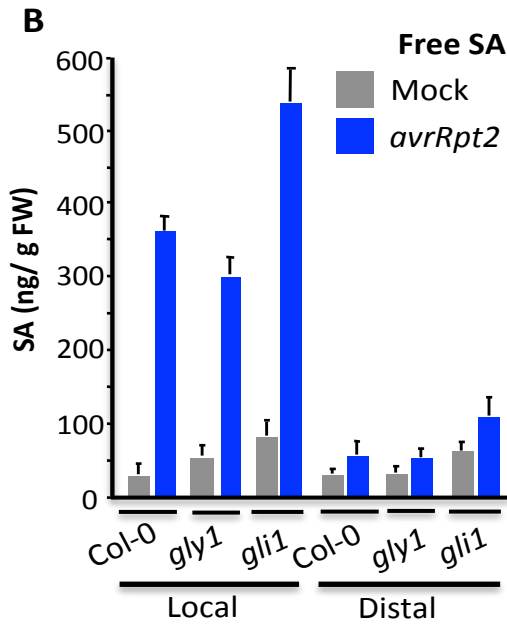
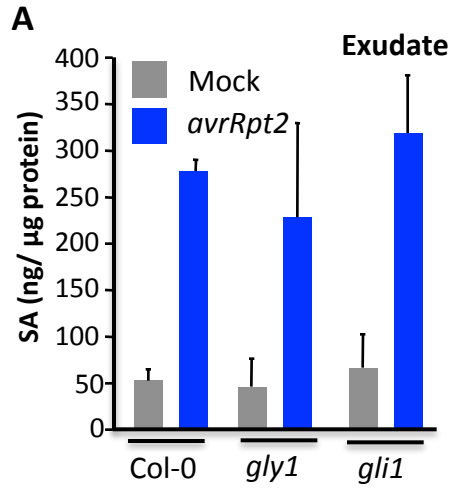
**Figure 3.5. Pathogen-induced increase in G3P precedes that of SA, AA and JA.**

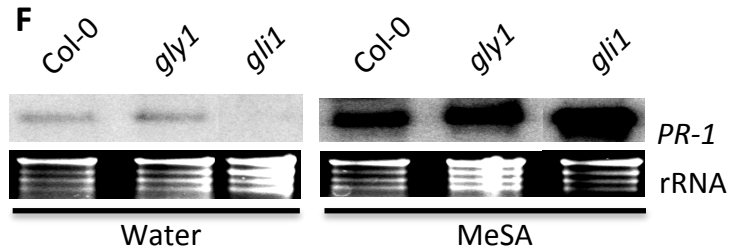
(A) SA, (B) AA, (C) JA, and (D) G3P levels in petiole exudates of Col-0 plants at 0, 6, 24 and 48 h post inoculation (hpi) with the avr pathogen (*avrRpt2*). Asterisk denotes significant difference with samples harvested at 0 hpi (*t* test, *P*<0.05). The error bars in a-d represent SD.



**Figure 3.6. G3P levels increase in response to pathogen inoculation.**

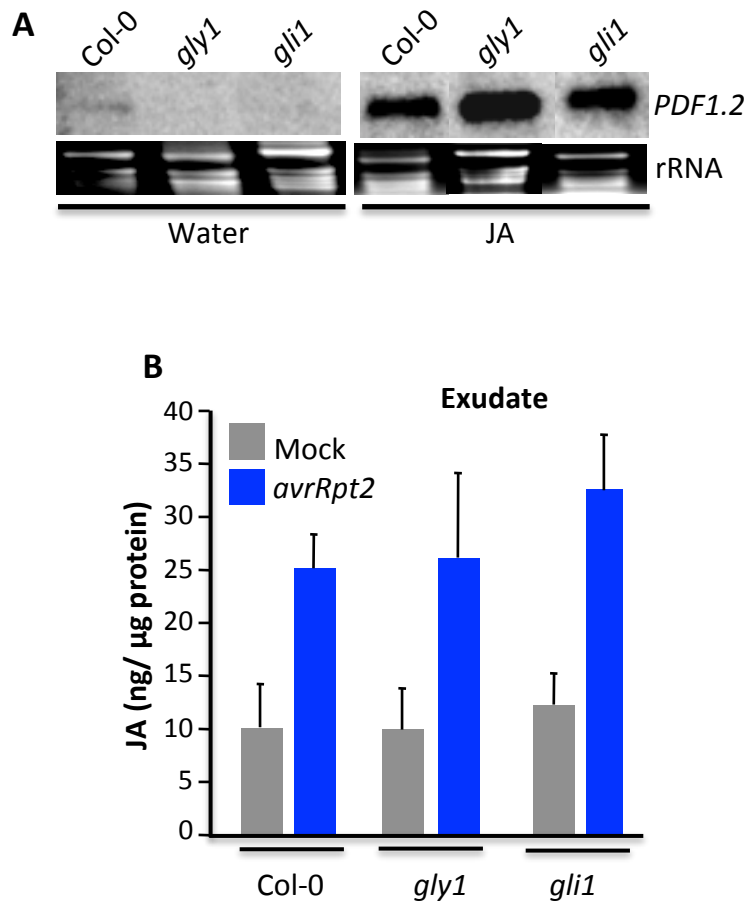
(A) G3P levels in petiole exudates of Col-0, *gly1*, *gli1* and *G3Pdh* KO plants at 0 and 24 h post inoculation with the avr pathogen (*avrRpt2*). (B) G3P levels in local or distal leaves of Col-0, *gly1*, *gli1* and *G3Pdh* KO plants at 0 and 24 h post inoculation with the avr pathogen (*avrRpt2*). The error bars in A and B represent SD.





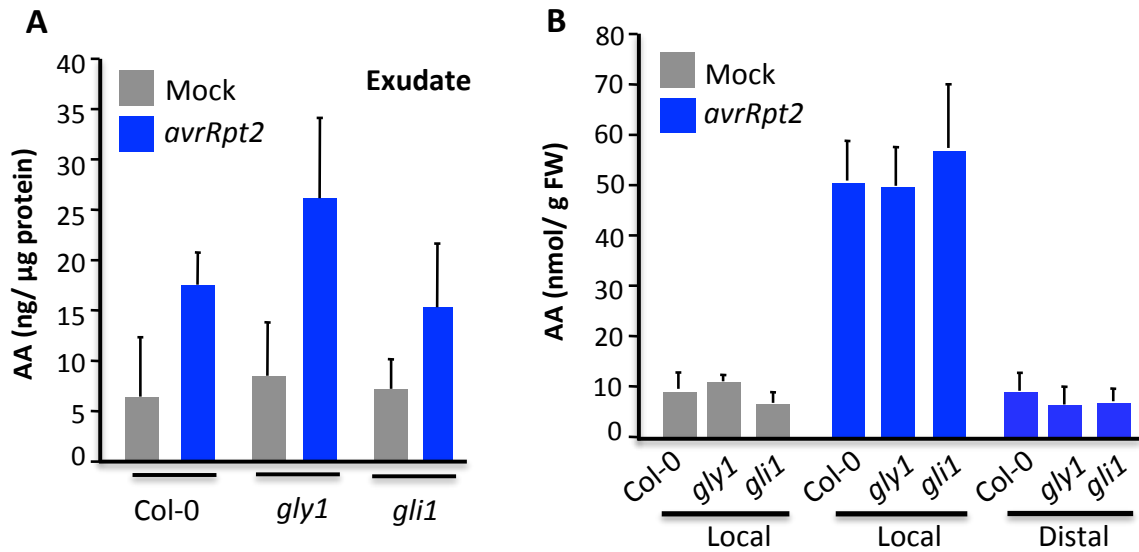
**Figure 3.7. The *gly1* and *gli1* plants are not impaired in SA or MeSA pathways.**

(A) SA levels in petiole exudates of *Col-0*, *gly1* and *gli1* plants at 24 h post inoculation with  $MgCl_2$  (mock) or the avr pathogen (*avrRpt2*). (B-C) SA and SAG levels in local and distal tissues of *Col-0*, *gly1* and *gli1* plants at 48 h post inoculation with  $MgCl_2$  (mock) or the avr pathogen (*avrRpt2*). The error bars in a-c represent SD. (D) Expression of the *PR-1* gene in distal tissues of *Col-0*, *gly1* and *gli1* plants at 48 h post inoculation with the avr pathogen (*avrRpt2*). (E) Expression of *PR-1* gene in water- or BTH-treated *Col-0*, *gly1* and *gli1* plants. (F) Expression of the *PR-1* gene in water- or MeSA-treated *Col-0*, *gly1* and *gli1* plants. Leaf samples were harvested 48 h post treatments (in D-F) and ethidium bromide staining of rRNA was used as a loading control in D, E, F.



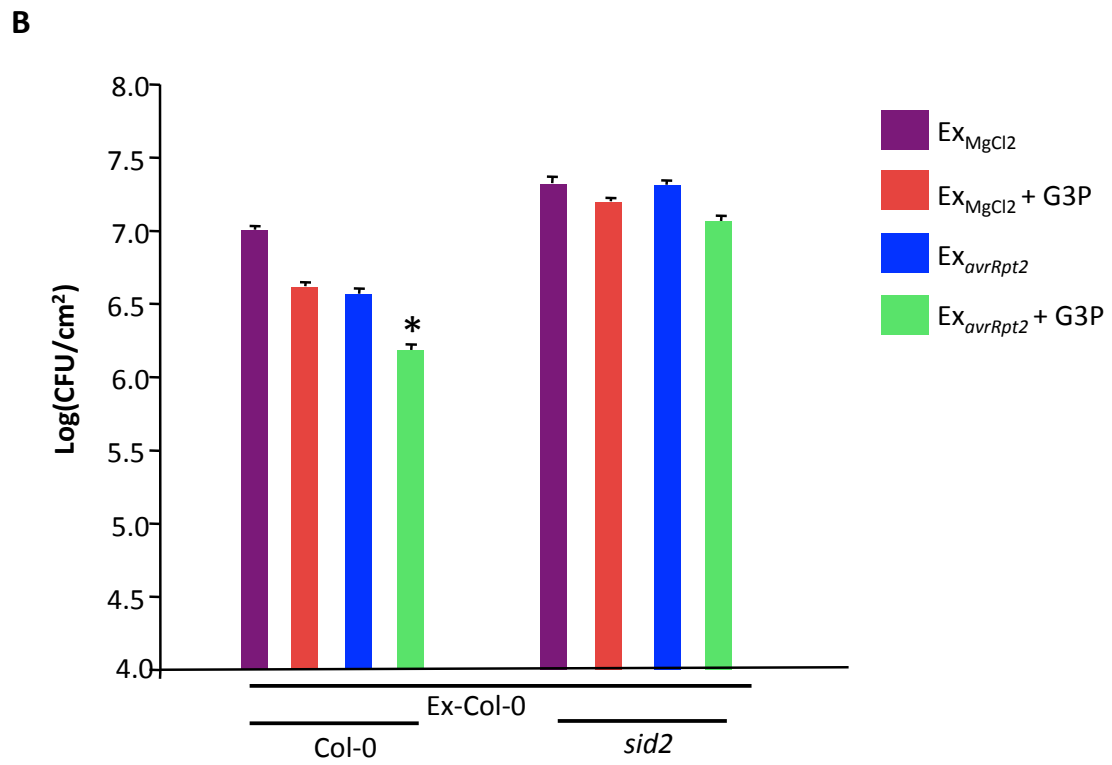
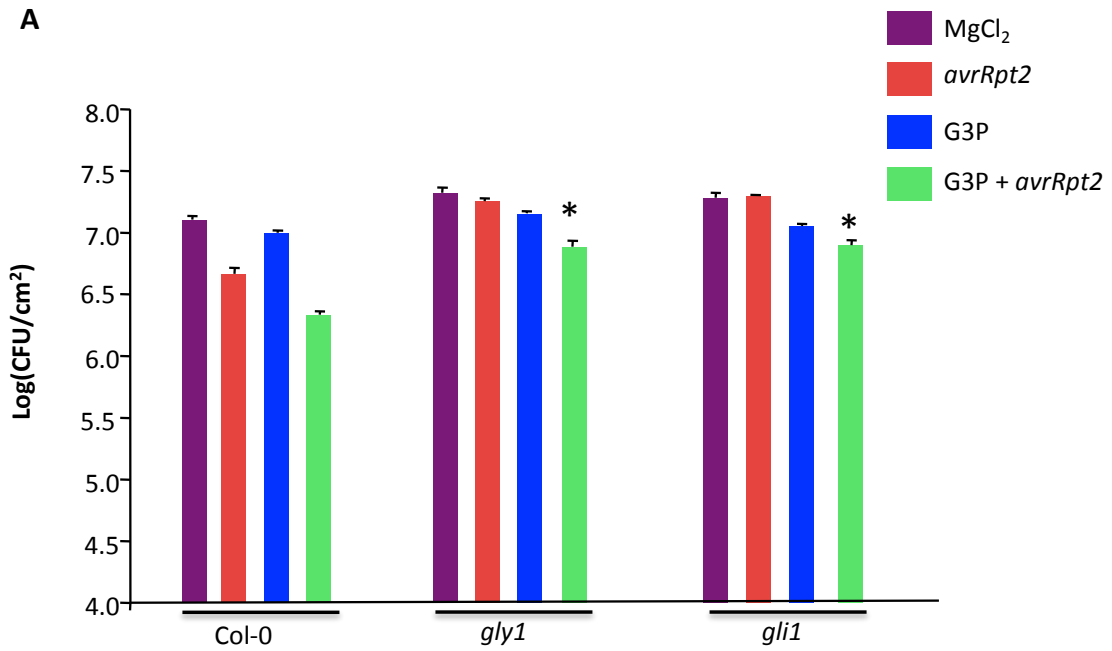
**Figure 3.8. The *gly1* and *gli1* plants are not impaired in JA pathways.**

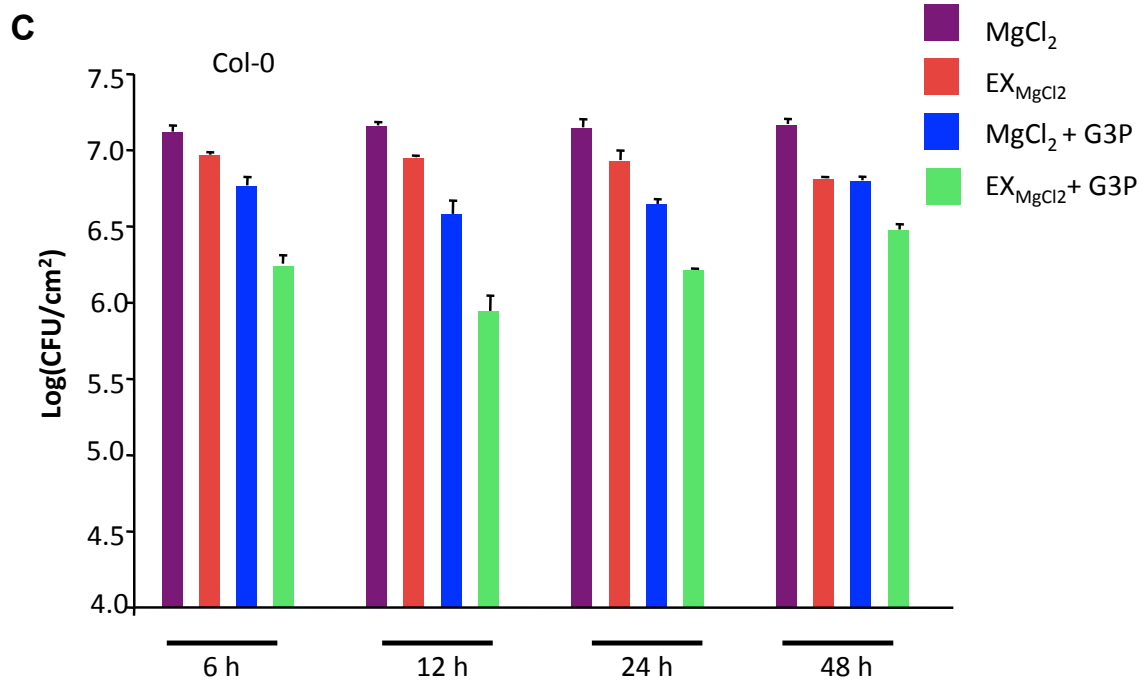
(A) Expression of the *PDF1.2* gene in water- or JA-treated Col-0, *gly1* and *gli1* plants. Leaf samples were harvested 48 h post treatments and ethidium bromide staining of rRNA was used as a loading control. (B) JA levels in petiole exudates of Col-0, *gly1* and *gli1* plants at 24 h post inoculation with MgCl<sub>2</sub> (mock) or the avr pathogen (*avrRpt2*). The error bars represent SD.



**Figure 3.9. The *gly1* and *gli1* plants are not impaired in AA pathways.**

(A) AA levels in petiole exudates of Col-0, *gly1* and *gli1* plants at 24 h post inoculation with MgCl<sub>2</sub> (mock) or the avr pathogen (*avrRpt2*). (B) AA levels in local and distal tissues of Col-0, *gly1* and *gli1* plants at 24 h post inoculation with MgCl<sub>2</sub> (mock) or the avr pathogen (*avrRpt2*). The error bars in h-k represent SD.

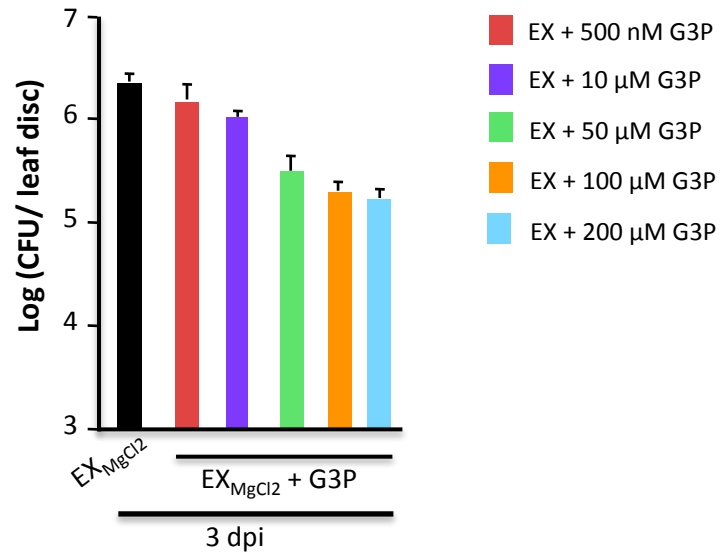




**Figure 3.10. Exogenous application of G3P improves SAR in Col-0 plants, and G3P-conferred SAR is dependent on SID2.**

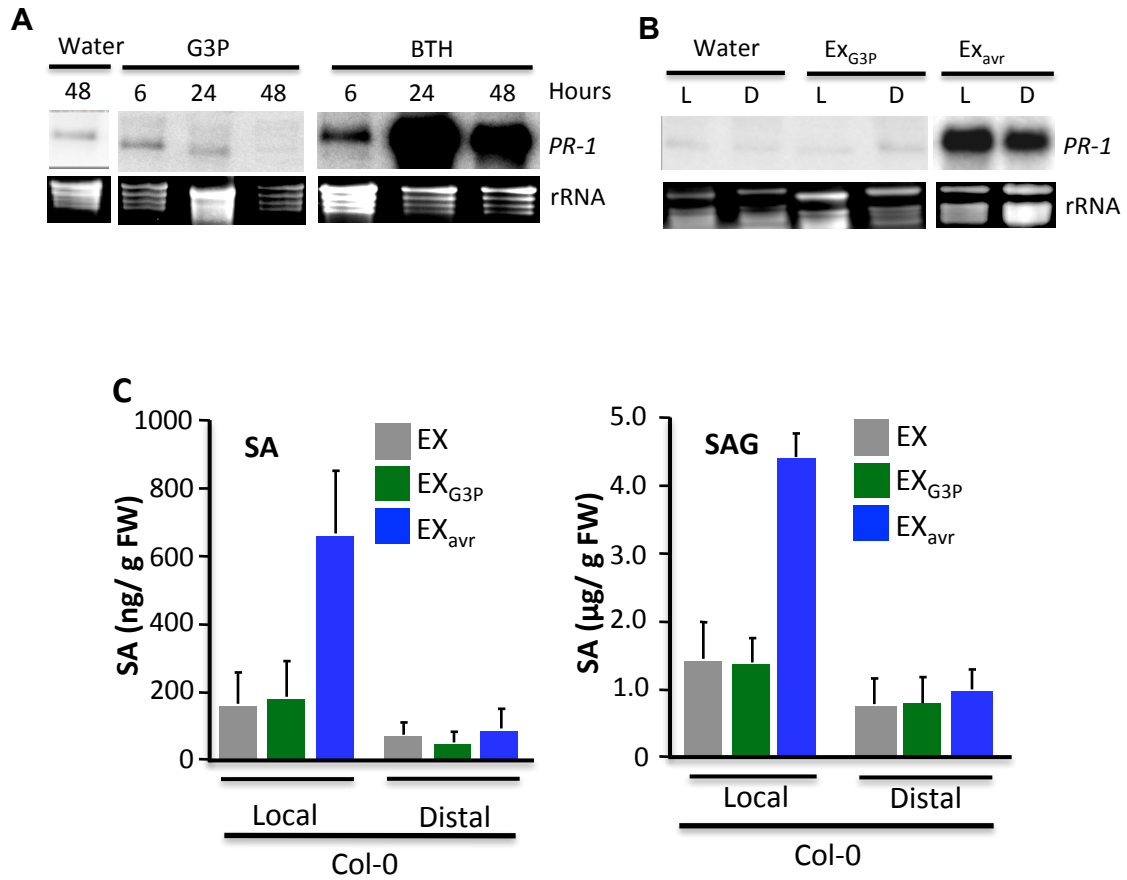
(A) SAR response in Col-0 (wild-type), *gly1* and *gli1* plants. I inoculated primary leaves with MgCl<sub>2</sub>, avrRpt2, G3P or avrRpt2 + G3P and the distal leaves 24 h later with a virulent strain of *P. syringae*. After 48h, the average number of colony forming units from 7 to 8 replications of 1 cm<sup>2</sup> disks from these leaves was estimated. Asterisks denote a significant difference with respective MgCl<sub>2</sub> treatment. (*t*-test,  $P < 0.005$ ) (B) SAR response in Col-0 and *sid2* plants infiltrated with exudates collected from Col-0 plants. Exudates were collected post inoculation with MgCl<sub>2</sub> (EX<sub>MgCl<sub>2</sub></sub>) or avrRpt2 (EX<sub>avrRpt2</sub>). Asterisks denote a significant difference with respective MgCl<sub>2</sub> treatment. (*t*-test,  $P < 0.001$ ) (C) SAR in Col-0 plants after infiltrating primary leaves with MgCl<sub>2</sub>, EX<sub>MgCl<sub>2</sub></sub>, MgCl<sub>2</sub> + G3P or EX<sub>MgCl<sub>2</sub></sub> + G3P. EX<sub>MgCl<sub>2</sub></sub> was collected from the wild-type (Col-0) plants. I inoculated the distal leaves with virulent pathogen at 6, 12, 24 or 48 h post infiltration of primary leaves. The error bars in A-C represent SD. EX, exudates..





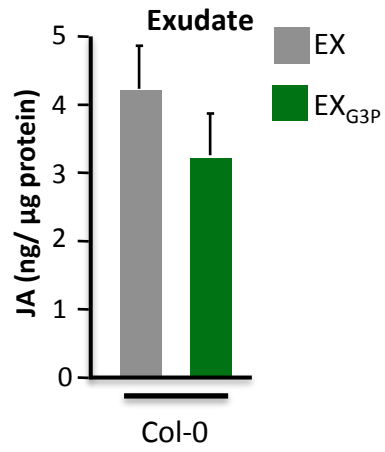
**Figure 3.11. Dose-response relationship for G3P.**

SAR in Col-0 plants after infiltrating primary leaves with EX containing 500 nM-200 μM concentrations of G3P. EX were collected from the wt (Col-0) plants. The distal leaves were inoculated with virulent pathogen at 24 h post infiltration of primary leaves with G3P. The error bars represent SD.



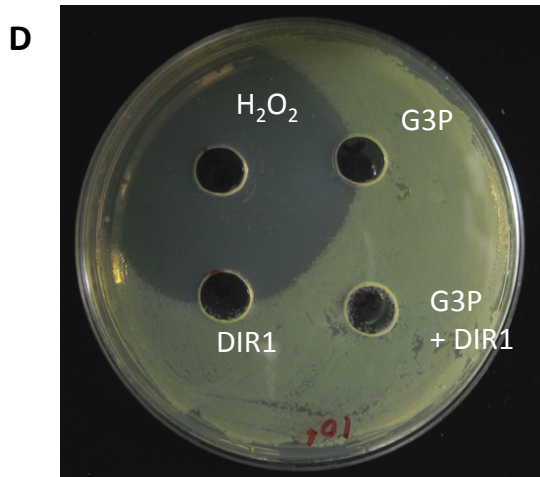
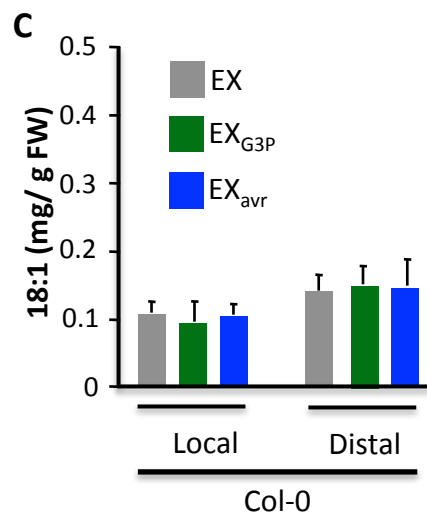
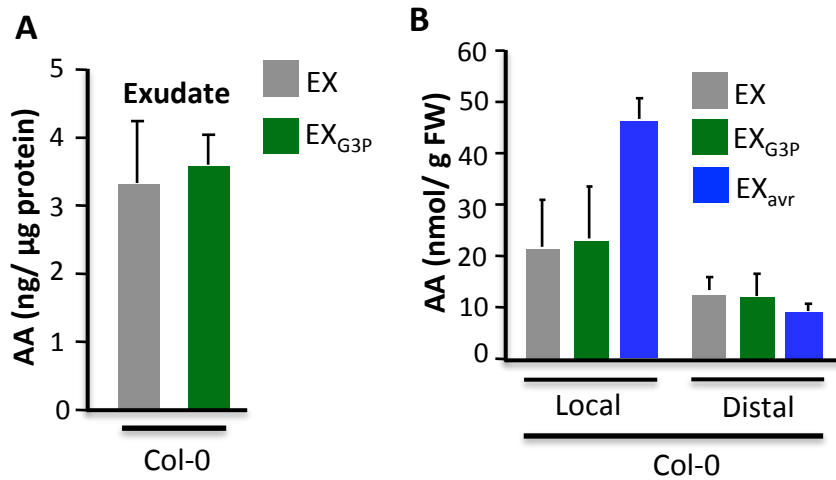
**Figure 3.12. G3P does not alter SA levels.**

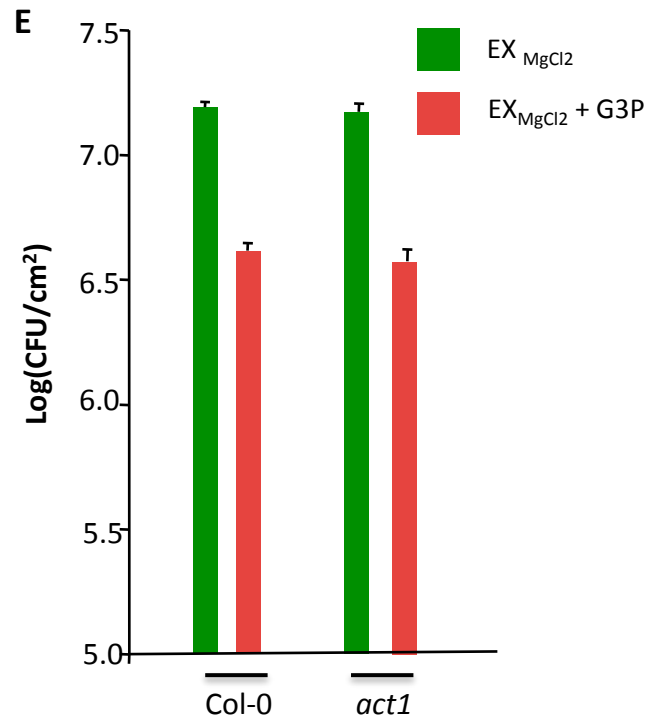
(A) Expression of the *PR-1* gene in water-, G3P- or BTH-treated Col-0 plants at indicated times post treatment. Ethidium bromide staining of rRNA was used as a loading control. (B) Expression of the *PR-1* in Col-0 plants at 48 h post infiltration with EX, EX + G3P or EX<sub>avr</sub>. L and D indicate local and distal leaves, respectively. (C) SA and SAG levels in local and distal tissues of Col-0 plants infiltration with EX, EX + G3P or EX<sub>avr</sub>.



**Figure 3.13. G3P does not alter JA levels.**

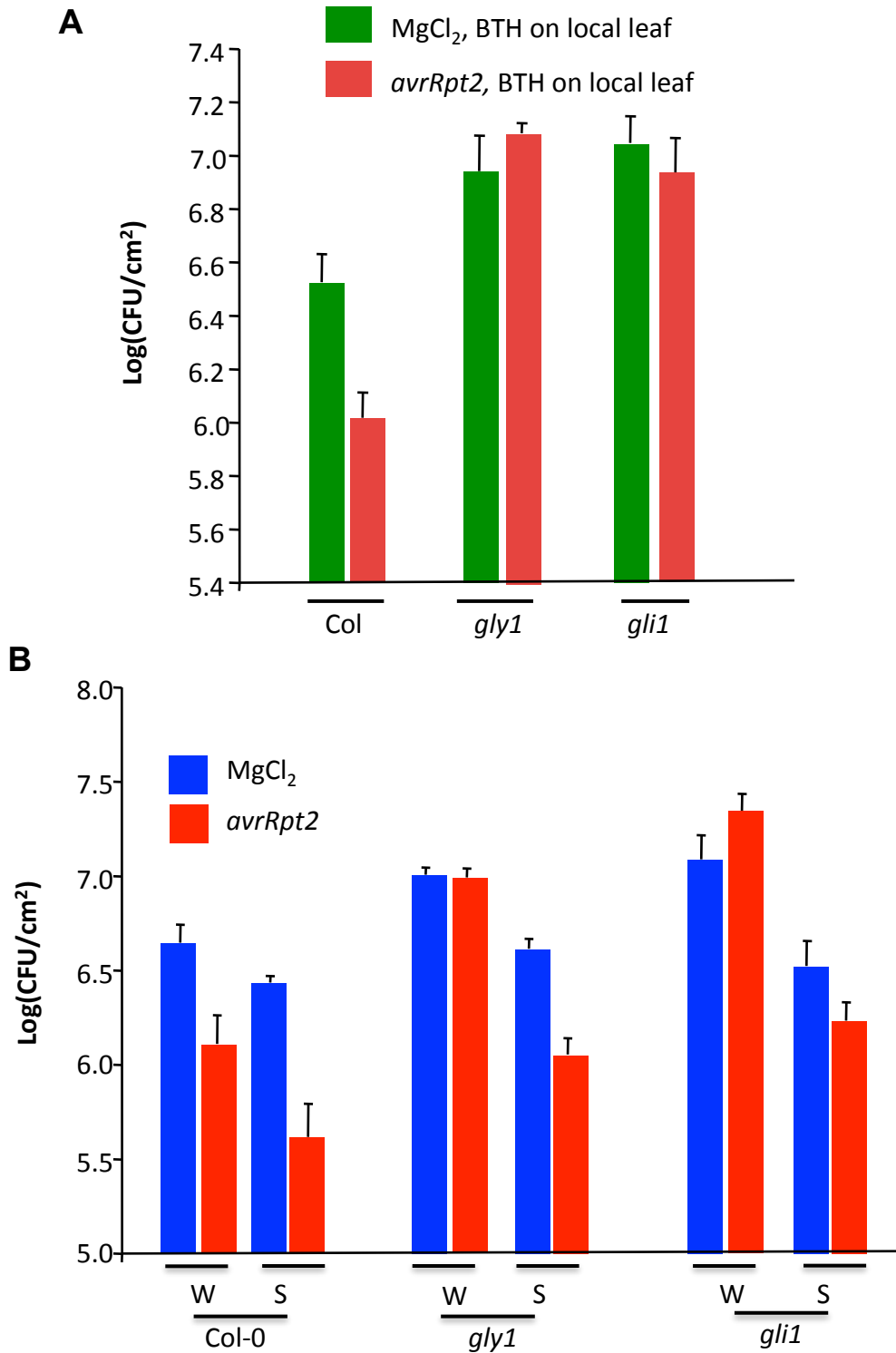
JA levels in petiole EX of Col-0 plants at 24 h post treatments with EX or EX + G3P.





**Figure 3.14. G3P does not alter AA or oleic acid (18:1) levels or show antimicrobial activity.**

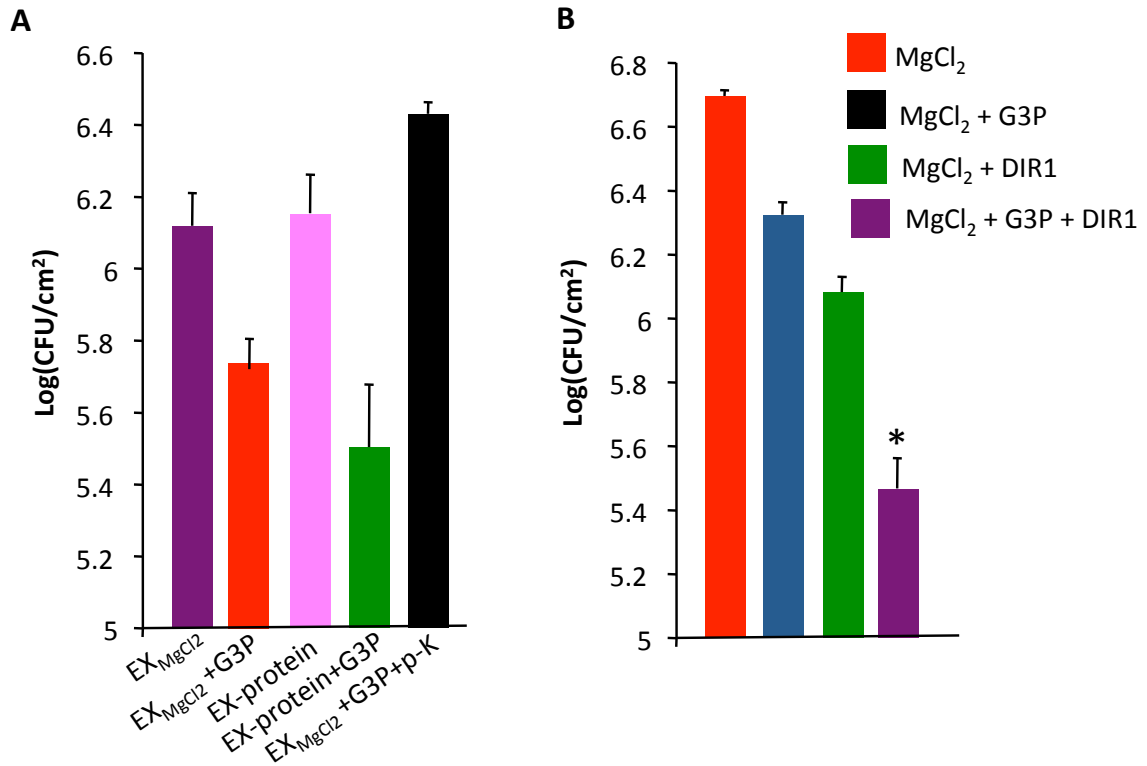
(A) AA levels in wild type petiole exudate at 24 h post treatments with EX or EX + G3P. (B) AA levels in local and distal tissues of Col-0 plants at 24 h post treatments with EX, EX + G3P or EX<sub>avr</sub>. (C) Relative levels of 18:1 in 4-week-old Col-0 plants infiltrated with EX, EX + G3P or EX<sub>avr</sub>. The values are presented as means of 6-8 replicates. FW indicates fresh weight. (D) Plate assay for testing antimicrobial activity. The bacterial culture was plated at a density of  $10^6$  CFU/ml and allowed to grow in the presence of 50  $\mu$ M H<sub>2</sub>O<sub>2</sub>, 100  $\mu$ M G3P, 20  $\mu$ g of DIR1 or G3P + DIR1. (E) SAR in Col-0 and *act1* plants after infiltrating primary leaves with EX<sub>MgCl2</sub> or EX<sub>MgCl2</sub> + G3P. EX<sub>MgCl2</sub> were collected from the wt (Col-0) plants. The distal leaves were inoculated with virulent pathogen 24 h post infiltration of primary leaves. The error bars represent SD.



**Figure 3.15. Whole plant pretreatment with SA, but not local application, restores SAR in *gly1* and *gli1* plants**

**Figure 3.15. (Continued)**

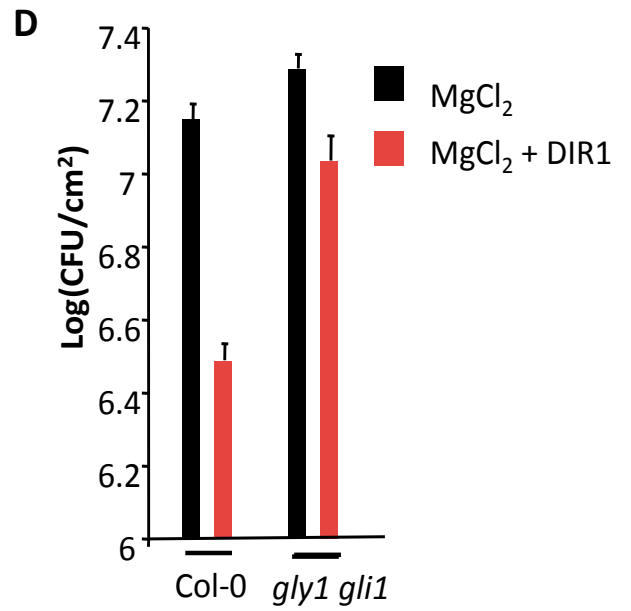
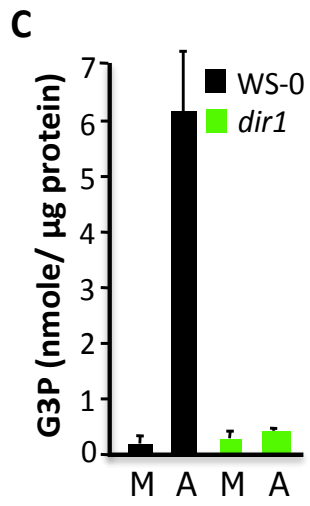
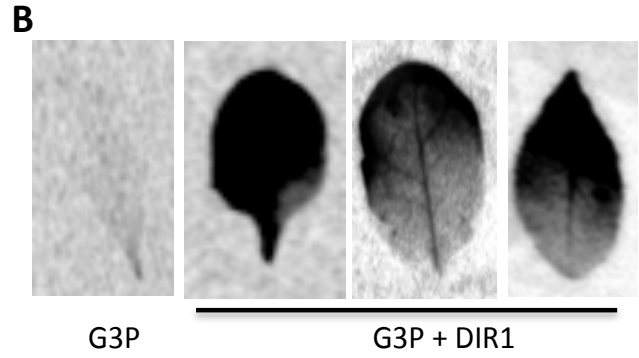
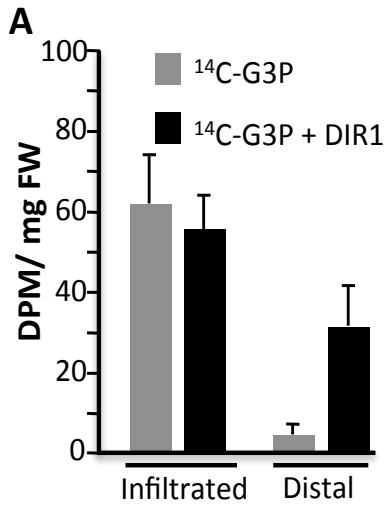
(A) SAR response in Col-0, *gly1* and *gli1* plants that were pretreated with BTH on their local leaves for 24 h prior to infiltration with MgCl<sub>2</sub> or *avrRpt2*. (B) SAR response in Col-0, *gly1* and *gli1* plants that were pretreated with water (W) or SA (S) for 24 h prior to infiltration with MgCl<sub>2</sub> or *avrRpt2*. The error bars represent SD.



**Figure 3.16. G3P-conferred SAR is dependent on DIR1.**

(A) SAR in Col-0 plants infiltrated with EX<sub>MgCl<sub>2</sub></sub>, EX<sub>MgCl<sub>2</sub></sub> + G3P, total protein extracted from petiole exudates (EX-protein), EX-protein + G3P and EX-protein pretreated with proteinase K (p-k) before addition of G3P. (B) SAR response in Col-0 (wild-type) plants infiltrated with MgCl<sub>2</sub> or MgCl<sub>2</sub> containing G3P and/or DIR1. The error bars in a–c represent SD. EX, exudates. Asterisk denotes a significant difference with respective MgCl<sub>2</sub> treatment. (*t*-test, *P* < 0.001)





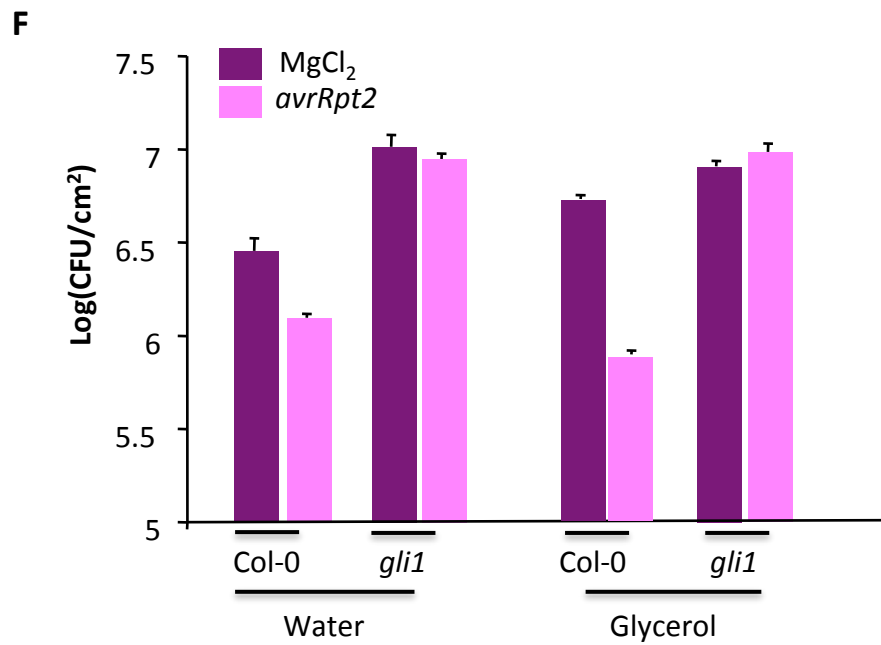
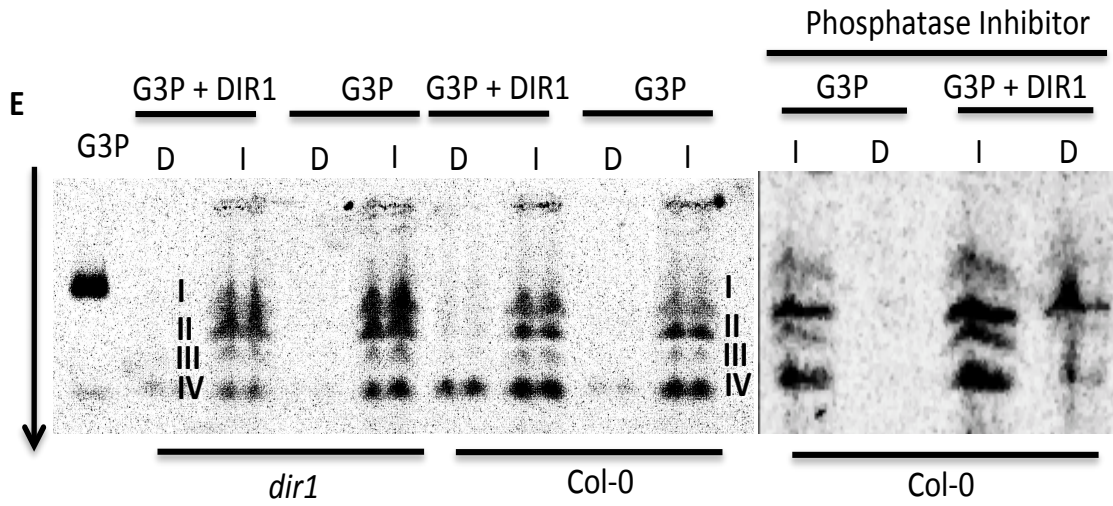


**Figure 3.17. G3P and DIR1 are dependent on each other for translocation into distal tissues.**

**Figure 3.17. (Continued)**

(A) Quantification of radioactivity in local (infiltrated) and distal tissues of leaves infiltrated with  $^{14}\text{C}$ -G3P or  $^{14}\text{C}$ -G3P + DIR1. DPM, disintegrations per minute. (B) Autoradiograph showing images of distal leaves collected from plants that were infiltrated with  $^{14}\text{C}$ -G3P or  $^{14}\text{C}$ -G3P + DIR1. I sampled the leaves 24 h post treatments. (C) G3P levels in petiole exudates of WS-0 (wild-type) and *dir1* plants collected 24 h after mock (M) or *avrRpt2* (A) inoculations. (D) SAR response in Col-0 (wild-type) and *gly1 gli1* plants infiltrated with  $\text{MgCl}_2$  or  $\text{MgCl}_2$ + DIR1 in the local leaves. (E) Autoradiograph of extracts from infiltrated (I) and distal (D) leaves of wild-type and *dir1* plants infiltrated with  $^{14}\text{C}$ -G3P or  $^{14}\text{C}$ -G3P + DIR1 with or without phosphatase inhibitor, normalized for protein content and run on a cellulose thin-layer chromatography plate. Arrow indicates direction of the run. (G) SAR in indicated genotypes treated with water or glycerol 6 h before mock ( $\text{MgCl}_2$ ) or *avrRpt2* inoculations. Water or glycerol was infiltrated in same leaves that were later inoculated with  $\text{MgCl}_2$  or *avrRpt2*. The error bars represent SD.

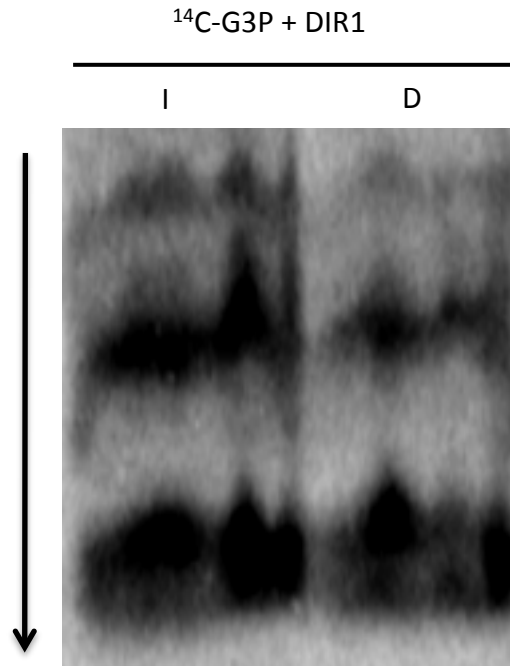


**Figure 3.18. Autoradiograph of extracts from infiltrated (I) and distal (D) leaves of plants infiltrated with  $^{14}\text{C-G3P} + \text{DIR1}$ .**

Extracts were concentrated and normalized for protein content before loading onto a cellulose TLC plate. Arrow indicates direction of the run.

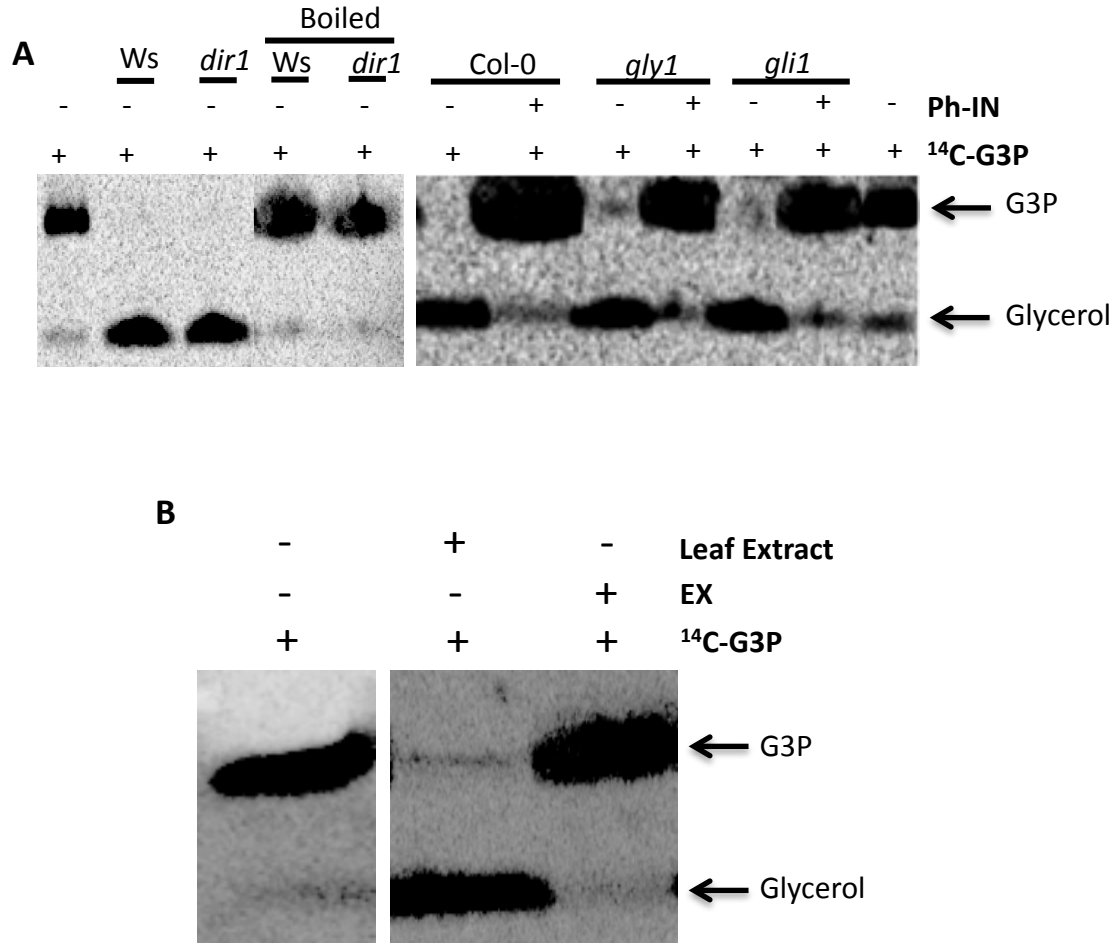


**Figure 3.19. Arabidopsis plants express phosphatase that converts G3P to glycerol.** (A) Leaf extracts from WS-0, *dir1*, Col-0, *gly1* and *gli1* plants were incubated with 20  $\mu$ M <sup>14</sup>C-G3P and the reaction was run on a cellulose TLC plate. Heat treatment (boiling) or addition of phosphatase inhibitors (Ph-IN) prevented the conversion of G3P to glycerol. The glycerol band was confirmed by GC-MS analysis. (B) Comparison of phosphatase activity in total proteins prepared from leaf extracts and petiole exudates (EX).

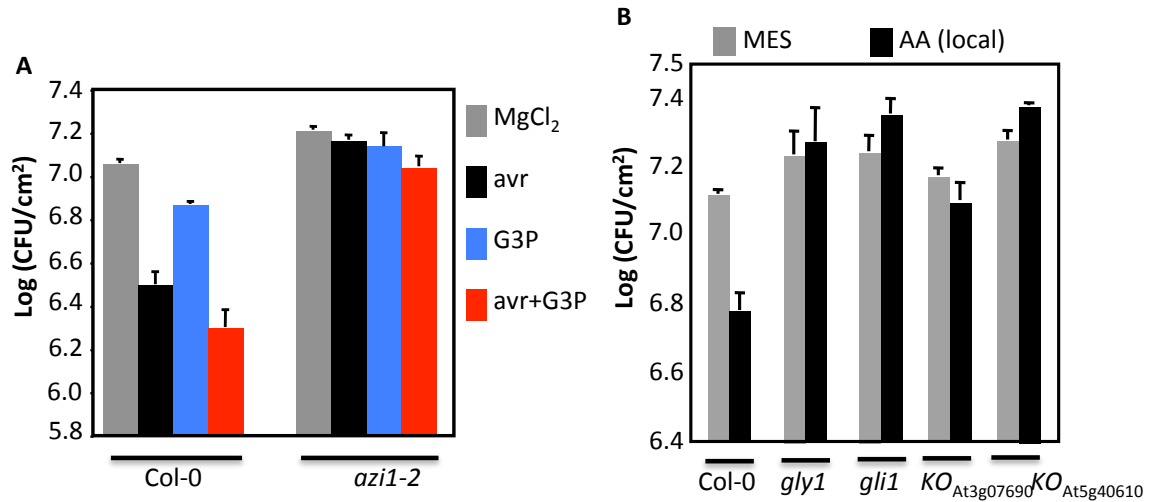


**Figure. 3.20 Arabidopsis mutants impaired in G3P biosynthesis are insensitive to AA.**

**(A)** SAR response in Col-0 and *azi1* plants. Primary leaves were inoculated with MgCl<sub>2</sub>, *avrRpt2*, G3P, or *avrRpt2*+G3P and the distal leaves were inoculated 24 h later with a virulent strain of *P. syringae*. 72 hours pi, distal leaves were ground and the number of colony forming units per 7-8 replications of a 1cm<sup>2</sup> leaf disk, assessed. **(B)** SAR response in Col-0, *gly1*, *gli1* or *g3pdh* KO plants treated locally with MES buffer or AA (as AA was dissolved in MES buffer) for 24 h prior to inoculation of distal leaves with virulent strain of *P. syringae*. The error bars represents SD.

## Chapter 4

### The role of G3P in basal defense against the hemibiotrophic fungal pathogen *Colletotrichum higginsianum*

#### Introduction

Fungal pathogenesis is thought to involve suppression of host defenses as well as nutrient uptake by the pathogen, resulting in altered host metabolism (Dulermo et al., 2009; AbuQamer et al., 2006). The efficient movement of nutrients from host to pathogen is an essential component of pathogenicity (Hancock and Huisman, 1981) and it suggests that primary metabolic pathways might interface with disease-related signaling. As plant defense requires energy, which is normally derived from the primary metabolic processes. This is supported by the fact that fatty acid (FA) and carbohydrate metabolism play important roles in plant defense and are involved in cross-talk with various phytohormones, including salicylic acid (SA), jasmonic acid (JA), and abscisic acid (Ehness et al., 1997; Price et al., 2003; Schaaf et al., 1995; Scheideler et al., 2002; Kachroo et al., 2003; Kachroo et al., 2005; Scharschmidt et al., 2007; Chandra-Shekara et al., 2007). Similarly, glycerol metabolism participates in both host defense and pathogenesis. A glycerol derived metabolite, glycerol-3-phosphate (G3P), which serves as a precursor to membrane glycerolipid biosynthesis, can be derived via the GLYCEROL KINASE (GK)-mediated phosphorylation of glycerol, or via G3P DEHYDROGENASE (G3Pdh)-mediated reduction of dihydroxyacetone phosphate. The *Arabidopsis* genome encodes five isoforms of G3Pdh that likely contribute to the G3P pool. Two of them are localized to the cytosol (G3Pdh<sub>CYT1</sub> and G3Pdh<sub>CYT2</sub>), the chloroplast (GLY1 and G3Pdh<sub>CHL</sub>) and the mitochondria (G3Pdh<sub>MIT</sub>). It has been suggested that glycerol is a primary transferred carbon metabolite during intercellular growth of *Colletotrichum gloeosporioides* on its host, round leaved mallow (*Malva pusilla*) (Wei et al., 2004). This, together with the observation that glycerol metabolism participates in host defense (Kachroo et al., 2004, 2005; Chandra Shekara et al., 2007; Kachroo et al., 2008), suggested a role for glycerol metabolism in both host defense and

pathogenesis.

The hemibiotrophic fungus *Colletotrichum higginsianum* is pathogenic to *Arabidopsis thaliana* (O'Connell et al., 2004; Narusaka et al., 2004). Hemibiotrophs, like true biotrophs, establish an intimate intracellular contact with their host cells during the initial phases of infection. The defining characteristic of necrotrophic pathogens is that they kill host tissues in advance of, or concurrent with, colonization, and feed on the dead cells (Schulz-Lafert and Panstruga, 2003; Williams, 1979; Yoder and Turgeon, 2001). Examples include *Alternaria brassicicola* and *Botrytis cinerea*, both of which have been studied as pathogens of *Arabidopsis* (Glazebrook, 2005). Because they undergo both biotrophic and necrotrophic development at different points in the disease cycle, *Colletotrichum* fungi are uniquely suitable for studies aimed at uncovering unifying principles underlying both types of interaction (Perfect et al., 1999). In this study, I have evaluated the response of various *Arabidopsis* mutants that are altered in glycerol metabolism to *C. higginsianum*. Results presented in this chapter show that glycerol metabolic activities in the host, leading to synthesis of G3P, are important for basal defense against *C. higginsianum*.

## Results

### **G3P levels correlate with infection response to *C. higginsianum***

Earlier work has suggested that glycerol is a primary transferred carbon metabolite during intercellular growth of *Colletotrichum gloesporioides* on its host (Wei et al., 2004). The *GLII*-encoded GLYCEROL KINASE uses glycerol as a substrate (Kang et al., 2003), while *GLYI*- encoded G3P DEHYDROGENASE uses DHAP (Kachroo et al., 2004). Furthermore, prior work in our laboratory had already established that *glyI* and *gliI* mutations conferred enhanced susceptibility to *C. higginsianum*. To determine if high endogenous glycerol levels in the *Arabidopsis glyI* and *gliI* mutants supported more growth of pathogen, I measured the glycerol levels. Plants mutated in *GLII* accumulated



~5 fold higher levels of glycerol while glycerol levels in *gly1* were comparable to wild-type [Columbia (Col-0) ecotype] plants (**Fig 4.1A**). However, the glycerol levels did not correlate with infection symptoms since *gly1* showed more susceptibility compared to *gli1* (**Figs 4.1B and C**). Since both *gly1* and *gli1* plants are affected in steps leading to synthesis of G3P, an alternate possibility further suggested that G3P levels could be important for basal defense to *C. higginsianum*. I next determined levels of glycerol in Arabidopsis plants inoculated with *C. higginsianum*, and found that the glycerol levels were reduced to ~35% at four days post inoculation (dpi), in comparison to controls (**Fig. 4.1 D**). A similar phenomenon observed in *C. gloeosporioides*-inoculated round-leaved mallow plants was interpreted as pathogen utilization of host glycerol (Wei et al., 2004). An alternative possibility was that host glycerol was decreasing because it was being metabolized to G3P by the plant in response to pathogen infection. I measured the G3P levels in mock- and pathogen-inoculated plants, and indeed, *C. higginsianum*-inoculated plants accumulated ~four-fold higher levels of G3P than controls (**Fig. 4.1E**). However, a stoichiometric correlation was not observed between the decrease in glycerol and the increase in G3P, which could be because there are at several enzymes that contribute to the synthesis of G3P.

I next quantified G3P levels in *act1* plants, which showed enhanced resistance to *C. higginsianum* (Venugopal et al., 2008; also see **Figs 4.2A and B**). ACT1 catalyzes the acylation of oleic acid (18:1) on the G3P backbone (**Fig. 3.1**, Kunst et al., 1988). Since *act1* plants accumulate 18:1 (Kunst et al., 1988; Kachroo et al., 2003), they would also be expected to accumulate G3P, as *act1* is unable to catalyses acylation of G3P with 18:1. Basal levels of G3P were slightly increased in *act1*, compared to wt (**Fig 4.2C**). Next, I measured changes in G3P levels in *C. higginsianum*-inoculated wt, *act1*, *gli1* and *gly1* plants. Since *gly1* plants were nearly killed within 96 h of pathogen inoculation, G3P levels were monitored only up to 72 h post-inoculation (hpi). In comparison with wt plants, pathogen inoculation resulted in ~two-fold higher levels of G3P in *act1* and ~two-fold reduced levels of G3P in *gly1* and *gli1* plants at 72 hpi (**Figs 4.2C and D**).

In addition to G3P, the levels of glucose and fructose also increased significantly in *C. higginsianum*-inoculated wt plants (**Figs 4.2E and F**). In contrast, sucrose levels

decreased, while sorbitol levels increased only marginally, and galactose levels did not change significantly. I compared the levels of these sugars in water- and pathogen-treated wt, *gly1* and *act1* genotypes, in order to evaluate whether they were also associated with the pathogen response, like G3P. Pathogen-inoculated leaves of wt, *gly1* and *act1* plants accumulated similar amounts of fructose and galactose and varying levels of glucose, sucrose and sorbitol (**Figs 4.2E and F**). However, unlike G3P, the levels of glucose, sucrose and sorbitol did not correlate with the increased susceptibility and resistance of the *gly1* and *act1* plants, respectively. Together, these data provide further evidence that induced increases in levels of G3P is specifically associated with increased resistance to the pathogen.

#### **A mutation in *G3Pdh<sub>chl</sub>* and *G3Pdh<sub>cyt2</sub>* confer enhanced susceptibility to *C. higginsianum***

In addition to *GLY1*, the Arabidopsis genome encodes four other G3Pdh isoforms that are predicted to localize to cytosol, mitochondria or plastids (Wei et al., 2001; Shen et al., 2003). Earlier work from the host laboratory showed that GLY1 and GLI1 proteins localized to chloroplasts and cytosol, respectively (Chanda et al., 2011). To determine cellular localization of other G3Pdh isoforms, I created G3Pdh-GFP fusion constructs, expressed these transiently in *Nicotiana benthamiana* and analyzed the localization using confocal microscopy. As predicted, G3Pdh<sub>cyt1</sub> (At2g41540) and G3Pdh<sub>cyt2</sub> (At3g07690) localized to the cytosol, G3Pdh<sub>chl</sub> (At5g40610) localized to chloroplasts and G3Pdh<sub>mit</sub> (At3g10370) to small organelles, which appear to be mitochondria (**Fig 4.3A**). To test if enhanced susceptibility to *C. higginsianum* was specific to a mutation in the *GLY1* isoform of *G3Pdh*, I tested the response to *C. higginsianum* on *G3Pdh<sub>cyt1</sub>*, *G3Pdh<sub>cyt2</sub>* and *G3Pdh<sub>chl</sub>* mutant plants. Plants defective in the mitochondrial-targeted G3Pdh isoform (At3g10370) were kindly provided by Dr. Peter Eastmond (Rothamsted Research, West Common, Harpenden, Hertfordshire, United Kingdom). The KO were morphologically similar to wt (Col-0). The *G3Pdh<sub>chl</sub>* and *G3Pdh<sub>cyt2</sub>* KO plants showed more susceptibility to *C. higginsianum* compared to wt. In comparison, *G3Pdh<sub>cyt1</sub>* and *G3Pdh<sub>mit</sub>* KO plants showed a wt-like response (**Figs 4.3B and C**). The infection symptoms correlated with growth of the fungi on wild-type or KO plants (**Fig 4.3D**), and G3P levels (**Fig 4.3E**).

Together, these results suggest that besides GLY1 and GLI1, G3Pdh<sub>cyt2</sub> and G3Pdh<sub>chl</sub> also contribute to the pathogen induced G3P pool and are required for basal resistance to *C. higginsianum*.

To reconfirm if increased susceptibility to *C. higginsianum* in various *g3pdh* mutants was due to reduced accumulation of G3P, I evaluated the response of various genotypes after G3P pretreatment. Exogenous application of G3P enhanced resistance to *C. higginsianum* in both wild-type and *g3pdh* mutant plants (**Fig 4.4A and B**) suggesting that exogenous G3P was able to compensate for the loss of *G3Pdh* isoforms.

### **The enhanced susceptibility of *g3pdh* mutants is not due to a defect in SA, camalexin or ROS pathways**

To determine if a mutation in *g3pdh* conferred susceptibility by altering defense pathways regulated by SA, camalexin or ROS, I evaluated phenotypes specific to SA, camalexin and ROS in *g3pdh* mutants. Exogenous application of benzothiadiazole induced wt-like expression of the SA marker gene *PR-1* (**Fig 4.5A**). The wt and *g3pdh* mutant plants showed similar sensitivity to paraquat (methyl viologen), an agent that promotes the formation of ROS by inhibiting electron transport during photosynthesis. The plants were treated by placing a 5 µl droplet of 20 µM paraquat on individual leaves and the lesion size was monitored after 48 h posttreatment. The wt and *g3pdh* mutant plants exhibited similar levels of sensitivity to paraquat (**Figs 4.5B and C**). These results suggest that *g3pdh* mutants show wt-like responsiveness to SA and ROS and that susceptibility of *g3pdh* mutants to *C. higginsianum* is not due to altered sensitivity to SA or ROS.

The *PR-1* gene expression correlates well with free and bound forms of SA (Rochon, 2006). The wt (Col-0) plants inoculated with *C. higginsianum* induced high levels of *PR-1* gene expression (**Fig 4.5D**). The inoculated leaves of all *g3pdh* mutants showed a similar induction of *PR-1* gene expression, suggesting that *C. higginsianum* was capable of eliciting a normal SA-dependent defense response in these plants. Likewise, *C.*

*higginsianum* inoculated wt and *g3pdh* mutants showed a wt-like increase in their ROS levels; the inoculated leaves of wt and *g3pdh* mutant plants showed a ~2.5-fold increase in H<sub>2</sub>O<sub>2</sub> levels (**Fig 4.5E**). Since camalexin levels play an important role in defense against necrotrophic pathogen (Naruska et. al., 2004), I next assayed camalexin levels in *C. higginsianum*-inoculated wt and *g3pdh* mutants. Similar basal and pathogen-induced camalexin levels in wt and *g3pdh* mutants suggested that G3P levels do not impact camalexin biosynthesis (**Fig 4.5F**). Together, these results suggest that susceptibility of *g3pdh* plants was not associated with altered SA, camalexin or ROS pathways.

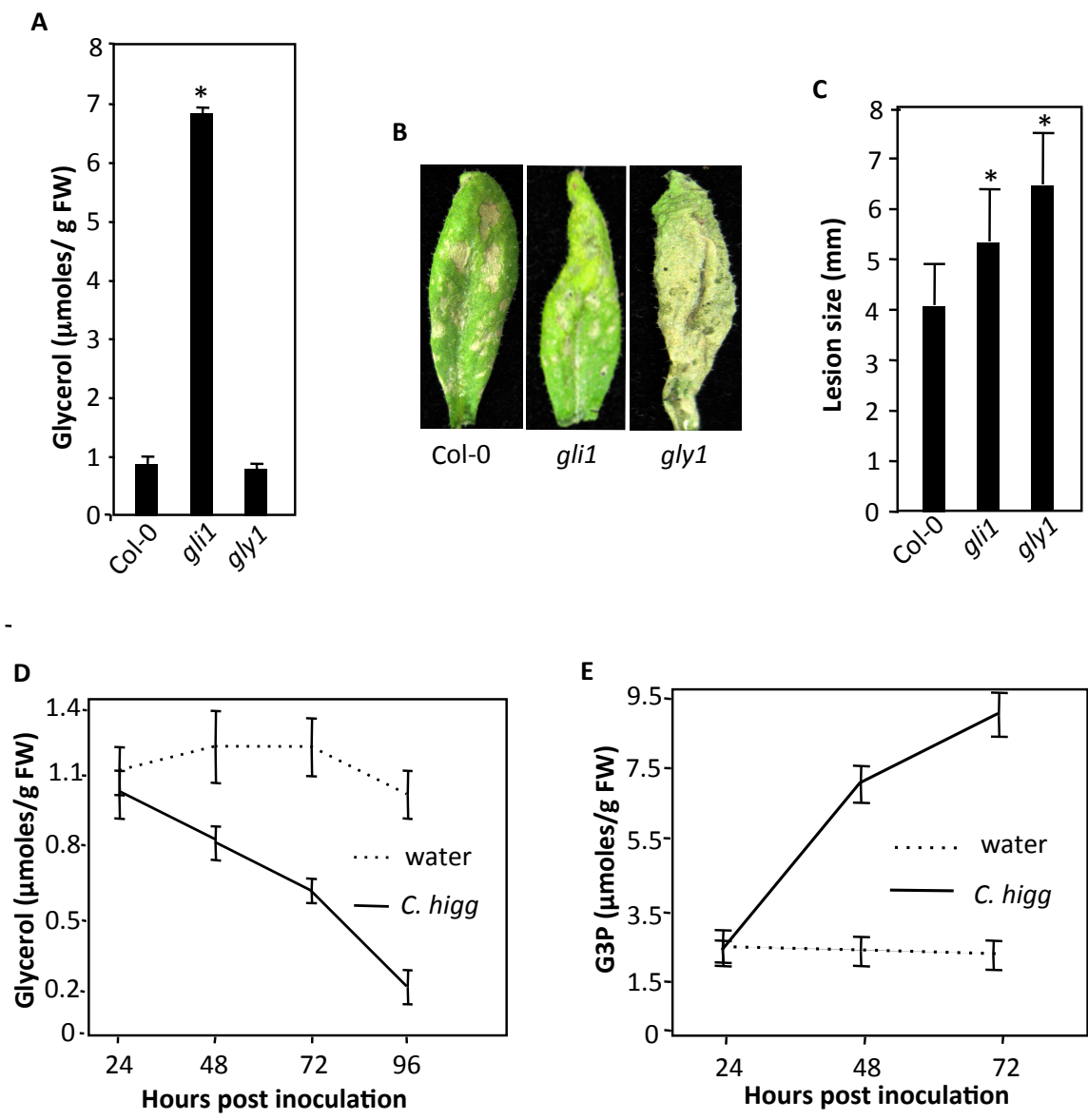
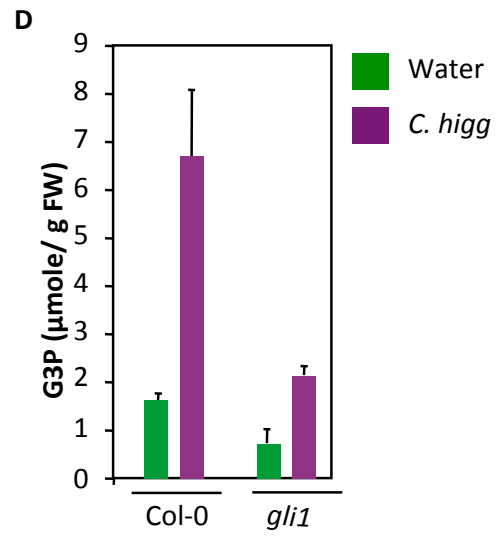
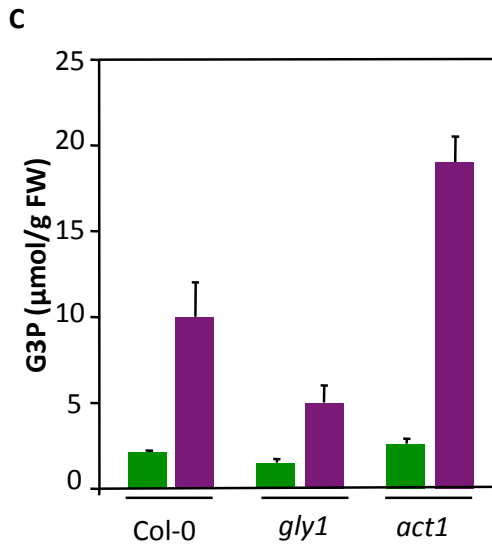
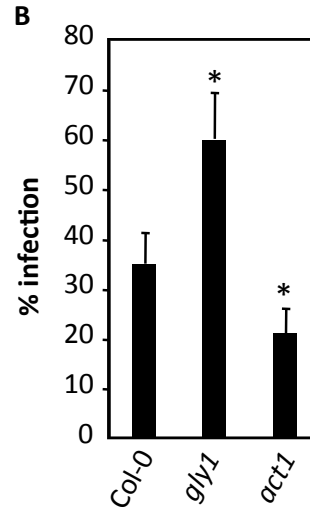
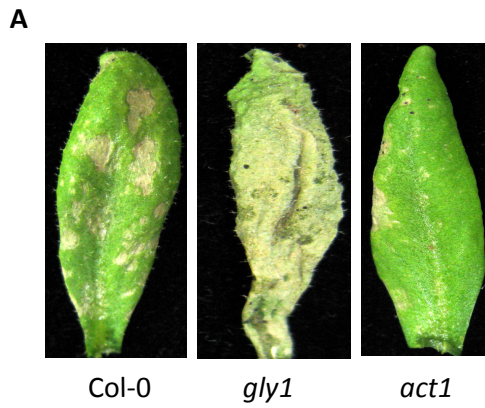
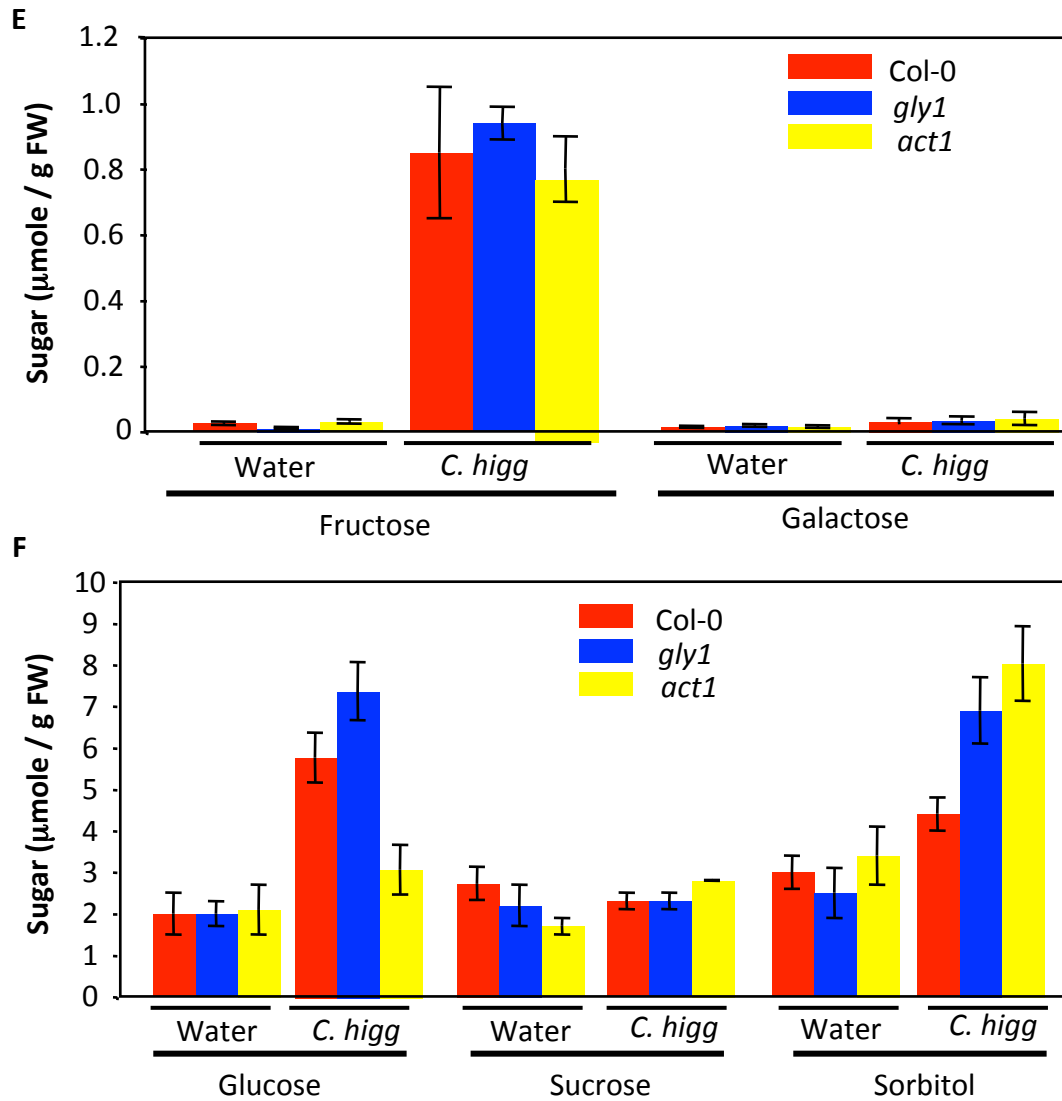


Figure. 4.1. Pathogen response, G3P and glycerol levels in *C. higginsianum* inoculated plants.

**Figure 4.1. (Continued)**

(A) Disease symptoms in Col-0, *gli1* and *gly1* leaves inoculated with  $10^6$  spores/mL of *C. higginsianum*. (B) Lesion size in spot inoculated genotypes. Plants were spot inoculated with  $10^6$  spores/mL of *C. higginsianum* and the lesion size was measured from 20-30 independent leaves at 6 dpi. Statistical significance was determined by using Student's *t* test. Asterisks indicate statistically significant data from that of the control (Col-0;  $P < 0.05$ ). Error bars indicate SD. (C) Basal glycerol levels in 4-week old Col-0, *gli1* and *gly1* plants. (D) Glycerol levels in mock (water)- or *C. higginsianum* –inoculated wild-type (Col-0) plants. Plants were spray inoculated ( $10^6$  spores/mL) and samples were collected at indicated times. (E) G3P levels in mock (water)- or *C. higginsianum* – inoculated wild-type (Col-0) plants. Plants were spray inoculated ( $10^6$  spores/mL) and samples were collected at indicated times.



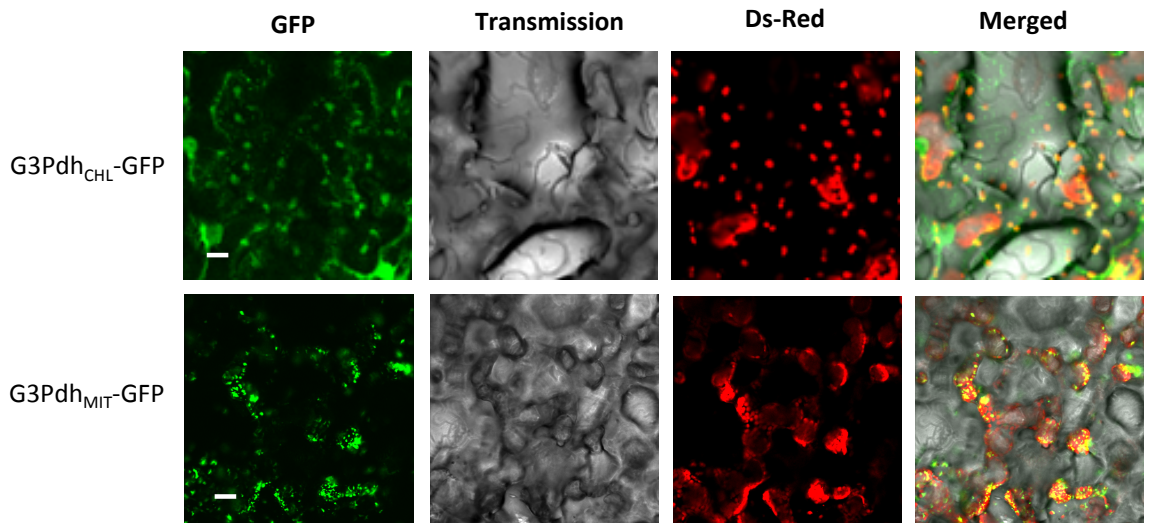
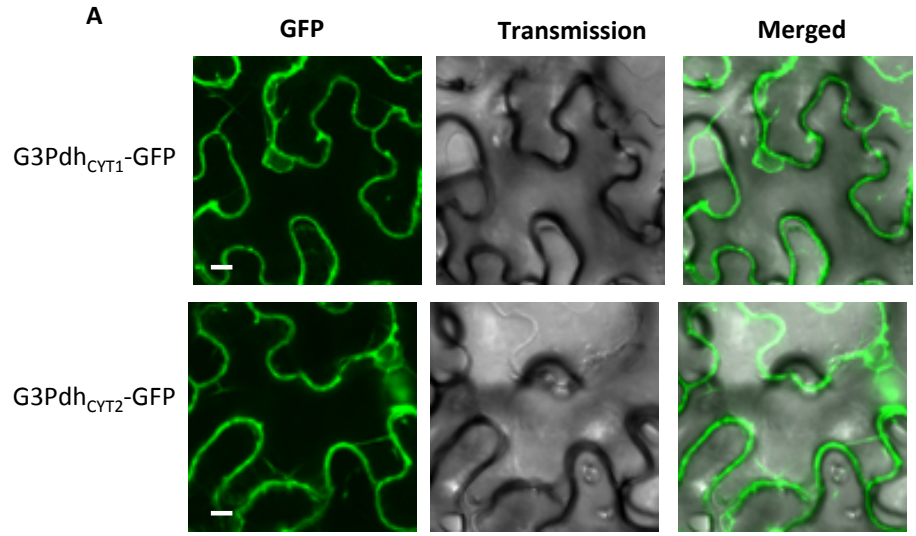


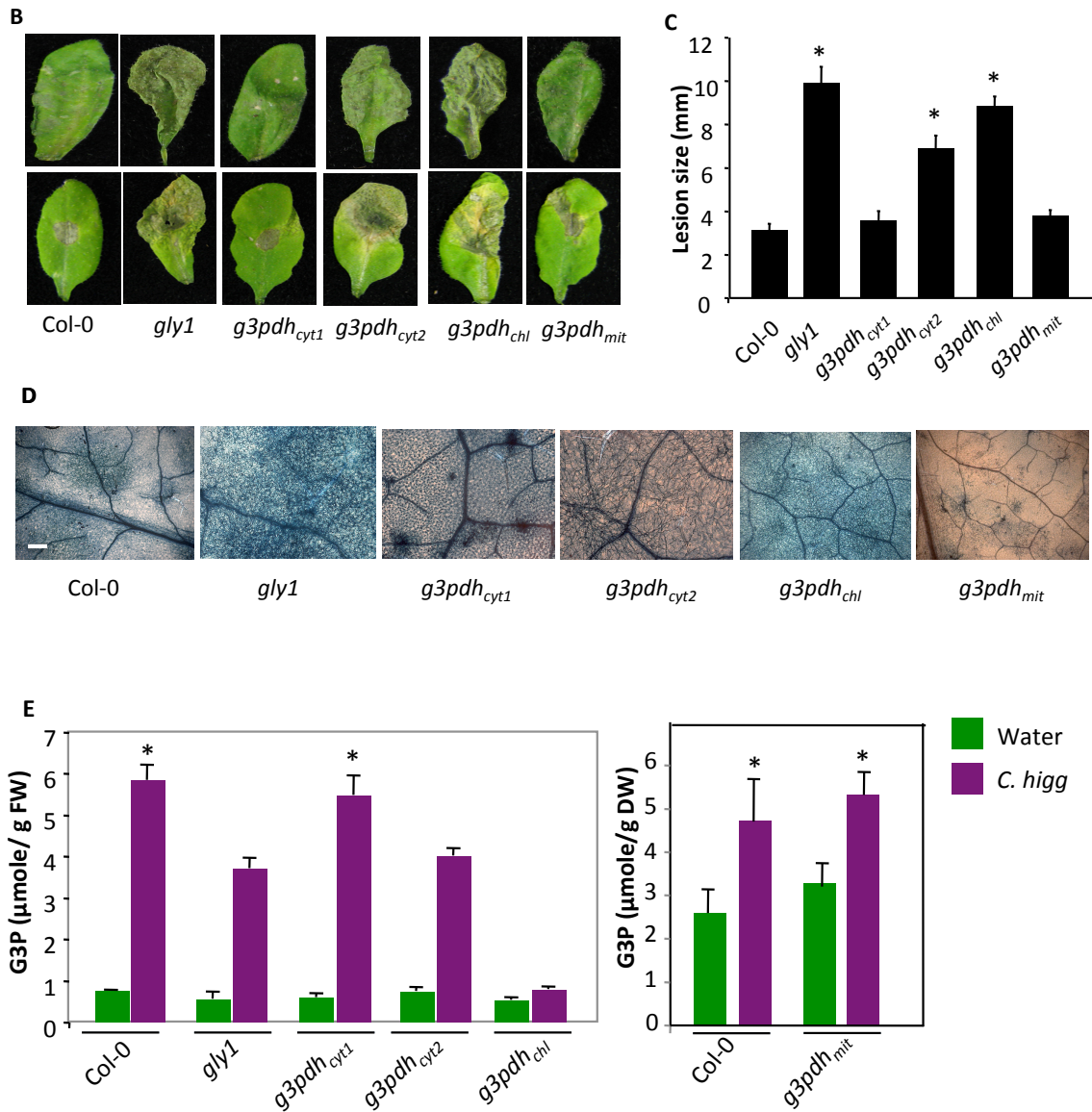
**Figure. 4.2. *In planta* growth and pathogen response in *Colletotrichum higginsianum*-inoculated plants and G3P and neutral sugar levels.**



**Figure. 4.2. (Continued)**

**(A)** Disease symptoms on Col-0, *gly1* and *act1*, plants spray- inoculated with  $10^6$  spores/mL of *C. higginsianum*. **(B)** Lesion size in spot-inoculated genotypes. The plants were spot-inoculated with  $10^6$  spores/mL *C. higginsianum* and the lesion size was measured from 20-30 independent leaves at 6 dpi. Statistical significance was determined using Students *t*-test. Asterisks indicate data statistically significant from that of control (Col-0) ( $P < 0.05$ ). Error bars indicate SD. **(C)** Basal and induced levels of G3P in four-week-old Col-0, *gly1* and *act1* plants. Plants were spray inoculated at ( $10^6$  spores/mL) and samples were collected at 72 hpi **(D)** Basal and induced levels of G3P in four-week-old Col-0 and *gli1* plants. Plants were spray inoculated ( $10^6$  spores/mL) and samples were collected at 72 hpi **(E, F)** Levels of neutral sugars in *C. higginsianum*-inoculated Col-0, *gly1* and *act1* plants. Plants were spray-inoculated at ( $10^6$  spores/mL) and samples were collected at indicated times.

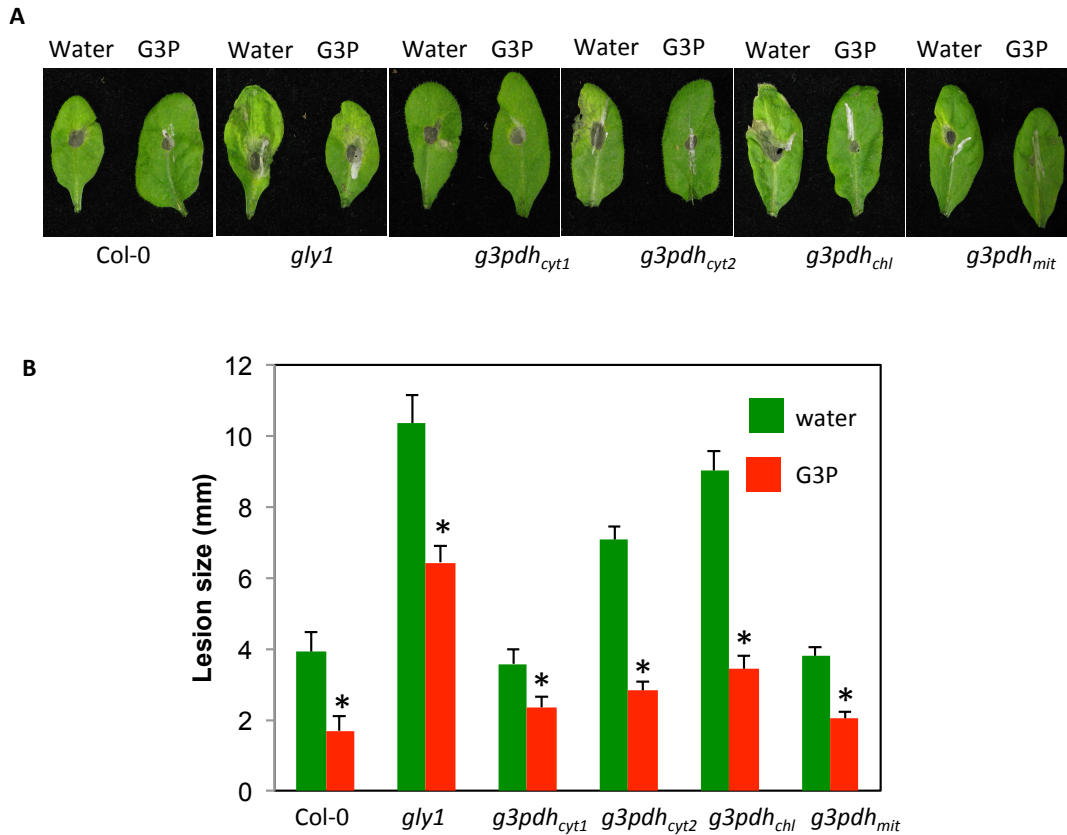




**Figure 4.3. A mutation in *G3Pdh<sub>chl</sub>* and *G3Pdh<sub>cyt2</sub>* confer enhanced susceptibility to *C. higginsianum*.**

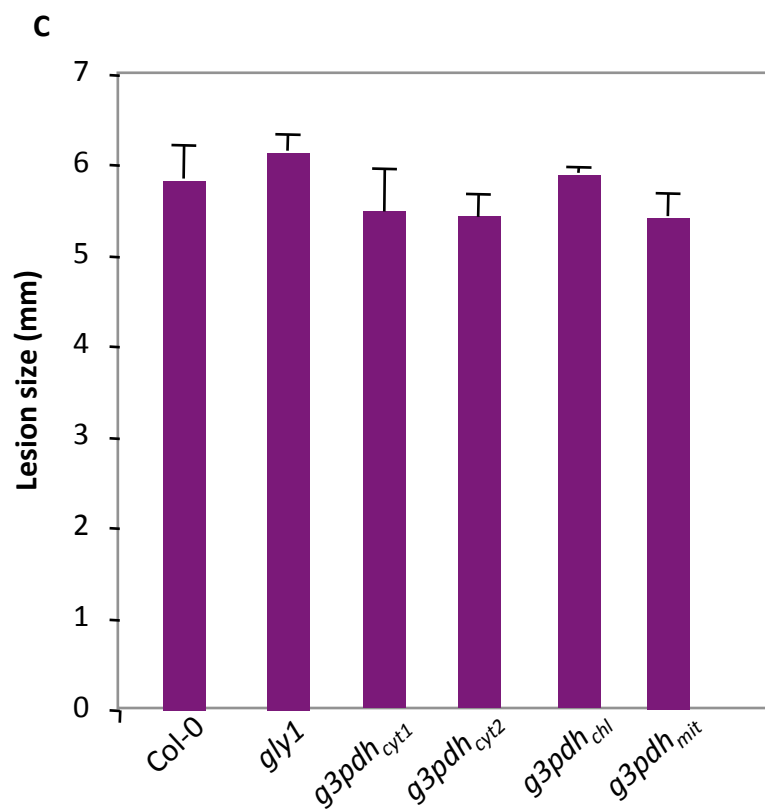
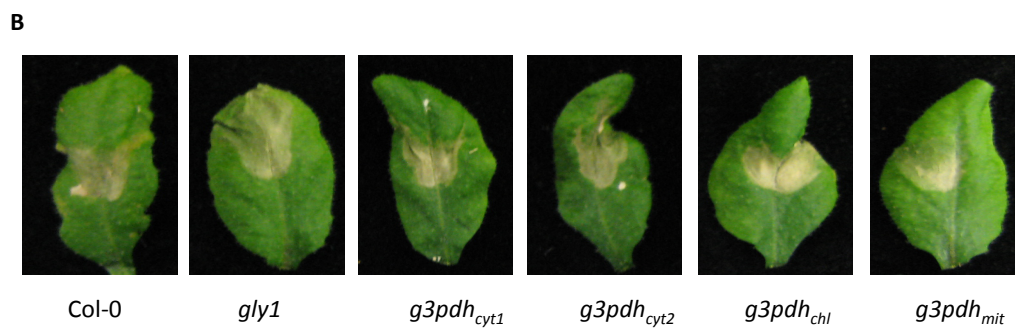
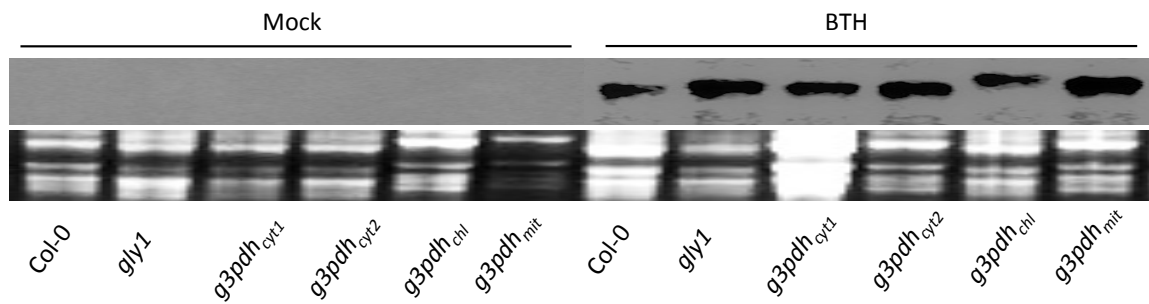
**Figure 4.3. (Continued)**

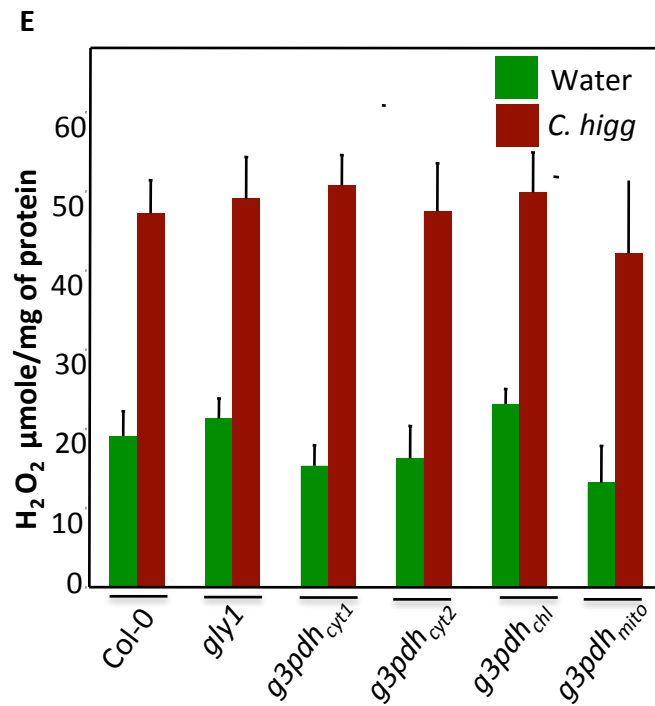
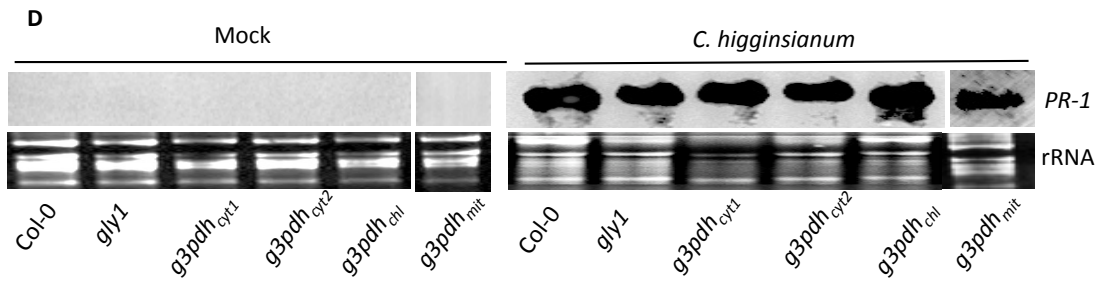
(A) Localisation of G3Pdh isoforms. Confocal micrograph showing localization of G3Pdh<sub>CYT1</sub>, G3Pdh<sub>CYT2</sub>, G3Pdh<sub>chl</sub>, G3Pdh<sub>Mit</sub> –GFP in *N. benthamiana* plants. Scale bar, of 10 µm. (B) Disease symptoms in Col-0, *gly1*, *g3pdh<sub>cyt1</sub>*, *g3pdh<sub>cyt2</sub>*, *g3pdh<sub>chl</sub>* and *g3pdh<sub>mit</sub>* leaves spray and spot inoculated with 10<sup>6</sup> spores/ml of *C. higginsianum*. (C) Lesion size of Col-0, *gly1*, *g3pdh<sub>cyt1</sub>*, *g3pdh<sub>cyt2</sub>*, *g3pdh<sub>chl</sub>* and *g3pdh<sub>mit</sub>* leaves spot inoculated with 10<sup>6</sup> spores/mL of *C. higginsianum*. Lesion size was measured from 20-30 independent leaves at 6 dpi. (D) Microscopy of trypan blue-stained leaves from size of Col-0, *gly1*, *g3pdh<sub>cyt1</sub>*, *g3pdh<sub>cyt2</sub>*, *g3pdh<sub>chl</sub>* and *g3pdh<sub>mit</sub>* leaves plants inoculated with *C. higginsianum* at (10<sup>6</sup> spores/mL). The leaves were harvested at 3 dpi. The scale bar represents the size of 10 µm. (E) Basal and induced levels of G3P in Col-0, *gly1*, *g3pdh<sub>cyt1</sub>*, *g3pdh<sub>cyt2</sub>*, *g3pdh<sub>chl</sub>* and *g3pdh<sub>mit</sub>* four-week-old plants. Plants were spray inoculated at (10<sup>6</sup> spores/mL) and samples were collected at 72 hpi. Statistical significance was determined using Students *t*-test. Asterisks indicate data statistically significant from that of control (Col-0) (P<0.05). Error bars indicate SD.



**Figure 4.4. Pathogen response in plants pretreated with G3P**

(A) Disease symptoms in spot inoculated mock- and G3P-pretreated Col-0, *gly1*, *g3pdh<sub>cyt1</sub>*, *g3pdh<sub>cyt2</sub>*, *g3pdh<sub>chl</sub>* and *g3pdh<sub>mit</sub>* plants. (B) Lesion size in spot- inoculated Col-0, *gly1*, *g3pdh<sub>cyt1</sub>*, *g3pdh<sub>cyt2</sub>*, *g3pdh<sub>chl</sub>* and *g3pdh<sub>mit</sub>* plants treated with water or G3P. The lesion size was measured from ~20 independent leaves at 7 dpi. Error bars indicate SD. The lesion size was measured from 20-30 independent leaves at 7 dpi. Statistical significance was determined using Student's *t*-test. Asterisks indicate data statistically significant from that of water treatment ( $P < 0.001$ ). Error bars indicate SD.





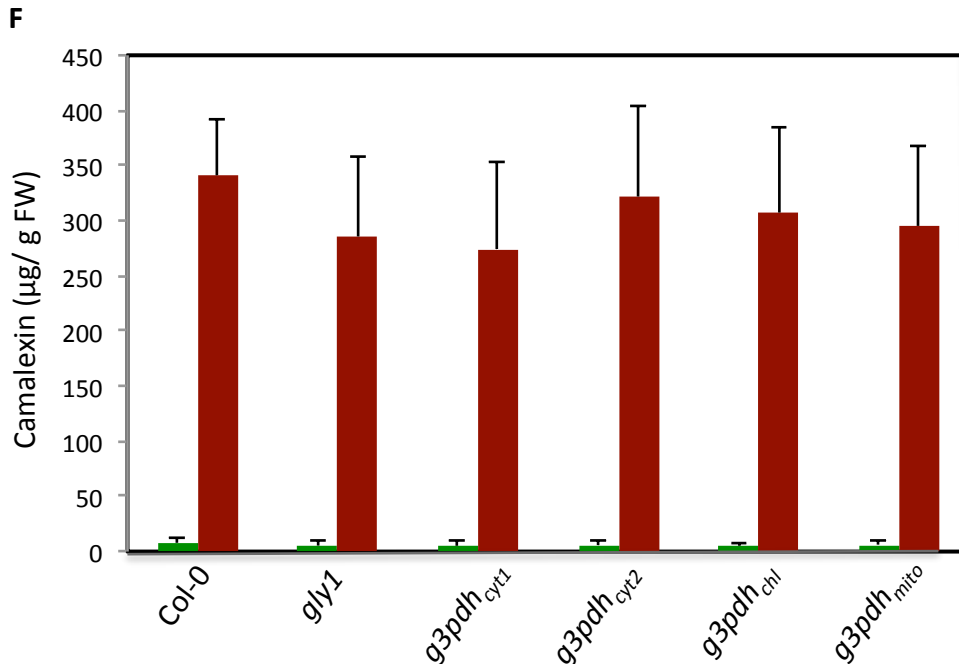


**Figure. 4.5. The enhanced susceptibility of *g3pdh* mutants is not due to a defect in SA, camalexin or ROS pathways**

(A) Northern blot analysis of *PR-1* gene expression in Col-0, *gly1* and *g3pdh<sub>cyt1</sub>*, *g3pdh<sub>cyt2</sub>*, *g3pdh<sub>chl</sub>* and *g3pdh<sub>mit</sub>* plants spray-inoculated with water or Benzothiadiazole (BTH). The samples were collected at 2 dpi. RNA gel blot analysis was performed on ~7 µg of total RNA and ethidium bromide staining of rRNA was used as a loading control. (B) Typical morphological phenotype seen in leaves spot inoculated with 20 µM of paraquat. The leaves were photographed 2 d posttreatment. (C) Lesion size in Col-0, *gly1*, *g3pdh<sub>cyt1</sub>*, *g3pdh<sub>cyt2</sub>*, *g3pdh<sub>chl</sub>* and *g3pdh<sub>mit</sub>* leaves treated with 10 µM of paraquat. The lesion size was measured from approximately 15 independent leaves at 2 d posttreatment. (D) Northern blot analysis of *PR-1* gene expression in Col-0, *gly1* and *g3pdh<sub>cyt1</sub>*, *g3pdh<sub>cyt2</sub>*, *g3pdh<sub>chl</sub>* and *g3pdh<sub>mit</sub>* plants spray-inoculated with water or 10<sup>6</sup> spores/mL of *C. higginsianum*. (E) Basal and *C. higginsianum* induced H<sub>2</sub>O<sub>2</sub> levels in four-week old Col-0 and *gly1* plants. The plants were spray-inoculated with 10<sup>6</sup> spores of *C. higginsianum* and the samples were collected at 3 dpi. (F) Camalexin levels in water- and *C. higginsianum*-inoculated wt (Col-0) *gly1* and *g3pdh<sub>cyt1</sub>*, *g3pdh<sub>cyt2</sub>*, *g3pdh<sub>chl</sub>* and *g3pdh<sub>mit</sub>* plants spray-inoculated with water or 10<sup>6</sup> spores/mL of *C. higginsianum*. The samples were collected at 3 dpi



## Chapter 5

### Discussion

Based on their mode of lifestyle pathogens are broadly classified as biotrophic or necrotrophic pathogens. The difference in these pathogens being that biotrophic pathogens feed on living host tissue but do not cause death of the host. In contrast, necrotrophic pathogens cause necrosis of the host tissues leading to their death (Glazebrook, 2005). A third group of pathogens, known as hemibiotrophs, live as both biotroph and necrotroph during their life cycle on the host. Both biotrophic and necrotrophic pathogens utilize host resources for their survival. Plants counter these pathogens by reprogramming their primary metabolic pathways (Berger et al., 2004) and therefore several primary metabolites play an important role in plant defense (Rolland et al., 2002). For example, colonization by *Botrytis cinerea* is associated with multiple metabolic changes including increased expression of genes involved in sugar, amino acid, and mineral transport and nutrient cycling (AbuQamer et al., 2006). In this study, I have characterized the role of primary metabolite glycerol-3-phosphate (G3P) in plant defense. I show that G3P levels play an important role in plant defense against hemibiotrophic pathogen *Colletotrichum higginsianum* and in systemic immunity triggered upon activation of resistance (R)-mediated signaling.

G3P is synthesized via GLYCEROL KINASE (GK) catalyzed phosphorylation of glycerol or G3P DEHYDROGENASE (G3Pdh) catalyzed reduction of dihydroxyacetone phosphate. The Arabidopsis genome encodes one isoform of GK (*GLII*) and five isoforms of G3Pdh, suggesting that combined activities of various G3P biosynthesis enzymes contribute to the total G3P pool. This is further consistent with the fact that mutation in *GLII* and three isoforms of *G3Pdh* (*GLY1*, *G3Pdh<sub>cyt2</sub>*, *G3Pdh<sub>chl</sub>*) lowered pathogen-induced G3P levels and resulted in increased susceptibility to *C. higginsianum* and compromised systemic acquired resistance (SAR). Compromised basal resistance and SAR were not associated with impaired glycerolipid levels as except *gly1* rest other

*g3pdh* mutants showed normal FA and glycerolipid levels. Similarly, the *gli1* plants also showed wild-type-like glycerolipid profile. Furthermore, *act1* plants showed reduced glycerolipid levels but normal SAR and enhanced resistance to *C. higginsianum*. A requirement for glycerolipid pathway in SAR is further discounted by the result that *FATTY ACID DESATURASE* mutants that are defective in desaturation of membrane lipids show normal SAR and wild-type-like response to *C. higginsianum* (Xia et. al., 2010).

Although, plants deficient in G3P biosynthesis showed enhanced susceptibility to *C. higginsianum*, they showed normal levels of *PR-1* gene expression and accumulated wild type-like levels of SA. This and the result that SA pretreatment restored resistance to *C. higginsianum* suggest that SA likely acts independent and downstream of G3P. Increased susceptibility to *C. higginsianum* was not associated with levels of reactive oxygen species (ROS) or camalexin, which have been shown to play a role in defense against necrotrophic pathogen (Kariola et. al., 2005; Thomma et al., 1998); the *g3pdh* plants accumulated wild-type-like levels of ROS and camalexin and displayed wild-type-like sensitivity to ROS inducing agent paraquat. A wild-type-like pathogen response seen in camalexin deficient *act1 pad3* plants suggests that G3P acts downstream and/or independent of camalexin.

The plastidal G3P pool regulates levels of oleic acid (18:1), a key defense-signaling molecule. A mutation in the stearoyl-acyl carrier protein (ACP) desaturase (*SSI2*) leads to constitutive *PR (PATHOGENESIS RELATED)* gene expression, increased SA levels and resistance to oomycete and bacterial pathogens (Kachroo et al., 2004). The low 18:1 levels and constitutive defense phenotype in *ssi2* plants are restored by a loss-of-function mutation in the *ACT1*-encoded G3P acyltransferase, or the *GLY1* gene. The *GLY1* catalyzed biosynthesis of G3P serves as a substrate for the *ACT1*-catalyzed reaction. The 18:1 levels can also be lowered by exogenous application of glycerol, which increases G3P resulting in the depletion of 18:1 in an *ACT1*-dependent manner (Kachroo et al., 2004). Glycerol plays an important role in various metabolic processes (Aubert et. al., 1994) and the host glycerol was suggested to trigger *in planta* growth of the fungus *Colletotrichum gloeosporioides* (Wei et al., 2004). Consistent with this hypothesis, *GLII*

mutant plants, which contain high basal levels of glycerol, showed enhanced susceptibility to *C. higginsianum*. However, *gly1* plants, which accumulated wild-type-like glycerol, also showed enhanced susceptibility to *C. higginsianum*. A common feature shared between *gly1* and *gli1* plants is that they show reduced accumulation of pathogen-induced G3P levels. This together with the fact that exogenous G3P restores enhanced susceptible phenotype of *gli1* and *gly1* plants suggests that G3P levels play an important role in basal resistance against *C. higginsianum*. This is further supported by the observation that *act1* plants, which accumulate higher levels of G3P, show enhanced resistance to *C. higginsianum*.

G3P levels also increase in response to inoculations with the bacterial pathogen *P. syringae* expressing the cognate avirulent effector. This increase in G3P levels was detected in both local and distal tissues as well as the vascular exudate. Notably, plants inoculated with *P. syringae* showed faster and higher levels of G3P compared to plants inoculated with *C. higginsianum*. This is consistent with the fact that R-mediated activation often leads to stronger induction of defense responses. Plants mutated in G3P biosynthetic activities failed to induce SAR, which was restored when plants were treated with G3P. Exogenous G3P did not induce the SA pathway, a well-known inducer of SAR. However, a mutation in *SID2* compromised G3P induced SAR, suggesting that SA was required for G3P conferred SAR. The basal SA levels in SA-deficient *sid2* plants were significantly lower compared to wild-type plants, suggesting that basal SA might be sufficient for SAR. This is further supported by an earlier study that showed that ability to accumulate SA does not correlate with induction of SAR (Cameron et. al., 1999). This together with the observation that *gly1* and *gli1* plants accumulate normal pathogen-induced SA suggests that induction of SA does not require G3P biosynthetic activities. The *gly1* and *gli1* mutants show normal response to exogenous MeSA treatments, suggesting that these plants are not defective in methylesterase activity, which is required for normal SAR (Park et. al., 2007).

Interestingly, exogenous azelaic acid (AA), a dicarboxylic acid that confers SAR on wild-type plants, was unable to confer SAR on *gly1* and *gli1* plants. Moreover, G3P conferred

SAR was dependent on AZI1 (Azelaic Acid Insensitive 1), which shows homology to lipid transfer protein family and also is required for AA-conferred SAR. Together these results suggest that AA- and G3P-triggered SAR might overlap. More work will be required to clarify this. My results also show that the G3P is converted to a derivative, which is translocated to distal tissues in a DIR1-dependent manner. The molecular and biochemical basis of this translocation remains unclear. A likely possibility is that G3P-derivative might form a complex with DIR1 and that the translocation of this complex is required for transcriptional reprogramming of distal tissues. In conclusion, this study shows that G3P is a critical signaling molecule that participates in basal resistance against *C. higginsianum* and during SAR.

## References:

1. AbuQamar S, Chen X, Dhawan R, Bluhm B, Salmeron J, Lam S, Dietrich RA, and Mengiste T (2006) Expression profiling and mutant analysis reveals complex regulatory networks involved in Arabidopsis response to Botrytis infection. *Plant J* **48**: 28-44
2. Ahn I-P, Kim S, and Lee Y-H (2005) Vitamin B1 functions as an activator of plant disease resistance. *Plant Physiol* **138**: 1505-1515
3. Asahi T, Kojima M, and Kosuge T (1979) The energetics of parasitism, pathogenism, and resistance in plant disease. In: *Plant Disease An Advanced Treatise Vol. IV*. Horsfall JG and Cowling EB, eds. Academic Press Inc. pp. 47-74
4. Attaran, E., Zeier, T.E., Griebel, T. & Zeier, J. (2009) Methyl salicylate production and jasmonate signaling are not essential for systemic acquired resistance in Arabidopsis. *Plant Cell* **21**: 954–971
5. Aubert S, Gout E, Bligny R, and Douce R (1994) Multiple effects of glycerol on plant cell metabolism. *J Biol Chem* **269**: 21420-21427
6. Berger S, Sinha AK and Roitsch T (2007) Plant physiology meets phytopathology: plant primary metabolism and plant-pathogen interactions. *J Exp Bot* **58**: 4019-4026
7. Bessire M, Chassot C, Jacquat AC, Humphry M, Borel S, Petétot JM, Métraux JP, Nawrath C (2007) A permeable cuticle in Arabidopsis leads to a strong resistance

to *Botrytis cinerea*. *EMBO J* **26**: 2158-2168

8. Boller T, Felix G (2009) A renaissance of elicitors: perception of microbe-associated molecular patterns and danger signals by pattern-recognition receptors. *Annu Rev Plant Biol* **60**: 379–406
9. Brisson D, Vohl M-C, St-Pierre J, Hudson T and Gaudet D (2001) Glycerol: a neglected variable in metabolic processes? *Bioessays* **23**: 534-542
10. C. Zipfel, S. Robatzek, L. Navarro, E.J. Oakeley, J.D. Jones, G. Felix, T. Boller (2004) Bacterial disease resistance in *Arabidopsis* through flagellin perception. *Nature* **428**, 764–767
11. Chandra-Shekara AC Navarre D, Kachroo A, Kang H-G, Klessig DF, Kachroo P (2004) Signaling requirements and role of salicylic acid in *HRT*- and *rrt*-mediated resistance to turnip crinkle virus in *Arabidopsis*. *Plant J.* **40**, 647-659
12. Chandra-Shekara AC, Gupte M, Navarre DA, Raina S, Raina R, Klessig D and Kachroo P (2006) Light-dependent hypersensitive response and resistance signaling to turnip crinkle virus in *Arabidopsis*. *Plant J* **45**: 320-335
13. Chandra-Shekara AC, Venugopal SC, Barman SR, Kachroo A and Kachroo P (2007) Plastidial fatty acid levels regulate resistance gene-dependent defense signaling in *Arabidopsis*. *Proc Natl Acad Sci USA* **104**: 7277-7282
14. Chaturvedi, R. et al. (2008) Plastid omega-3-fatty acid desaturase-dependent accumulation of systemic acquired resistance inducing activity in petiole exudates of *Arabidopsis thaliana* is independent of jasmonic acid. *Plant J.* **54**: 106–117
15. Clough SJ and Bent AF (1998) Floral dip: a simplified method for *Agrobacterium*

- mediated transformation of *Arabidopsis thaliana*. Plant J. **16**: 735-743

16. Dangl, J. L. & Jones, J. D. G. (2001) Plant pathogens and integrated defence responses to infection. Nature **411**: 826–833
17. Dong X (2004) NPR1, all things considered. Curr Opin Plant Biol **7**: 547-552
18. Downie B (1994) Sugar content and endo-beta-mannanase activity in white spruce (*Picea glauca* [Moench.] Voss.) seeds during germination. Ph. D. thesis, University of Guelph, Guelph, Ontario, Canada.
19. Durrant WE and Dong X (2004) Systemic acquired resistance. Ann Rev Phytopathol **42**: 185-209
20. Durrant, W.E. & Dong, X. (2004) Systemic acquired resistance. Annu. Rev. Phytopathol. **42**: 185–209
21. Eastmond PJ (2004) Glycerol-insensitive Arabidopsis mutants: *gli1* seedlings lack glycerol kinase, accumulate glycerol and are more resistant to abiotic stress. Plant J **37**: 617-625
22. Ehness R, Ecker M, Godt DE and Roitsch T (1997) Glucose and stress independently regulate source and sink metabolism and defense mechanisms via signal transduction pathways involving protein phosphorylation. Plant Cell **9**: 1825-1841
23. Feys BJ and Parker JE (2000). Interplay of signaling pathways in plant disease resistance. Trends in Genetics **16**: 449-455
24. Fillinger, S. et al. (2001) Molecular and physiological characterization of the NAD-dependent glycerol 3-phosphate dehydrogenase in the filamentous fungus *Aspergillus nidulans*. Mol. Microbiol. **39**: 145–157

25. Flor H (1971) Current status of gene-for-gene concept. *Annu Rev Phytopathol* **9**: 275- 296
26. Glazebrook J (2001) Genes controlling expression of defense responses in *Arabidopsis* – 2001 status. *Curr Opin Plant Biol* **4**: 301-308
27. Glazebrook J (2005) Contrasting mechanisms of defense against biotrophic and necrotrophic pathogens. *Annu Rev Phytopathol* **43**: 205-227
28. Gomez-Ariza J, Campo S, Rufat M, Estopa M, Messeguer J, San Segundo B and Coca M (2007) Sucrose-mediated priming of plant defense responses and broad-spectrum disease resistance by overexpression of the maize pathogenesis-related PRms proteins in rice plant. *Mol Plant-Microbe Interact* **20**: 832-842
29. Gorvin EM and Levine A (2000) The hypersensitive response facilitates plant infection by the necrotrophic pathogen *Botrytis cinerea*. *Curr Biol* **10**: 751-757
30. Hancock JG and Huisman OC (1981) Nutrient movement in host-pathogen systems. *Annu Rev Phytopathol* **19**: 309-331
31. Heil, M. & Ton, J (2008) Long-distance signalling in plant defence. *Trends Plant Sci.* **13**: 264–272
32. Huckelhoven R (2007) Cell wall-associated mechanisms of disease resistance and susceptibility. *Annu Rev Phytopathol* **45**: 2.1-2.27
33. Iriti, M. & Faoro, F. (2007) Review of innate and specific immunity in plants and animals. *Mycopathologia* **164**: 57–64



34. Jones, J.D., and Dangl, J.L. (2006) The plant immune system. *Nature* **444**, 323–329
35. Jung, H.W., Tschaplinski, T.J., Wang, L., Glazebrook, J. & Greenberg, J.T. (2009) Priming in systemic plant immunity. *Science* **324**: 89–91
36. Kachroo A and Kachroo P (2006) Salicylic Acid-, Jasmonic Acid- and Ethylene-Mediated Regulation of Plant Defense Signaling. In *Genetic Regulation of Plant Defense Mechanisms*, Ed. Jane Setlow, Springer pubs. **28**: 55-83
37. Kachroo A, Daqi F, Havens W, Navarre D, Kachroo P and Ghabrial S (2008) An oleic acid-mediated pathway induces constitutive defense signaling and enhanced resistance to multiple pathogens in soybean. *Mol Plant-Microbe Interact* **21**: 564-575
38. Kachroo A, Lapchyk L, Fukushigae H, Hildebrand D, Klessig D and Kachroo P (2003) Plastidial fatty acid signaling modulates salicylic acid- and jasmonic acid-mediated defense pathways in the *Arabidopsis ssi2* mutant. *Plant cell* **15**: 2952-2965
39. Kachroo A, Venugopal SC, Lapchyk L, Falcone D, Hildebrand D and Kachroo P (2004) Oleic acid levels regulated by glycerolipid metabolism modulate defense gene expression in *Arabidopsis*. *Proc Natl Acad Sci USA* **101**: 5152-5157
40. Kachroo P, Venugopal SC, Navarre DA, Lapchyk L, and Kachroo A (2005) Role of salicylic acid and fatty acid desaturation pathways in *ssi2*-mediated signaling. *Plant Physiol* **139**: 1717-1735
41. Kang L, Li J, Zhao T, Xiao F, Tang X, Thilmony R, He SY and Zhou J-M (2003) Interplay of the *Arabidopsis* nonhost resistance gene *NHO1* with bacterial virulence. *Proc Natl Acad Sci USA* **100**: 3915-3924

42. Koeck M, Hardham AR, Dodds PN (2011) The role of effectors of biotrophic and hemibiotrophic fungi in infection. *Cell Microbiol* **13**: 1849–57
43. Kotchoni SO and Gachomo EW (2006) The reactive oxygen species network pathways: an essential prerequisite for perception of pathogen attack and the acquired disease resistance in plants. *J Biosci* **31**: 389-404
44. Kunst L, Browse J and Somerville C (1988) Altered regulation of lipid biosynthesis in a mutant of *Arabidopsis* deficient in chloroplast glycerol-3-phosphate acyltransferase activity. *Proc Natl Acad Sci USA* **85**: 4143-4147
45. Lascombe, M.-B. et al. (2008) The structure of “defective in induced resistance” protein of *Arabidopsis thaliana*, DIR1, reveals a new type of lipid transfer protein. *Protein Sci.* **17**: 1522–1530
46. Lipka V, Dittgen J, Bednarek P, Bhat R, Wiermer M, Stein M, Landtag J, Brandt W, Rosahl S, Scheel D, Llorente F, Molina A, Parker J, Somerville S, Schulze-Lefert P (2005) Pre- and postinvasion defenses both contribute to nonhost resistance in *Arabidopsis*. *Science* **310**: 1180-1183
47. Liu G, Kennedy R, Greenshields DL, Peng G, Forseille L, Selvaraj G, Wei Y (2007) Detached and attached *Arabidopsis* leaf assays reveal distinctive defense responses against hemibiotrophic *Colletotrichum spp.* *Mol Plant-Microbe Interact* **20**: 1308-1319
48. Liu, P.-P., Yang, Y., Pichersky, E. & Klessig, D.F. (2010) Altering expression of Benzoic acid/salicylic acid carboxyl methyltransferase 1 compromises systemic acquired resistance and PAMP-triggered immunity in *Arabidopsis*. *Mol. Plant Microbe Interact.* **23**: 82–90
49. Lu, M., Tang, X. & Zhou, J.-M. (2001) *Arabidopsis* NHO1 is required for general

resistance against *Pseudomonas* bacteria. *Plant Cell* **13**: 437–447

50. Maldonado, A.M., Doerner, P., Dixon, R.A., Lamb, C.J. & Cameron, R.K. (2002) A putative lipid transfer protein involved in systemic resistance signaling in *Arabidopsis*. *Nature* **419**: 399–403
51. Mengiste T, Chen X, Salmeron J and Dietrich R (2003) The *BOS1* Gene Encodes an R2R3MYB Transcription Factor Protein That Is Required for Biotic and Abiotic Stress Responses in *Arabidopsis*. *Plant Cell* **15**: 2551-2565
52. Miquel M, Cassagne C and Browse J (1998) A new class of *Arabidopsis* mutants with reduced hexadecatrienoic acid fatty acid levels. *Plant Physiol* **117**: 923-930
53. Miquel, M., Cassagne, C. & Browse, J. (1998) A new class of *Arabidopsis* mutants with reduced hexadecatrienoic acid fatty acid levels. *Plant Physiol.* **117**: 923–930
54. Nandi A, Welti R and Shah J (2004) The *Arabidopsis thaliana* dihydroxyacetone phosphate reductase gene *Suppressor of fatty acid desaturase Deficiency1* is required for glycerolipid metabolism and for the activation of systemic acquired resistance. *Plant Cell* **16**: 465-477
55. Nandi, A., Welti, R. & Shah, J. (2004) The *Arabidopsis thaliana* dihydroxyacetone phosphate reductase gene *SUPPRESSOR OF FATTY ACID DESATURASE DEFICIENCY1* is required for glycerolipid metabolism and for the activation of systemic acquired resistance. *Plant Cell* **16**: 465–477
56. Narusaka Y, Narusaka M, Park P, Kubo Y, Hirayama T, Seki M, Shiraiishi T, Ishida J, Nakashima M, Enju A, Sakurai T, Satou M, Kobayashi M, Shinozaki K (2004) *RCHI*, a locus in *Arabidopsis* that confers resistance to the hemibiotrophic fungal pathogen *Colletotrichum higginsianum*. *Mol Plant-Microbe Interact* **17**:

57. Nürnberger, T. & Kemmerling, B. (2009) Pathogen-associated molecular patterns (PAMP) and PAMP-triggered immunity. *Annu. Plant Rev.* **34**: 16–47
58. O’Connell R, Herbert C, Sreenivasaprasad S, Khatib M, Esquerre-Tugaye M-T, Dumas B (2004) A novel *Arabidopsis-Colletotrichum* pathosystem for the molecular dissection of plant-fungal interactions. *Mol Plant-Microbe Interact* **17**: 272-282
59. Oliver RP and Ipcho SVS (2004) Arabidopsis pathology breathes new life into the necrotrophs-vs.-biotrophs classification of fungal pathogens. *Mol Plant Pathol* **5**: 347-352
60. Panstruga, R. (2003). Establishing compatibility between plants and obligate biotrophic pathogens. *Curr. Opin. Plant Biol.* **6**: 320–326
61. Park SW, Kaimoyo E, Kumar D, Mosher S. & Klessig D. (2007) Methyl salicylate is a critical mobile signal for plant systemic acquired resistance. *Science* **318**: 113–116
62. Penninckx IA, Thomma BP, Buchala A, Mettraux JP, Broekaert WF (1998) Concomitant activation of jasmonate and ethylene response pathways is required for induction of a plant defensin gene in Arabidopsis. *Plant Cell* **10**: 2103-2113
63. Pennypacker BW (2000). Differential impact of carbon assimilation on the expression of quantitative and qualitative resistance in alfalfa (*Medicago sativa*). *Physiol Mol Plant Pathol* **57**: 87-93
64. Perfect SE, Hughes HB, O’Connell RJ and Green JR (1999) *Colletotrichum*: a model genus for studies on pathology and fungal-plant interactions. *Fungal Genet*

Biol **27**: 186- 198

65. Pieterse, C.M.J., Leon-Reyes, A., Van der Ent, S. *and* Van Wees, S.C.M. (2009) Networking by small-molecule hormones in plant immunity. *Nat. Chem. Biol.* **5**, 308–316. *Plant Signal. Behav.* **4**: 746–749
66. Price J, Li T-C, Kang SG, Na JK and Jang JC (2003) Mechanisms of glucose signaling during germination of Arabidopsis. *Plant Physiol* **132**: 1424-14389
67. Quettier, A.-L., Shaw, E. & Eastmond, P.J. (2008) SUGAR-DEPENDENT6 encodes a mitochondrial flavin adenine dinucleotide-dependent glycerol-3-P dehydrogenase, which is required for glycerol catabolism and postgerminative seedling growth in
68. R.A.L. van der Hoorn, S. Kamoun (2008) From guard to decoy: a new model for perception of plant pathogen effectors *Plant Cell*, **20**: 2009–2017
69. Rasmussen, J.B., Hammerschmidt, R. & Zook, M.N. (1991) Systemic induction of salicylic acid accumulation in cucumber after inoculation with *Pseudomonas syringae* pv *syringae*. *Plant Physiol.* **97**: 1342–1347
70. Robert B. Abramovitch<sup>1</sup>, Jeffrey C. Anderson<sup>1</sup> & Gregory B. Martin (2002) Bacterial elicitation and evasion of plant innate immunity *Nature Reviews Molecular Cell Biology* **7**: 601-611
71. Robert, H.S. & Friml, J. (2009) Auxin and other signals on the move in plants. *Nat. Chem. Biol.* **5**: 325–332
72. Rolland F, Moore B and Sheen J (2002) Sugar sensing and signaling in plants. *Plant Cell* S185-S205

73. Schaaf J, Walter MH and Hess D (1995) Primary metabolism in plant defense. *Plant Physiol* **108**: 949-960
74. Schaarschmidt S, Kopka J, Ludwig-Muller J and Hause B (2007) Regulation of arbuscular mycorrhization by apoplastic invertases: enhanced invertase activity in the leaf apoplast affects the symbiotic interaction. *Plant J* **51**: 390-405
75. Scheideler M, Schlaich NL, Fellenberg K, Beissbarth T, Hauser NC, Vingron M, Slusarenko AJ and Hoheisel JD (2002) Monitoring the switch from housekeeping to pathogen defense metabolisms in *Arabidopsis thaliana* using cDNA arrays. *Proc Natl Acad Sci USA* **277**: 10555-10561
76. Schulz-Lefert P and Panstruga R (2003) Establishment of biotrophy by parasitic fungi and reprogramming of host cells for disease resistance. *Annu Rev Phytopathol* **41**: 641- 667
77. Shen W, Wei Y, Dauk M, Zheng Z and Zou J (2003) Identification of a mitochondrial glycerol-3-phosphate dehydrogenase from *Arabidopsis thaliana*: evidence for a mitochondrial glycerol-3-phosphate shuttle in plants. *FEBS Lett* **536**: 92-96
78. Shen W, Wei Y, Dauk M, Zheng Z and Zou J (2006) Involvement of a glycerol-3-phosphate dehydrogenase in modulating the NADH/NAD ratio provides evidence of a mitochondrial glycerol-3-phosphate shuttle in *Arabidopsis*. *Plant Cell* **18**: 422-441
79. Shen, W. et al. (2006) Involvement of a glycerol-3-phosphate dehydrogenase in modulating the NADH/NAD ratio provides evidence of a mitochondrial glycerol-3-phosphate shuttle in *Arabidopsis*. *Plant Cell* **18**: 422–441
80. Shen, W., Wei, Y., Dauk, M., Zheng, Z. & Zou, J. (2003) Identification of a

mitochondrial glycerol-3-phosphate dehydrogenase from *Arabidopsis thaliana*: evidence for a mitochondrial glycerol-3-phosphate shuttle in plants. *FEBS Lett.* **536**: 92–96

81. Smith-Becker, J. et al. (1998) Accumulation of salicylic acid and 4-hydroxybenzoic acid in phloem of cucumber during systemic acquired resistance is preceded by a transient increase in phenylalanine ammonia-lyase activity in petioles and stems. *Plant Physiol.* **116**: 231–238
82. Solomon PS, Tan K-C and Oliver RP (2003) The nutrient supply of pathogenic fungi; a fertile field for study. *Mol Plant Pathol* **4**: 203-210
83. Steven H. Spoell & Xinnian Dong (2012) How do plants achieve immunity? Defence without specialized immune cells *Nat. Rev. Immun.* **12**: 89-100
84. Taiz L and Zeiger E (2006) In: *Plant Physiology*, Eds Taiz L, Zeiger E.
85. Tang D, Simonich MT and Innes RW (2007) Mutations in *LACS2*, a Long-Chain Acyl- Coenzyme A Synthetase, enhance susceptibility to avirulent *Pseudomonas syringae* but confer resistance to *Botrytis cinerea* in *Arabidopsis*. *Plant Physiol* **144**: 1093-1103
86. Thilmony, R., Underwood, W. & He, S. Y. Genome-wide transcriptional analysis of the *Arabidopsis thaliana* interaction with the plant pathogen *Pseudomonas syringae* pv. tomato DC3000 and the human pathogen *Escherichia coli* O157:H7. *Plant J.* **46**: 34–53 (2006).
87. Thomma BP, Penninckx IA, Broekaert WF and Cammue BP (2001) The complexity of disease signaling in *Arabidopsis*. *Curr Opin Immunol* **13**: 63-68
88. Truman, W., Bennett, M.H., Kubigsteltig, I., Turnbull, C. & Grant, M. (2007)

Arabidopsis systemic immunity uses conserved defense signaling pathways and is mediated by jasmonates. Proc. Natl. Acad. Sci. USA **104**: 1075–1080

89. Truman, W.M., Bennett, M.H., Turnbull, C.G. & Grant, M.R. (2010) Arabidopsis auxin mutants are compromised in systemic acquired resistance and exhibit aberrant accumulation of various indolic compounds. Plant Physiol. **152**: 1562–1573
90. Venugopal, S.C., Chanda, B., Vaillancourt, L., Kachroo, A. & Kachroo, P. (2009) The common metabolite glycerol-3-phosphate is a novel regulator of defense signaling.
91. Vlot, A.C. et al. (2008) Identification of likely orthologs of tobacco salicylic acid binding protein 2 and their role in systemic resistance in Arabidopsis thaliana. Plant J. **56**: 445-456
92. Vlot, A.C., Dempsey, D.A. & Klessig, D.F. (2009) Salicylic acid, a multifaceted hormone to combat disease. Annu. Rev. Phytopathol. **47**: 177–206
93. Vlot, A.C., Klessig, D.F. & Park, S.-W. (2008) Systemic acquired resistance: the elusive signal(s). Curr. Opin. Plant Biol. **11**: 436–442
94. Wei Y, Periappuram C, Datla R, Selvaraj G and Zou J (2001) Molecular and biochemical characterization of a plastidic glycerol-3-phosphate dehydrogenase from Arabidopsis. Plant Physiol Biochem **39**: 841-848
95. Wei Y, Shen W, Dauk M, Wang F, Selvaraj G and Zou J (2004) Targeted gene disruption of glycerol-3-phosphate dehydrogenase in *Colletotrichum gloeosporioides*
96. Wei, Y., Periappuram, C., Datla, R., Selvaraj, G. & Zou, J. (2001) Molecular and



biochemical characterization of a plastidic glycerol-3-phosphate dehydrogenase from *Arabidopsis*. *Plant Physiol. Biochem.* **39**: 841–848

97. Wildermuth, M.C., Dewdney, J., Wu, G. & Ausubel, F.M. (2001) Isochorismate synthase is required to synthesize salicylic acid for plant defence. *Nature* **414**: 562–565
98. Williams PH (1979) How fungi induce disease. In. *Plant Disease An Advanced Treatise*.
99. Wladimir I. L. Tameling & Frank L. W. Takken (2008) Resistance proteins: scouts of the plant innate immune system *Eur J Plant Pathol* **121**: 243–255
100. Xia, Y. et al. (2009) An intact cuticle in distal tissues is essential for the induction of systemic acquired resistance in plants. *Cell Host Microbe* **5**: 151–165
101. Xia, Y. et al. (2010) The *glabra1* mutation affects cuticle formation and plant responses to microbes. *Plant Physiol.* **154**: 833–846
102. Yoder OC and Turgeon BG (2001) Fungal genomics and pathogenicity. *Curr Opin Plant Biol* **4**: 315–321
103. Zhou N, Tootle TL, Tsui F, Klessig DF and Glazebrook J (1998) PAD4 functions upstream from salicylic acid to control defense responses in *Arabidopsis*. *Plant Cell* **10**: 1021–1030
104. Zipfel C, Kunze G, Chinchilla D, Caniard A, Jones JD, Boller T, Felix G (2006) Perception of the bacterial PAMP EF-Tu by the receptor EFR restricts *Agrobacterium*-mediated transformation. *Cell* **125**: 749–760

## APPENDIX-A

### LIST OF ABBREVIATIONS

Acronym/ abbreviation	Expansion
ACC	AcetylCoA carboxylase
AA	Azelaic acid
ACP	Acyl carrier protein
ACT1	Glycerol-3-phosphate acyl transferase
AZI1	Azelaic acid insensitive 1
BSA	Bovine serum albumin
BTH	Benzo[1,2,3]thiadiazole-7-carbothioic Acid <i>S</i> -Methyl Ester
BHT	Butylated hydroxy toluene
CaCl <sub>2</sub>	Calcium chloride
CAPS	Cleaved Amplified Polymorphic Sequences
CF	Centrifuge
CFU	Colony forming unit
Co-IP	Co-immunoprecipitation
DIR1	Defective in induced resistance 1
DJA	Dihydro jasmonic acid
DHAP	Dihydroxyacetone phosphate
dATP	Deoxyribo adenosine triphosphate
dCAPS	Derived Cleaved Amplified Polymorphic Sequences
dCTP	Deoxyribo cytosine triphosphate
DEPC	Diethyl pyrocarbonate
DGDG	Digalactosyldiacylglycerol
DIR1	Defective in induced resistance 1
DMSO	Dimethyl sulfoxide
DNA	Deoxyribonucleic acid
dNTP	Deoxyribo nucleic triphosphate

<b>Acronym/ abbreviation</b>	<b>Expansion</b>
<b>DPI</b>	Days post inoculation
<b>DPM</b>	Disintegration per minute
<b>DPT</b>	Days post treatment
<b>DTT</b>	Dithiothreitol
<b>DW</b>	Dry weight
<b>EDTA</b>	Ethylene diamine tetra acetic acid
<b>EGTA</b>	Ethylene glycol tetraacetic acid
<b>ER</b>	Endoplasmic reticulum
<b>EtBr</b>	Ethidium bromide
<b>FAD</b>	Fatty acid desaturase
<b>FA</b>	Fatty acid
<b>FAME</b>	Fatty acid methyl ester
<b>DW</b>	Dry weight
<b>g/mg/mg/ng</b>	Gram/ milligram/ microgram/ nanogram
<b>GLI1/GK</b>	Glycerol insensitive 1/ Glycerol kinase
<b>GC</b>	Gas chromatography
<b>GLY1</b>	Glycerol Dependent 1
<b>G3Pdh</b>	Glycerol-3-phosphate dehydrogenase
<b>G3P</b>	Glycerol-3-phosphate
<b>GFP</b>	Green fluorescent protein
<b>h/min/sec</b>	Hours/minutes/seconds
<b>JA</b>	Jasmonic acid
<b>K<sub>2</sub>HPO<sub>4</sub></b>	Potassium phosphate, dibasic
<b>KOH</b>	Potassium hydroxide
<b>L/mL/mL</b>	Liter/ milliliter/ microliter
<b>LTP</b>	Lipid transfer protein

<b>Acronym/ abbreviation</b>	<b>Expansion</b>
<b>M/mM/mM</b>	Molar/millimolar/ micromolar
<b>MeSA</b>	Methyl salicylic acid
<b>MeJA</b>	Methyl jasmonic acid
<b>MgCl<sub>2</sub></b>	Magnesium chloride
<b>MGDG</b>	Monogalactosyldiacylglycerol
<b>MOPS</b>	3-(N-morpholino)propanesulfonic acid
<b>MS</b>	Murashige and skoog
<b>MS media</b>	Murashige & Skoog media
<b>NHO1</b>	Non-host resistance gene 1
<b>NaCl</b>	Sodium chloride
<b>NaOAc</b>	Sodium acetate
<b>NaOH</b>	Sodium hydroxide
<b>PA</b>	Phosphatidic acid
<b>PG</b>	Phosphatidylglycerol
<b>PI</b>	Phosphatase inhibitor
<b>°C</b>	Degree centigrade
<b>PBS</b>	Phosphate buffered saline
<b>PC</b>	Phosphatidylcholine
<b>PCR</b>	Polymerase chain reaction
<b>PE</b>	Phosphatidylethaloamine
<b>PFD</b>	Photon flux density
<b>PG</b>	Phosphatidylglycerol
<b>PI</b>	Phosphatidylinositol
<b><i>PR-1</i></b>	Pathogenesis related 1
<b>PS</b>	Phosphatidylserine
<b>R</b>	Resistant or resistance

<b>Acronym/ abbreviation</b>	<b>Expansion</b>
<b>RFP</b>	Red fluorescent protein
<b>Rh</b>	Relative humidity
<b>RNA</b>	Ribonucleic acid
<b>SA</b>	Salicylic acid
<b>SAG</b>	Salicylic acid glucoside
<b>SAR</b>	Systemic acquired resistance
<b>SD</b>	Standard deviation
<b>SDS</b>	Sodiumdodecyl sulfate
<b>SFD1</b>	Suppressor of fatty acid desaturase 1
<b>SID2</b>	Salicylic acid insensitive 2
<b>SL</b>	Sulfolipid
<b>SSC</b>	Sodium chloride, sodium citrate
<b>TBE</b>	Tris- borate/ EDTA electrophoresis buffer
<b>TE</b>	TRIS-EDTA
<b>TRIS</b>	Hydroxymethyl Aminomethane
<b>Wt</b>	Wild-type
<b>μM</b>	Micron meter
<b>16:0</b>	Palmitic acid
<b>16:1</b>	Palmitoleic acid
<b>16:2</b>	Hexadecadienoic acid
<b>16:3</b>	Hexadecatrienoic acid
<b>18:0</b>	Stearic acid
<b>18:1</b>	Oleic acid
<b>18:2</b>	Linoleic acid
<b>18:3</b>	Linolenic acid

## Vita

### Bidisha Chanda

#### EDUCATION:

2005-2006: Masters of Philosophy (M.Phil). Jawaharlal Nehru University, New Delhi, India. M.Phil Thesis Title: Cloning and characterisation of reverse transcriptase gene present in EhLINE1 (a non-LTR retrotransposon) of *Entamoeba histolytica*.

2001-2003: M.S. (Agricultural Biotechnology), Assam Agricultural University, India. M.S. Thesis Title: Molecular and biochemical characterisation of jute degumming bacteria.

1997-2001: B.S. (Agricultural Sciences, Major in Plant Pathology), Assam Agricultural University, India.

#### MEMBERSHIP:

- American Society of Plant Biologists (**ASPB**).
- American Phytopathological Society (**APS**).

#### PUBLICATIONS:

1. MK. Mandal, AC. Chandra-Shekara, RD. Jeong, K. Yu, S. Zhu, **B. Chanda**, D Navarre, A Kachroo, P Kachroo (**2012**). Oleic acid-dependent modulation of NITRIC OXIDE ASSOCATED 1 protein levels regulate nitric oxide-mediated signaling in plant defense. *Plant Cell*, **24**: 1654-1674

2. MK. Mandal, **B. Chanda**, Y. Xia, K. Yu, K. Sekine, Q. Gao, D. Selote, Y. Hu, A. Stromberg, D. Navarre, A. Kachroo, and P. Kachroo (2011). Glycerol-3-phosphate in systemic immunity. *Plant Signaling & Behavior*, **1**: 6-11.
3. **B. Chanda**, Y. Xia, MK Mandal, K. Yu, K. Sekine, Q. Gao, D. Selote, Y. Hu, A. Stromberg, D. Navarre, A. Kachroo, and P. Kachroo (2011). Glycerol-3-phosphate a critical mobile inducer of systemic immunity in plants. *Nature Genetics*, **43**: 421–427.
4. S. Venugopal, **B. Chanda**, L. Vaillancourt, A. Kachroo and P. Kachroo (2009). The common metabolite glycerol-3-phosphate is a novel regulator of plant defense signaling. *Plant Signaling & Behavior*, **4**: 746–749.
5. **B. Chanda**, S. Venugopal, S. Kulshrestha, D. Navarre, B. Downie, L. Vaillancourt, A. Kachroo, and P. Kachroo (2008). Glycerol-3-phosphate levels are associated with basal resistance to the hemibiotrophic fungus *Colletotrichum higginsianum* in Arabidopsis. *Plant Physiology*, **147**: 2017-2029.

#### AWARDS/FELLOWSHIPS

- **2011**, Awarded travel grant by **ASPB** to attend the annual meeting.
- **2011**, Awarded travel grant by University of Kentucky Graduate School.
- **2011-2012**, Presidential award granted by University of Kentucky.
- **2008**, Awarded travel grant by University of Kentucky Graduate School.
- **2004**, Awarded two fellowships during M.Phil, Council of Scientific and Industrial Research and Govt. of India.
- **2001**, Awarded fellowship during MS, Department of Biotechnology, India.
- **1997**, Awarded fellowship during BS, Assam Agricultural University, India.